A COMPARISON OF FIXED PARAMETER VERSUS ADAPTIVE DIGITAL TRACKING FILTERS

by

Charles Keith Colonna

Thesis submitted to the Graduate Faculty of the

Virginia Poltyechnic Institute and State University

in partial fulfillment of the requirements for the degree of

MASTER OF SCIENCE

in

Electrical Engineering

APPROVED:

H. F. VanLandingham

T. E. Bechert

R. L. Moose

February, 1977

Blacksburg, Virginia

ACKNOWLEDGEMENT

Like any other achievement, my efforts are based upon the contribution of many others who gave me the needed academic background to undertake this study. I am grateful to , my major advisor who gave me the needed advice and guidance, and also to and , members of my graduate committee.

I am especially grateful to my wonderful wife , who supported me financially and spiritually during my graduate work. Her patience and endurance during the typing of this manuscript will not be forgotten.

TABLE OF CONTENTS

LISTS OF FIGURES

FIGURE Page

Chapter 1

Introduction

The fundamental idea of closed-loop control or feedback is to modify a system input in some way by information about the behavior of the system output. In classical terms, this input modification corresponds to closing the loop in such a manner as to place the poles of the closed-loop transfer function where they best serve system design specifications. In the modern or state space approach to a linear, time invariant system, this corresponds to feeding back a linear combination of the system states such that the system closed-loop matrix has a desired set of eigenvalues. For example with the discrete time system

$$\underline{x}(k+1)=\Phi\underline{x}(k)+\Gamma\underline{u}(k) \tag{1.1}$$

an appropriate state feedback matrix, F, could be designed such that the modified system

$$\underline{x}(k+1)=(\Phi+\Gamma F)\underline{x}(k)+\Gamma\underline{u}(k) \tag{1.2}$$

has desired eigenvalues to satisfy system transient performance specifications.

In a more general situation, part or all of the system states may not be available for direct measurement. In such cases when the system is observable [9], the states can be reconstructed by observing the system outputs and inputs. Figure 1.1 illustrates the use of reconstructed state variables in the feedback process where w(k) and v(k)

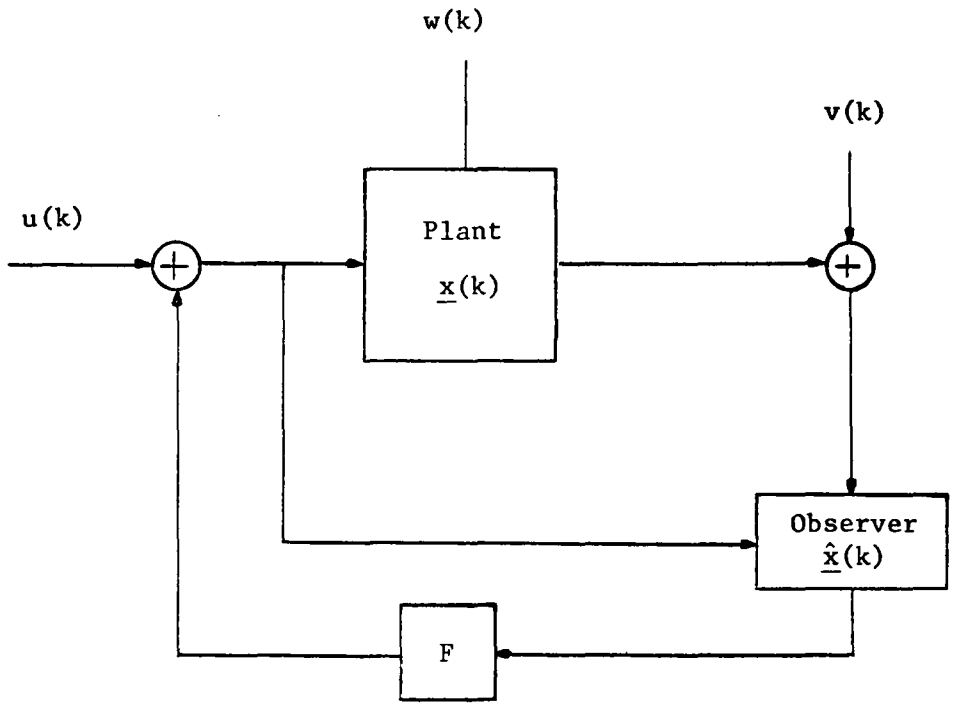

Figure 1.1 State Reconstruction Feedback

represent process noise and measurement noise respectively. In a completely deterministic system (i.e., $w(k)=v(k)=0$) the design of the observer is straight forward. For example with the system

$$\underline{x}(k+1)=\Phi\underline{x}(k)+\Gamma\underline{u}(k) \tag{1.3}$$

$$\underline{y}(k)=C\underline{x}(k)+D\underline{u}(k)$$

we can construct a second system [9]

$$\hat{\underline{x}}(k+1)=K\hat{\underline{x}}(k)+H\underline{y}(k)+G\underline{u}(k) \tag{1.4}$$

such that

$$\lim_{k\to\infty}[\tilde{\underline{x}}(k)]=0 \tag{1.5}$$

where

$$\tilde{\underline{x}}(k)\triangleq[\underline{x}(k)-\hat{\underline{x}}(k)] \tag{1.6}$$

Since

$$\tilde{\underline{x}}(k+1)=(\Phi-HC)\underline{x}(k)-K\hat{\underline{x}}(k)+(\Gamma-G-HD)\underline{u}(k) \tag{1.7}$$

we can let

$$G=\Gamma-HD \tag{1.8}$$

and

$$K=\Phi-HC \tag{1.9}$$

so that

$$\underset{\sim}{\tilde{x}}(k+1)=(\Phi-HC)\underset{\sim}{\tilde{x}}(k) \qquad (1.10)$$

Thus the observer error, $\tilde{x}$, will approach zero if $(\Phi-HC)$ is stable and the associated rate of approach is at the designer's discretion since the eigenvalues are determined by the arbitrary matrix H.

In the stochastic system (i.e., $v(k)\neq 0, w(k)\neq 0$) the choice of observer eigenvalues is much more difficult since a fast system will tend to track high frequency noise and a slow system may react too slowly to changes in the system state. This paper concerns itself with the simulation and comparison of various types of state estimators in a variety of process and measurement noise environments. The types of filters under test are the fixed parameter α-β filter, the double α-β filter, the 2nd order Kalman filter, the augmented Kalman filter, and the double Kalman filter.

The particular problem ensued is that of estimating the true position of a maneuvering vehicle from noisy radar or sonar data, assuming the maneuver capabilities of the vechicle are known.

Although the results are obtained directly from the problem of tracking a maneuvering vehicle, they may be extended to the more general control problem in which state reconstruction, in the presence of process and measurement noise, is desired. It is hoped that these simulations will yeild an indication of the relative advantages or disadvantages of the various tracking techniques in particular noise environments.

Chapter II

Plant Model

2.1 Continous-Time Plant

Chapter I introduced the role of state reconstruction in the overall closed-loop feedback problem and emphasized the ease of state estimation in a completely noise free observable system. This paper concerns itself with the more realistic problem of state estimation in a noisy environment. The problem is placed in the context of tracking maneuvering vehicles from noisy position data. This is the same problem encountered in most tactical weapons systems which require accurate tracking of manned maneuvering vehicles such as aircraft, ships, and submarines. In such systems, the target model selected for tracking applications must be sufficiently simple to permit ready implementation in weapons systems for which computation time is premium yet sufficiently sophisticated to provide satisfactory tracking accuracy. [1]

The model presented below is based on the fact that, without maneuvering, manned vehicles (such as aircraft, ships, and submarines) generally follow straight line trajectories. [1] The model is also useful for a single spatial dimension (such as x, y, z, range, bearing, or elevation), but the extension of the results to three dimensions can be considered simply as three independent models delivering three independent noisy measurements.

The targets under consideration normally move at constant velocity. Turns, evasive maneuvers, and accelerations due to atmospheric tur-

bulence may be viewed as pertubations upon the constant velocity trajectory. [1] In a single physical dimension, the continous-time target equations of motion may be represented by

$$\dot{\underline{x}}(t)=Ax(t)+Ba(t) \qquad (2.1)$$

where

$$\underline{x}(t)=\begin{bmatrix} x_1(t) \\ x_2(t) \end{bmatrix} = \begin{matrix} \text{target position at time t} \\ \text{target speed at time t} \end{matrix}$$

$a(t)=$ target acceleration at time t

and

$$A=\begin{bmatrix} 0 & 1 \\ 0 & 0 \end{bmatrix}; \qquad B=\begin{bmatrix} 0 \\ 1 \end{bmatrix}$$

It may be noted in Figure 1.1 that, in general, a state estimator has the deterministic plant input available for use in the state reconstruction process. However, in the problem at hand, the only data available to the observer are the noisy position measurments. The plant input function a(t) is a direct function of the pilot throttle and is not available for filtering of the noisy measurements. We must then model the system as having only a noise input and consider a(t) as a random process.

In order to accurately model a(t) as a random process, we must accurately model the first and second order statistics of the process (mean, variance, and autocorrelation). The statistical model below has

been utilized in tracking simulations and has been shown to provide a satisfactory representation of the targets maneuver characteristics. [1]

A probability density function applicable to the vehicles under consideration is shown in Figure 2.1 The target can accelerate at a maximum rate Am(-Am) and will do so with probability Pm. The target undergoes no acceleration with probability Po, and will accelerate between -Am and Am according to the appropriate uniform distribution. It is seen that the mean value of the acceleration is

$$\bar{a}(t)=E\{a(t)\}=0 \tag{2.2}$$

and the variance of the acceleration is

$$\sigma_a^2=E\{a^2(t)\}=\frac{Am^2}{3}[1+4Pm-Po] \tag{2.3}$$

The target maneuvers will be correlated in time since if a vehicle is accelerating in a given direction at time t, it will likely be accelerating in the same direction at time t+τ for small τ. A standard autocorrelation function for vehicle acceleration is

$$r(t)=E\{a(t)a(t+\tau)\}=\sigma_a^2 e^{-\gamma|\tau|} \qquad \gamma>0 \tag{2.4}$$

For the purpose of simulating the responses of the various tracking filters considered in this paper, three classes of vehicles were considered with varying values of maximum acceleration Am, and correlation coefficient γ . The three vehicles classes will be refered to as follows:

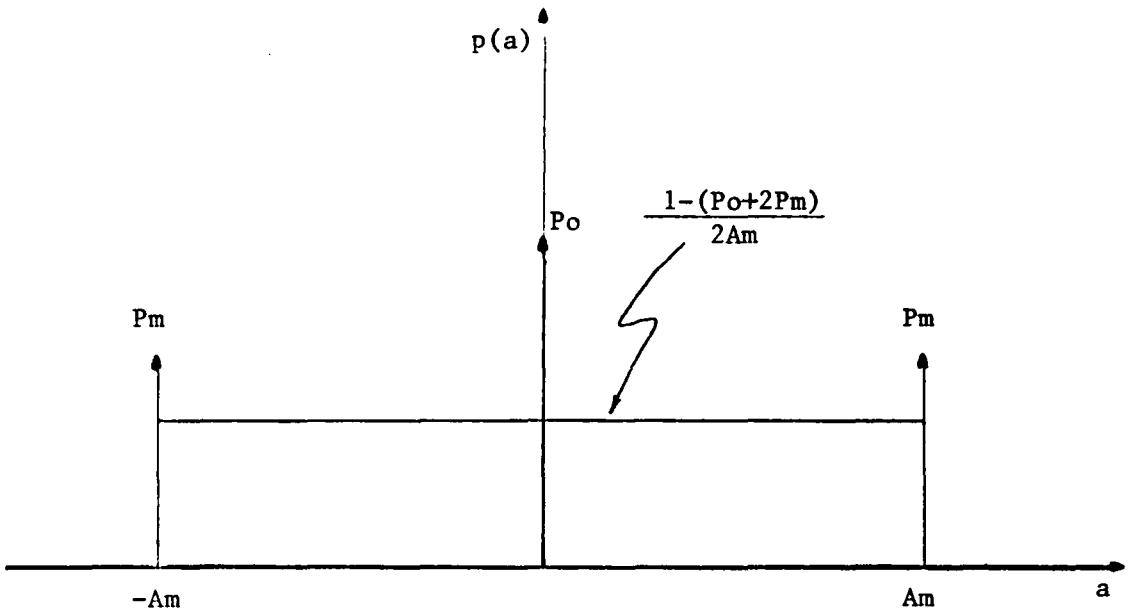

Figure 2.1 Probability Density Function of Acceleration

Class I	Am=150 ft./sec.^{2}	γ=1/2 sec.$^{-1}$
Class II	Am=100 ft./sec.^{2}	γ=1.5 sec.$^{-1}$
Class III	Am=50 ft./sec.^{2}	γ=1/10 sec.$^{-1}$

(2.5)

In each simulation, the data available to the various tracking filters is assumed to be of the form

$$z(t) = p(t)+v(t)$$

where

z(t) = position data available

p(t) = actual position

v(t) = white, gaussian, zero-mean noise

With the vehicle class fixed, each filter under test will be run through a range of measurement noise variance σ_m^2 of the white, zero-mean, gaussian sequence v(k) (section 2.2) ranging from 50 ft.^{2} to 400 ft.^{2}

2.2 Discrete-Time Plant

Given a continuous time plant

$$\dot{\underline{x}}(t)=A\underline{x}(t)+Bu(t) \qquad (2.1)$$

it is well documented [9] that a discrete time model

$$\underline{x}(k+1)=\Phi\underline{x}(k)+\Gamma\underline{u}(k) \qquad (2.6)$$

can be obtained through sample data arguements where

$$\Phi = e^{AT} \tag{2.7}$$

and

$$\Gamma = \int_0^T e^{At} B u(t) dt \tag{2.8}$$

For the plant under consideration

$$\Phi = \begin{bmatrix} 1 & T \\ 0 & 1 \end{bmatrix}, \quad \Gamma = \begin{bmatrix} T^2/2 \\ T \end{bmatrix} \tag{2.9}$$

However, there were two assumptions made which altered the system input matrix. The first assumption allowed the plant to have instantaneous changes in velocity. The second assumption allowed these accelerations to occur only at fixed intervals which for these simulations was set at one second. In order to approximate the vehicle classed as previously discussed and maintain the statistics of equations 2.2, 2.3, and 2.4, the input matrix was modified and the following discrete time system used for simulation.

$$\begin{bmatrix} x_1(k+1) \\ x_2(k+1) \end{bmatrix} = \begin{bmatrix} 1 & T \\ 0 & 1 \end{bmatrix} \begin{bmatrix} x_1(k) \\ x_2(k) \end{bmatrix} + \begin{bmatrix} 0 \\ 1 \end{bmatrix} a(k) \tag{2.8}$$

where

$$\begin{matrix} x_1(k) \\ x_2(k) \end{matrix} = \begin{matrix} \text{discrete-time position} \\ \text{discrete-time speed} \end{matrix}$$

and T.=.05 sec.

a(k) is the system input acceleration which takes on values other than zero only at one second intervals. The values of merrit from Figure 2.1 which were used in the filter simulation were Po=.95, Pm=.02 and Am as dictated by the vehicle class as previously discussed.

In the tracking filter simulations, the sample time T was held at .05 seconds throughout and the filter run through 10 seconds of tracking time. The actual positions for each of the three vehicle classes is shown in Figures 2.2 through 2.4. By altering the discrete-time system model and thus obtaining the piece-wise linear constant velocity trajectories, it was felt that the transient response of the tracking filters under consideration would become more evident while still reasonably approximating a continuously maneuvering vehicle. While the trajectories of Figures 2.2 through 2.4 are approximations to a continuously maneuvering vehicle, they may be quite accurate in track-while-scan systems where the sample time is large compared to the time constant of the vehicles being tracked.

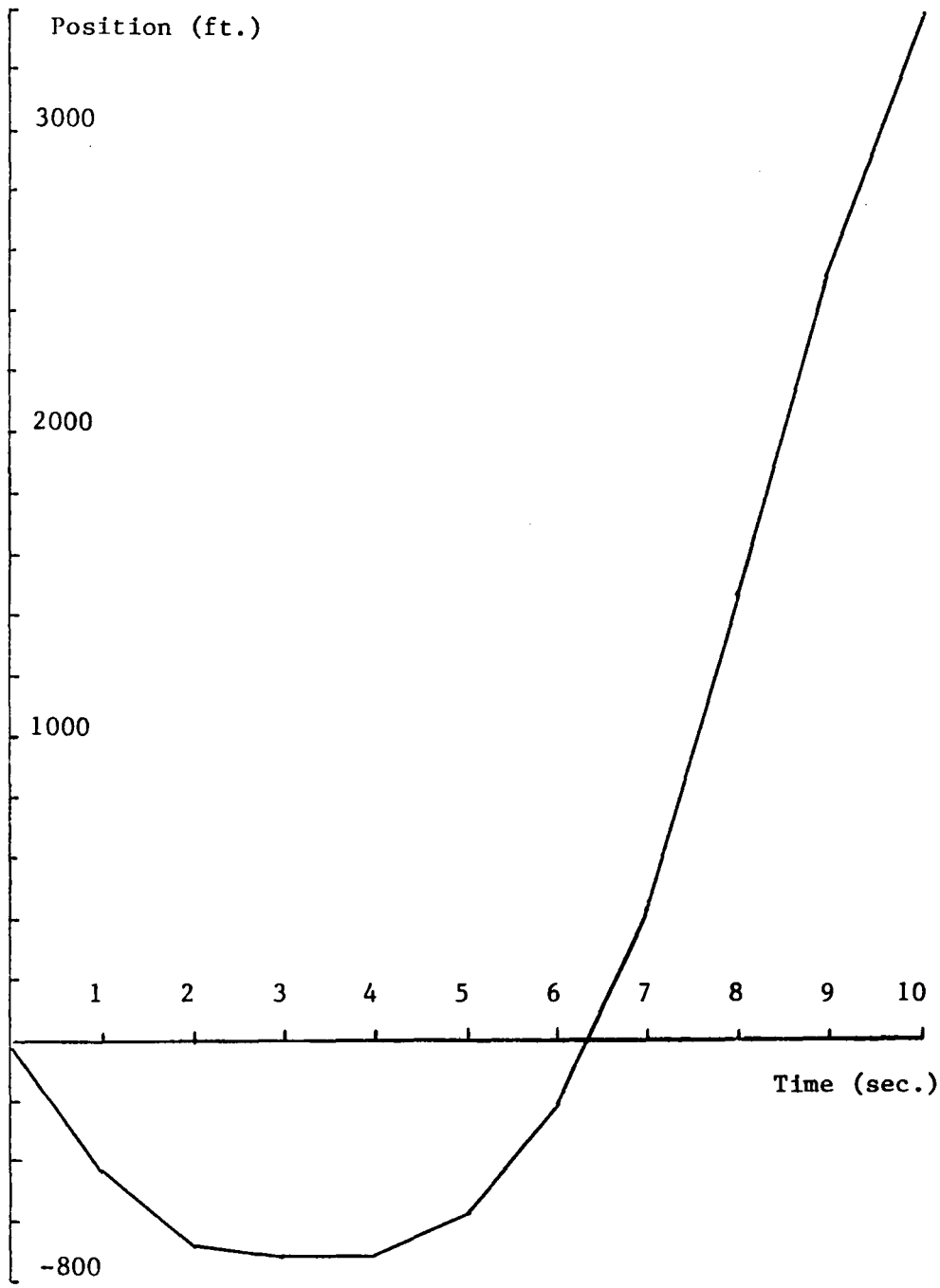

Figure 2.2 Class I Vehicle Trajectory

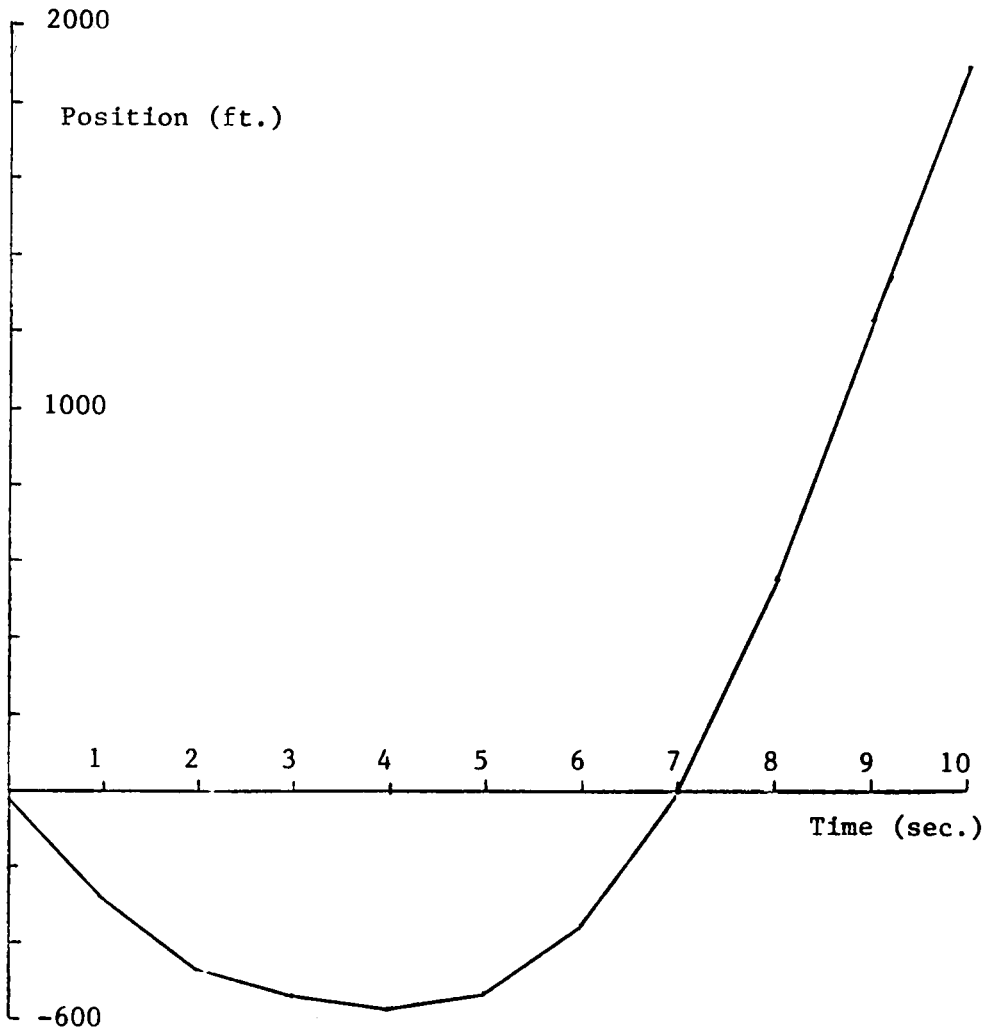

Figure 2.3 Class II Vehicle Trajectory

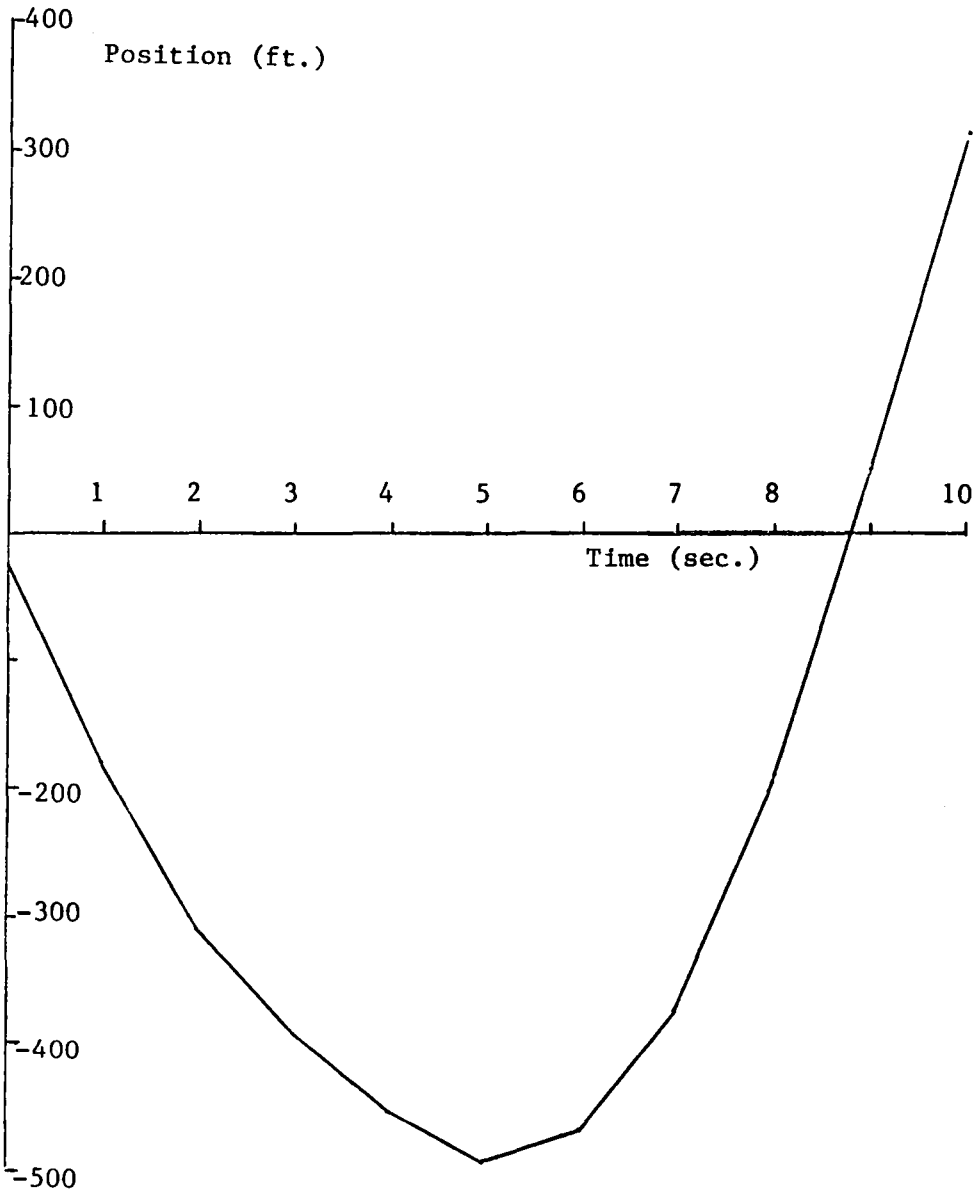

Figure 2.4 Class III Vehicle Trajectory

Chapter III

Alpha-Beta Filters

3.1 Fixed Parameter Alpha-Beta Filters

The use of α-β filters can be traced back to the middle to late 1950's [5] with work done by Sklansky and others. The basic idea is to design a digital filter which will process discrete, noisy, sampled input data and yield a smoothed estimate of position and (or) velocity. For example we wish to have a filter with unit impulse response, $g_x(k)$, such that for

$u(k)$ = raw input sampled data position sequence

$\bar{x}(k)$ = system smoothed-position output sequence

$\dot{\bar{x}}(k)$ = system smoothed velocity output sequence

we have the relations

$$\bar{x}(k) = \sum_{n=0}^{\infty} g_x(n)u(k-n) \tag{3.1}$$

and

$$\dot{\bar{x}}(k) = \sum_{n=0}^{\infty} g_{\dot{x}}(n)u(k-n) \tag{3.2}$$

The α-β filter is characterized as 2nd order with smoothing constants α and β which are used for smoothing position and velocity respectively [3]. The difference equations for the α-β filter are as follows:

$$\bar{x}(k) = x_p(k)+\alpha(u(k)-x_p(k)) \tag{3.3}$$

$$\dot{\bar{x}}(k) = \dot{\bar{x}}(k-1)+\frac{\beta}{T}(u(k)-x_p(k)) \tag{3.4}$$

$$x_p(k+1) = \bar{x}(k)+T\dot{\bar{x}}(k) \tag{3.5}$$

where

T = sampling period

and

$x_p(k)$= predicted position at time k

By use of the Z transform, the above difference equations can be used to characterize the transfer functions

$$G_x(Z)= \frac{Z[\alpha Z+(\beta-\alpha)]}{Z^2-(2-\alpha-\beta)Z+(1-\alpha)} \tag{3.6}$$

$$G_x(Z)= \frac{\dot{\bar{X}}(Z)}{U(Z)} = \frac{\beta Z(Z-1)}{Z^2-(2-\alpha-\beta)Z+(1-\alpha)} \tag{3.7}$$

In the design of these sampled data trackers, one must compromise between the conflicting requirements of good noise smoothing (long time constant, narrow bandwidth) and of good maneuver following (short time constant, wide bandwidth). Some compromise is always required. However, the smoothing equations should be constructed so as to give the "best" compromise. In order to do this, we must define what is meant by "best". T.R. Benedict and G.W.Border [3] have approached the problem of extending the deterministic α-β filter to include noise considerations.

Their method is to select perfectly freely the impulse response, $g_x(k)$, so as to minimize the scalar cost function

$$J=K_x(0)+\lambda D_x^2 \tag{3.8}$$

$K_x(0)$ and D_x^2 are performance measures for noise smoothing and maneuvering following respectively, where

$$K_x(0)=\frac{\text{steady state variance in position output}}{\text{variance in raw position input}} \tag{3.7}$$

$$D_x^2=\sum_{n=0}^{\infty}[(\text{unit increment ramp})-(\text{position ramp response})]^2$$

$$=\sum_{n=0}^{\infty}\left[n-\sum_{j=0}^{n} g_x(j)(n-j)\right]^2 \tag{3.10}$$

λ is the Lagrangian multiplier which weights the respective importance placed on noise smoothing versus maneuver following. This procedure has been carried out in reference. [3] The principal result of the development is that the optimal trend-following algorithm (in the sense of minimizing the scalar cost function), taken from the entire class of fixed parameter, linear, discrete-time operations is second order. In particular, the minimization results in

$$G(Z)=\frac{Z[(1-Z_1Z_2)Z+(2Z_1Z_2-Z_1-Z_2)]}{(Z-Z_1)(Z-Z_2)} \tag{3.11}$$

where

$$z_{1,2} = \frac{2-\alpha-\beta \pm j\sqrt{4\beta-(\alpha-\beta)^2}}{2} \tag{3.12}$$

Note that the pole-zero structure of the optimal tracker and the α-β tracker are identical. The loci of poles for the optimal tracker as λ is varied will be identical with the loci for the α-β tracker if and only if

$$\beta=\alpha^2/(2-\alpha) \tag{3.13}$$

This does not specify the optimum value of the single remaining parameter α. The choice of $\beta=\alpha^2/(2-\alpha)$ is essentially one of damping factor while the choice of α is one of bandwidth. Thus for a system with a given bandwidth, the choice $\beta=\alpha^2/(2-\alpha)$ optimizes the transient performance.

As stated, the above results of reference [3] do not indicate the value of α which should be selected in a particular situation. This selection must depend upon the system application where the relative importance of $K_x(0)$ and D_x can be ascertained. C.C. Schooler in reference [4], for the exact state model under consideration, has shown the smoothing parameters α and β to be related to the Kalman filter gains when the process and measurement noise statistics are gaussian. In particular, he has shown

$$\alpha(k)=K_1(k) \tag{3.14}$$

where

$K_1(k)$ = 1st element of Kalman gain matrix

For each of the vehicle classes and for selected values of measurement noise variances, the fixed parameter $\alpha=\beta$ filters were run for incremental values of α. In each case α was held constant at the value $\beta=\alpha^2/2-\alpha)$. Figure 3.1 is a plot of α versus average error for a class 1 vehicle with measurement noise variance $\sigma_m^2=50$. This plot is typical of the plots for the other vehicle classed and indicate a band of α in which the average error, $\bar{e}$, is minimum, where

$$\bar{e}= \frac{1}{200} \sum_{k=1}^{200} \left| \bar{x}(k)-p(k) \right|$$

In each case, the steady-state value of the 1st element of the Kalman gain matrix (Kalman filters will be discussed in Chapter 4) is within this band of α within which $\bar{e}$ is minimum. Therefore, for the simulation of the fixed parameter filters in tracking the various vehicle classes under consideration, the value of α was held at the steady state value of the 1st element of the Kalman gain matrix and β was held fixed at $\beta=\alpha^2/(2-\alpha)$.

Selected trajectories for the α-β filters are shown in Figures 3.2 through 3.7. Because of scaling problems, the entire ten seconds of simulation are not shown. Note that the improvement of the smoothed position versus the raw noisy input improves as the measurement noise variance increases.

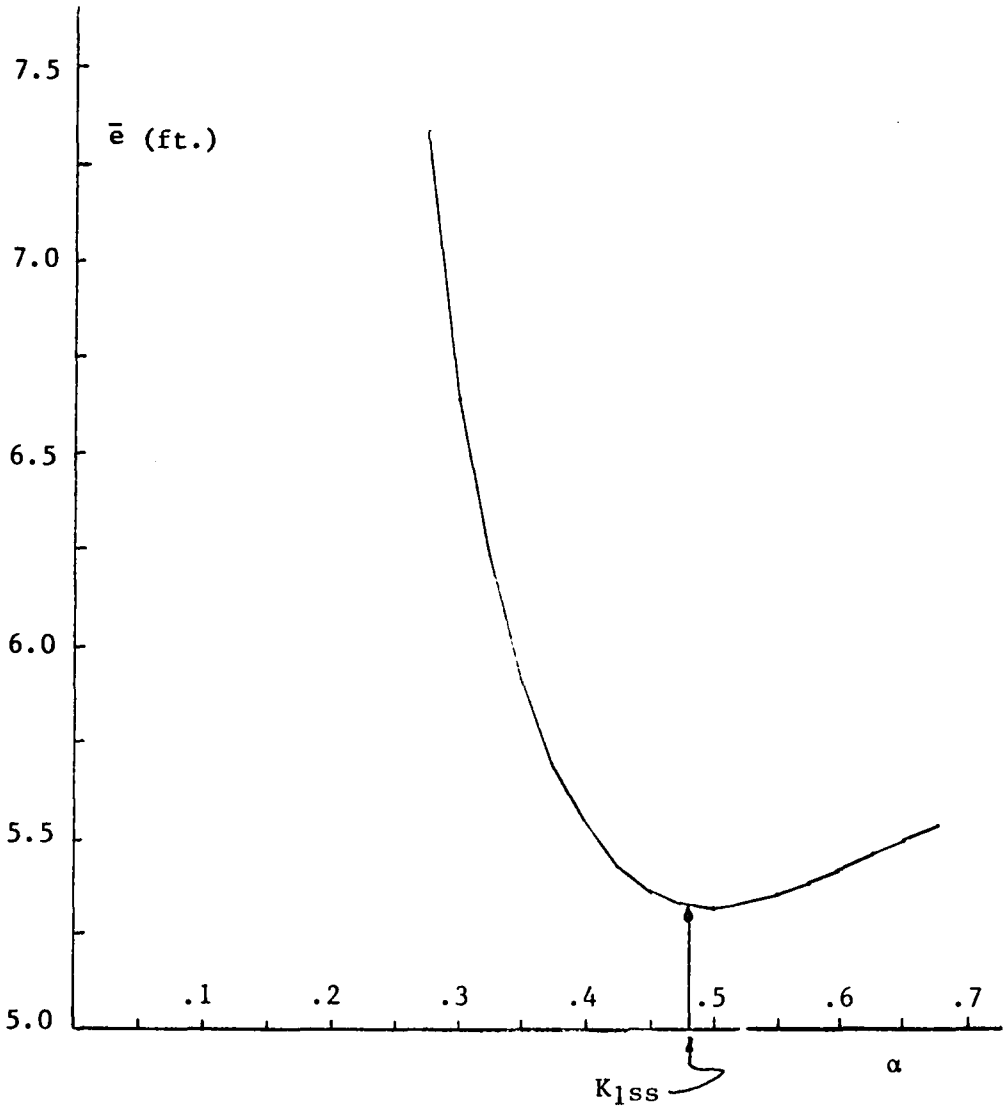

Figure 3.1 Alpha Versus Average Error for Class I vehicle with σ_m^2=50

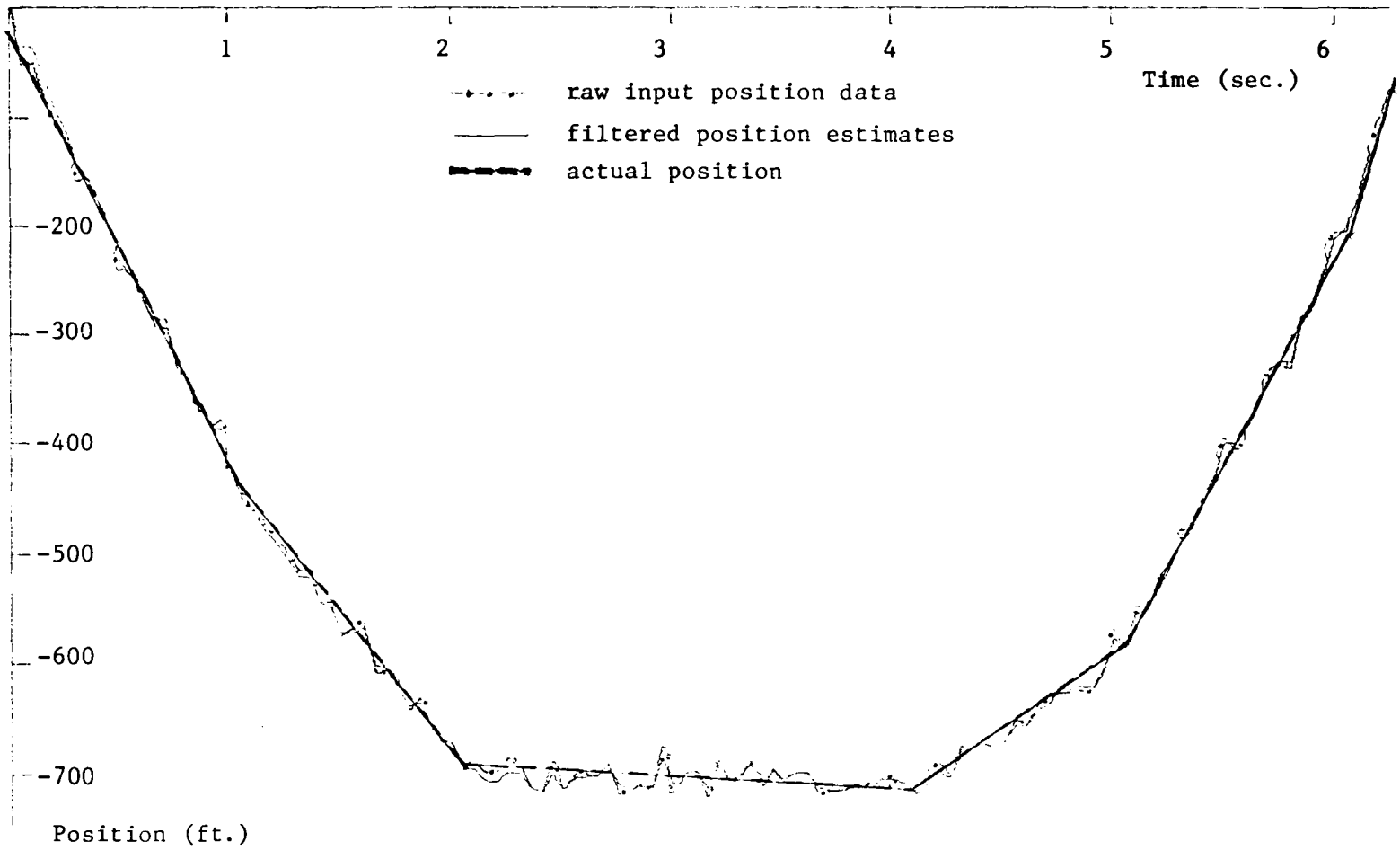

Figure 3.2 Fixed α-β Filter - Class I Vehicle, $\sigma_m^2=100$

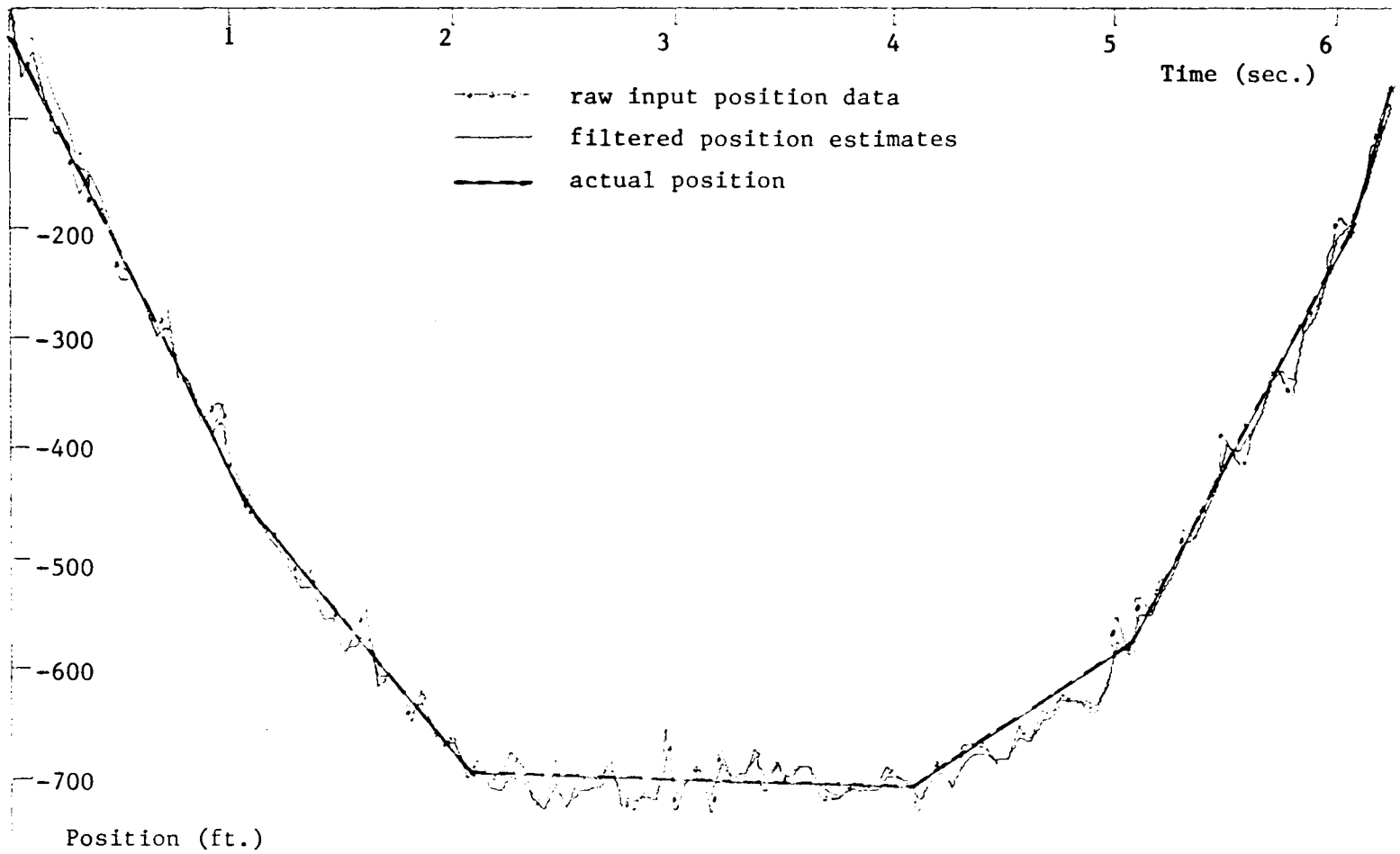

Figure 3.3 Fixed α-β Filter - Class I Vehicle, σ_m^2=300

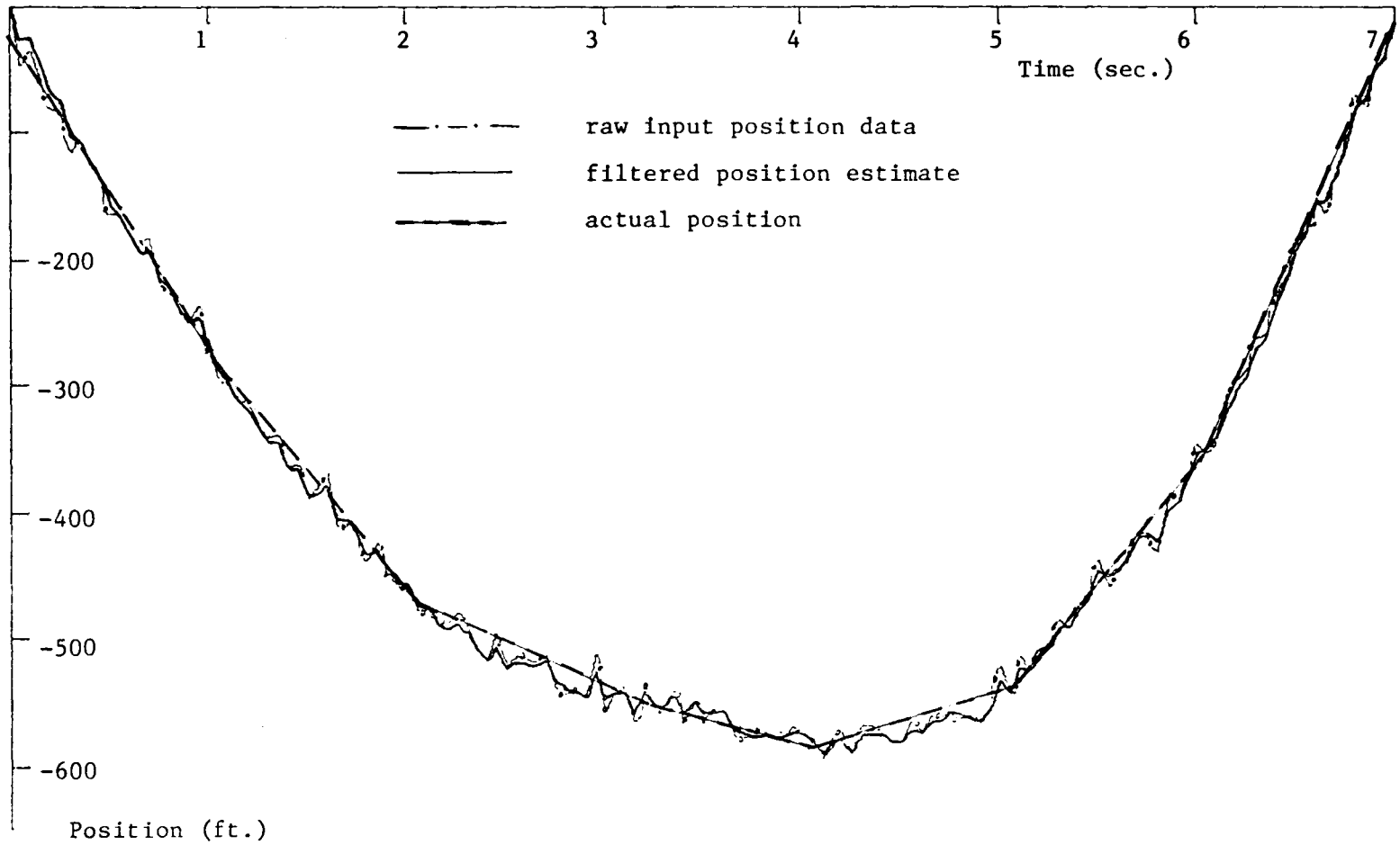

Figure 3.4 Fixed α-β Filter - Class II Vehicle, σ_m^2=100

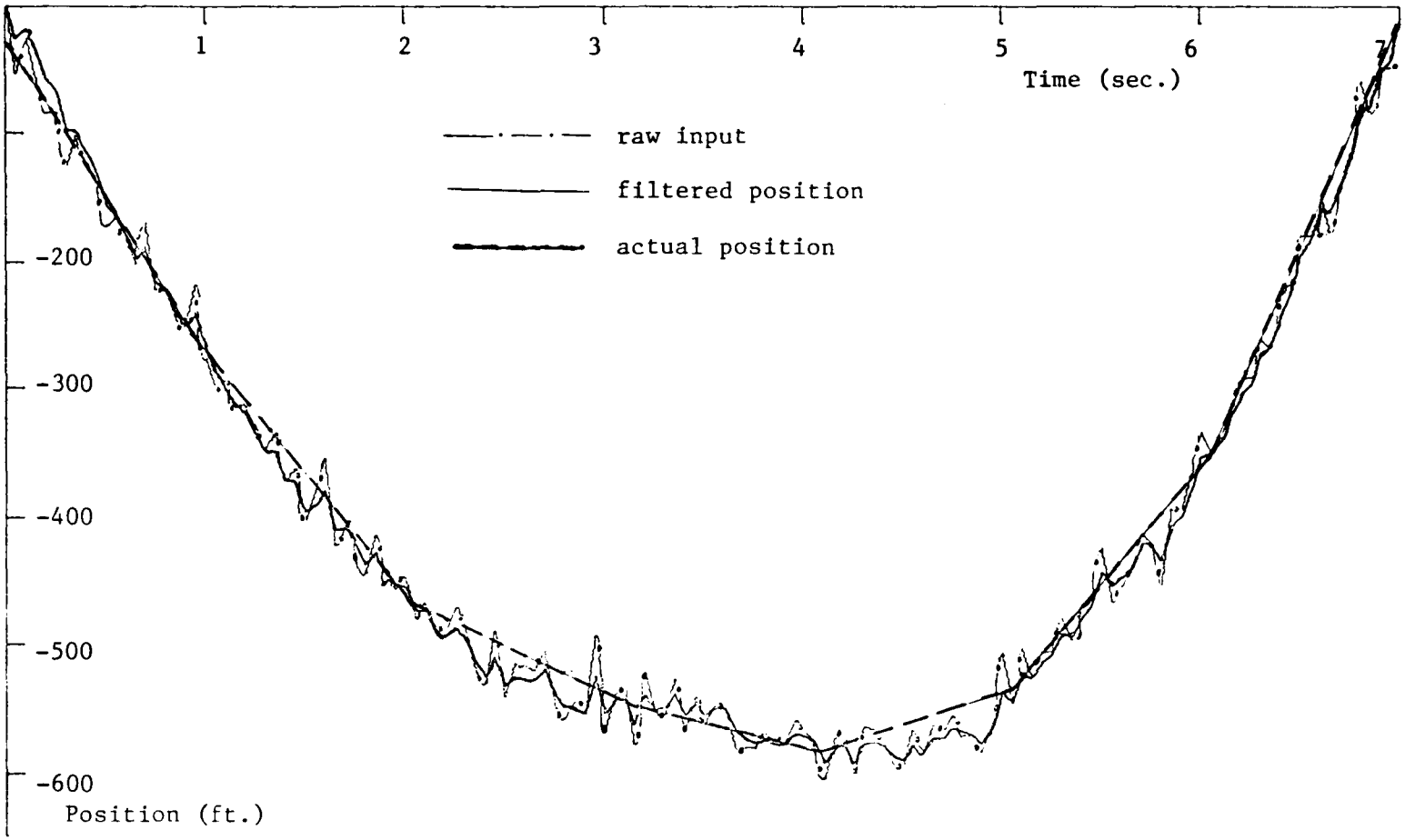

Figure 3.5 Fixed α-β Filter - Class II Vehicle σ_m^2=300

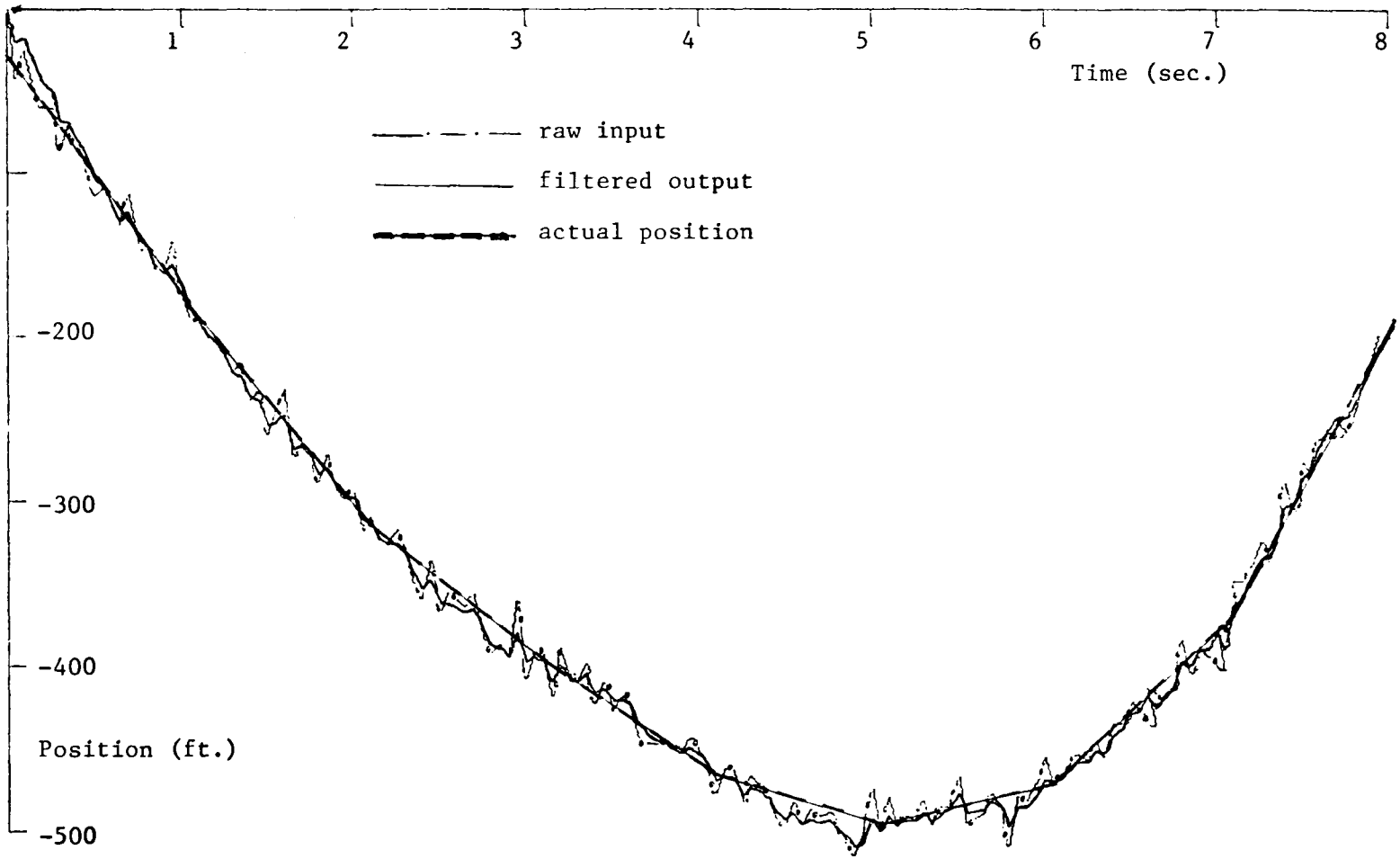

Figure 3.6 Fixed α-β Filter - Class III Vehicle $\sigma_m^2=100$

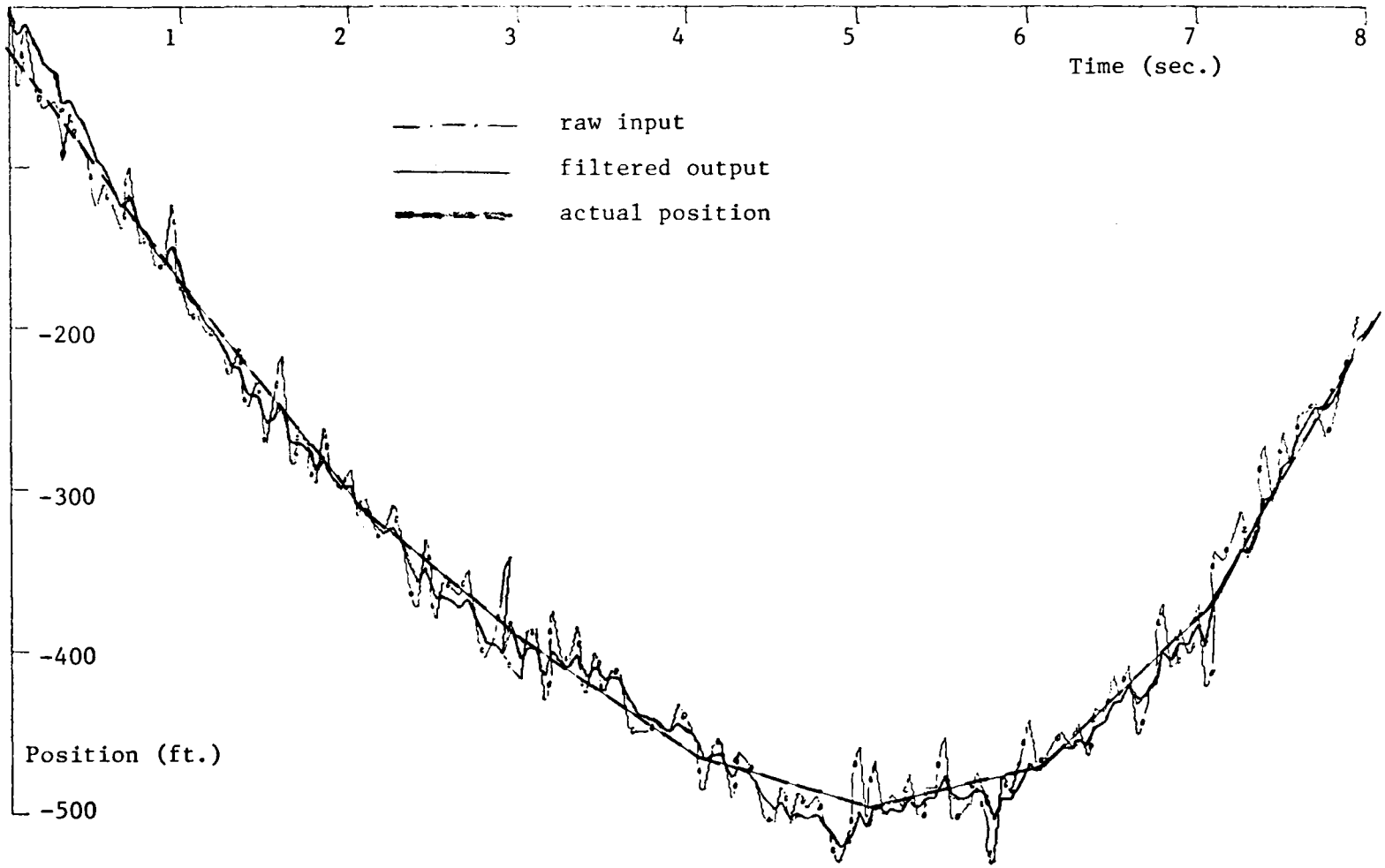

Figure 3.7 Fixed α-β Filter - Class III Vehicle σ_m^2=300

3.2 The Double α-β Filter

Section 3.1 presented an approach for optimizing the fixed parameter α-β filter. The optimization approach was to choose β to optimize the transient performance for a given α and to choose α to optimize the system bandwidth. This section investigates the use of a double α-β filter composed of two independent α-β filters of different bandwidth. Discrimination between the smoothed output of the wideband versus narrowband filters may yield improved estimates in the tracking problem.

An ideal double α-β filter would incorporate a narrowband, small α, filter which would show improved smoothed position estimates in the linear, constant velocity regions while performance following a maneuver would show considerable degradation. Increased maneuver detection would be gained by the use of estimates obtained from a second, wideband, α-β, filter. Once a maneuver had been detected via information of the wideband filter, the narrowband filter would be reset in some manner to insure the estimates once again track the appropriate constant velocity trajectory.

Figure 3.8 shows the frequency response of the fixed parameter α-β filter for various values of α with $\beta=\alpha^2/(2-\alpha)$. It is seen that the filter bandwidth is increased as α is increased from 0 to 1 with α=1 corresponding to an all pass filter (i.e.,no filtering). The narrowband filter must have a bandwidth which includes frequencies associated with the appropriate input accelerations but will eliminate much of the high frequency measurement noise.

It is shown in section 4.2 that the accelerations can be considered

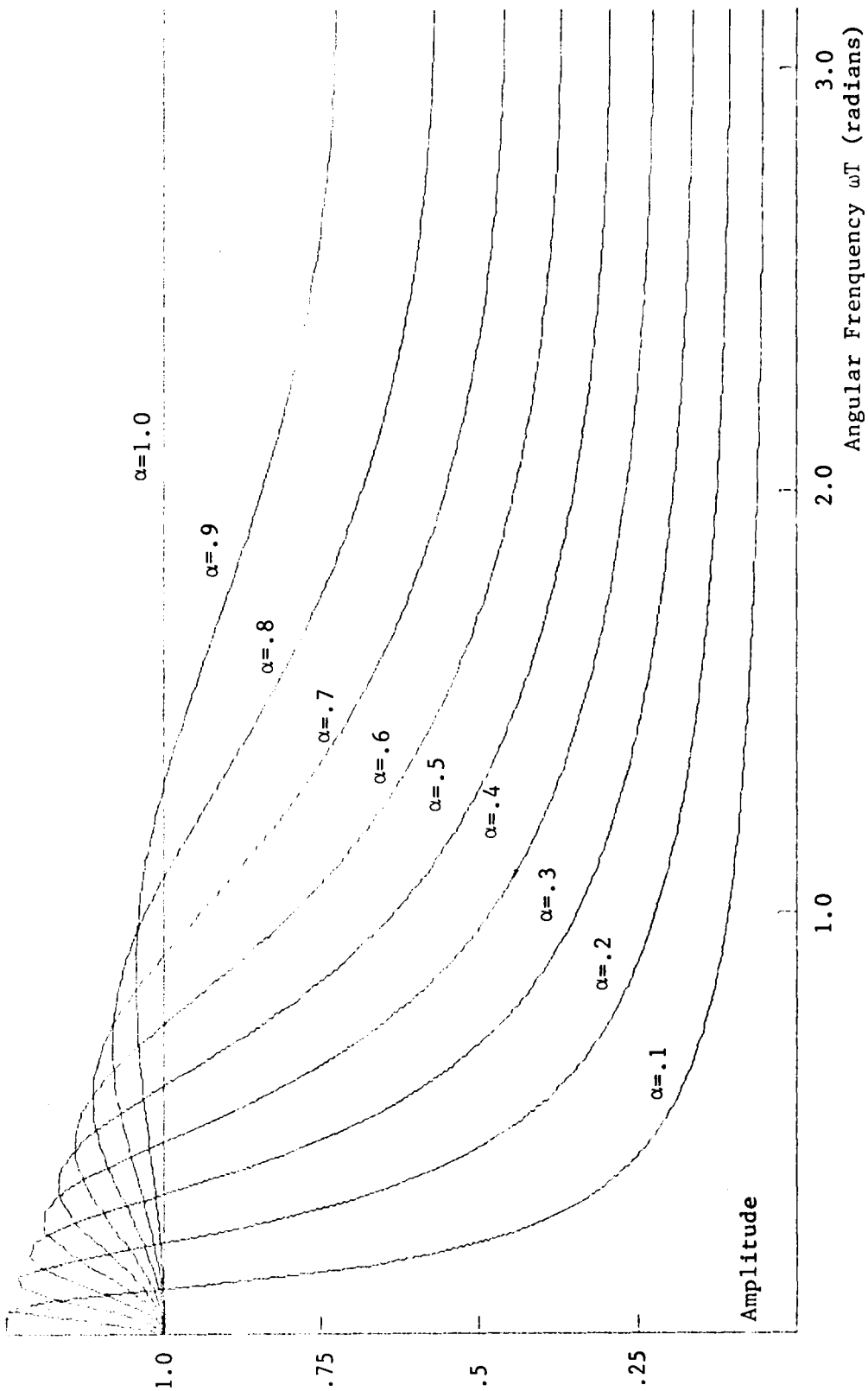

Figure 3.8 Frequency Response of the Fixed α-β Filter

as outputs of a linear filter, H(s), driven by an appropriate white noise. It is shown that

$$H(s)=\frac{1}{s+\gamma} \tag{3.15}$$

where γ=correlation coefficient of accelerations. The corresponding frequencies associated with the discrete time acceleration sequence are therefore within the band of γT radians. With T=.05 and the correlation coefficients of 2.5, it is seen that the frequencies associated with the maneuvers are within the bandwidth of the α=.1 filter. Sample trajectories of two fixed parameter α-β filters, with α_1=.1 and α=.6, are shown in Figure 3.9 for a class 1 vehicle with σ_m^2=50. It is seen that the α=.1 filter provides superior noise smoothing and would provide superior estimates if it could be reset to follow the appropriate straight line path. The problem of the double α-β filter then lies in the resetting procedure.

The flow diagram for the simulation of the double α-β filter with no resetting is shown in Figure 3.10. The variables x_1 and x_2 represent the states of the narrowband α-β filter and x_3 and x_4 represent the corresponding states of the wideband filter. The filters are of the exact same form, therefore the following state model is applicable to each.

$$\begin{aligned} \underline{x}_F(k+1) &= \Phi_F \underline{x}_F(k)+\Gamma_F u(k) \\ y_F(k) &= H_F \underline{x}_F(k)+D_F u(k) \end{aligned} \tag{3.16}$$

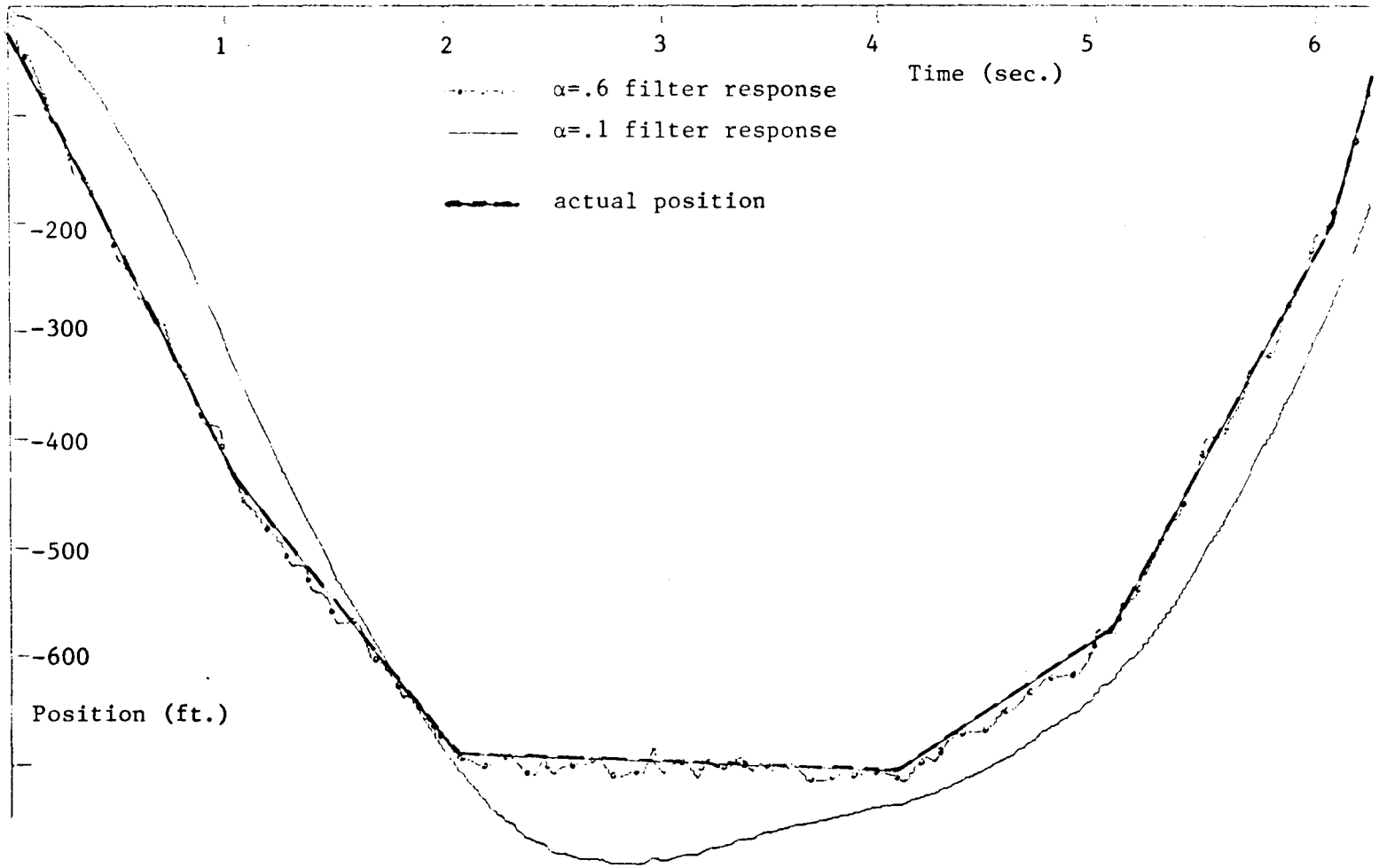

Figure 3.9 Wideband versus Narrowband Response of a Fixed α-β Filter, Class I Vehicle, $\sigma_m^2=50$

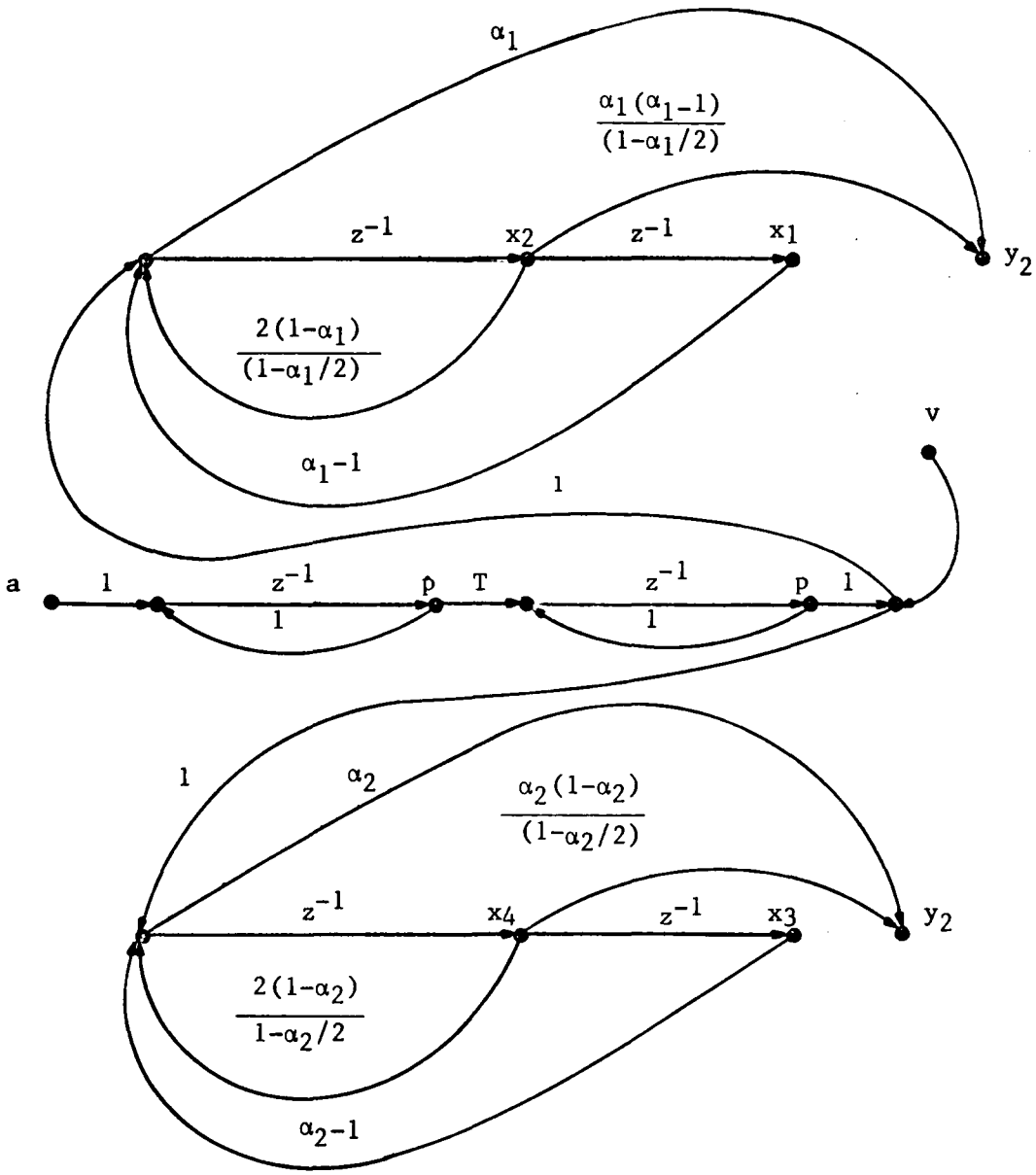

Figure 3.10 Flow Diagram for Simulation of Double α-β Filter

where

$\underline{x}_F(k)$= filter states at time k

$y_F(k)$=filter smoothed position at time k

u(k)= noisy position input at time k

and

$$\Phi_F=\begin{bmatrix} 0 & 1 \\ \alpha-1 & \frac{2(1-\alpha)}{1-\alpha/2} \end{bmatrix}, \quad \Gamma_F=\begin{bmatrix} 0 \\ 1 \end{bmatrix} \tag{3.17}$$

$$H_F=\begin{bmatrix} \alpha(\alpha-1) & \frac{\alpha(1-\alpha)}{1-\alpha/2} \end{bmatrix}$$

$$D_F=\alpha$$

Since the filters are of identical form, subscript 1 will indicate the matrices corresponding to the narrowband filter. Likewise, subscript 2 will indicate matices associated with the wideband filter.

In the system of Figure 3.10, when a maneuver detection occurs, states x_1 and x_2 must be reset via information obtained from filter #2(i.e., x_3,x_4, and y_2). In an analogous continuous time filter, at the time of maneuver detection, one would set the outputs and their derivatives equal (i.e.,$y_1(t)=y_2(t)$ and $\dot{y}_1(y)=\dot{y}_2(t)$) in order to obtain new state values of filter #1 in terms of the states of filter #2. In the discrete-time situation, the states of filter #1 may be reset by requiring

that the outputs of the filters be equal for two consecutive sample instants. For example, if a maneuver is detected at time k, we may set

$$y_1(k)=y_2(k)$$

$$y_1(k+1)=y_2(k+1) \tag{3.18}$$

This procedure leads to the resetting relation

$$\underline{x}_{1F}(k)=\left[\begin{matrix}H_1\\ \underline{H}_1\underline{\Phi}_1\end{matrix}\right]^{-1}\left\{\left[\begin{matrix}H_2\\ \underline{H}_2\underline{\Phi}_2\end{matrix}\right]x_{2F}(k)+(H_2-H_1)\Gamma u(k)+(D_2-D_1)u(k+1)\right\} \tag{3.19}$$

It is seen that this resetting procedure requires knowledge of the next input. The next input can be extimated from a present position estimate coupled with a present velocity estimate. Comparing equations 3.7 and 3.6, it is seen that the filter transfer function for the smoothed position and smoothed velocity have the same denominator. Therefore, velocity estimates can be obtained from the wideband filter of Figure 3.10 by adding two additional feedforward paths from states x_3 and x_4. Another approach would be to use equations equivalent to 3.19 by working backwards in time by requiring $y_1(k)=y_2(k)$ and $y_1(k-1)=y_2(k-1)$. Such requirements would result in a resetting relation equivalent to 3.19 in which the updated states of the narrowband filter would require the previous input instead of the next input.

The above resetting procedure is analytically sound, however it is

seen empirically to produce poor results. The high frequencey variations on x_3, x_4 and y_2, used to reset the narrowband filter, cause the transient performance of the narrowband filter to perform as poorly after resetting as before. Therefore, a resetting procedure must be devised which will reset x_1 and x_2 based only on information obtained from x_3, x_4 and y_2 at the time of resetting. The final resetting procedure used in these simulations was devised empirically.

Observation of the state trajectories of the wideband filter during tracking indicate that the average ratio x_4/x_3 remains relatively constant within the individual linear regions of the plant's trajectory. Figures 3.11, 3.12 and 3.13 show the average ratio x_4/x_3 as a function of time for each of the vehicle classes. The average ratio, RA, is taken to be the average over a moving window of three consecutive sample times, that is

$$RA(k)=\frac{1}{3}[R(k)+R(k-1)+R(k-2)] \tag{3.20}$$

This averaging process is used to smooth some of the high frequency noise on the trajectory of the ratio $R(k)=x_4(k)/x_3(k)$. The resetting procedure used in these simulations was to require

$$x_2(k)/x_1(k)=RA(k)=x_4(k)/x_3(k) \tag{3.21}$$

whenever a maneuver is thought to be detected. Thoughout these simulations, the bandwidth parameters α were taken as $\alpha_1=.1$ and $\alpha_2=K_{1ss}$ as in section 3.1. With $\alpha_1=.1$, the output equation of 3.16 and the relations of 3.17, 3.20 and 3.21, we have the following resetting relations

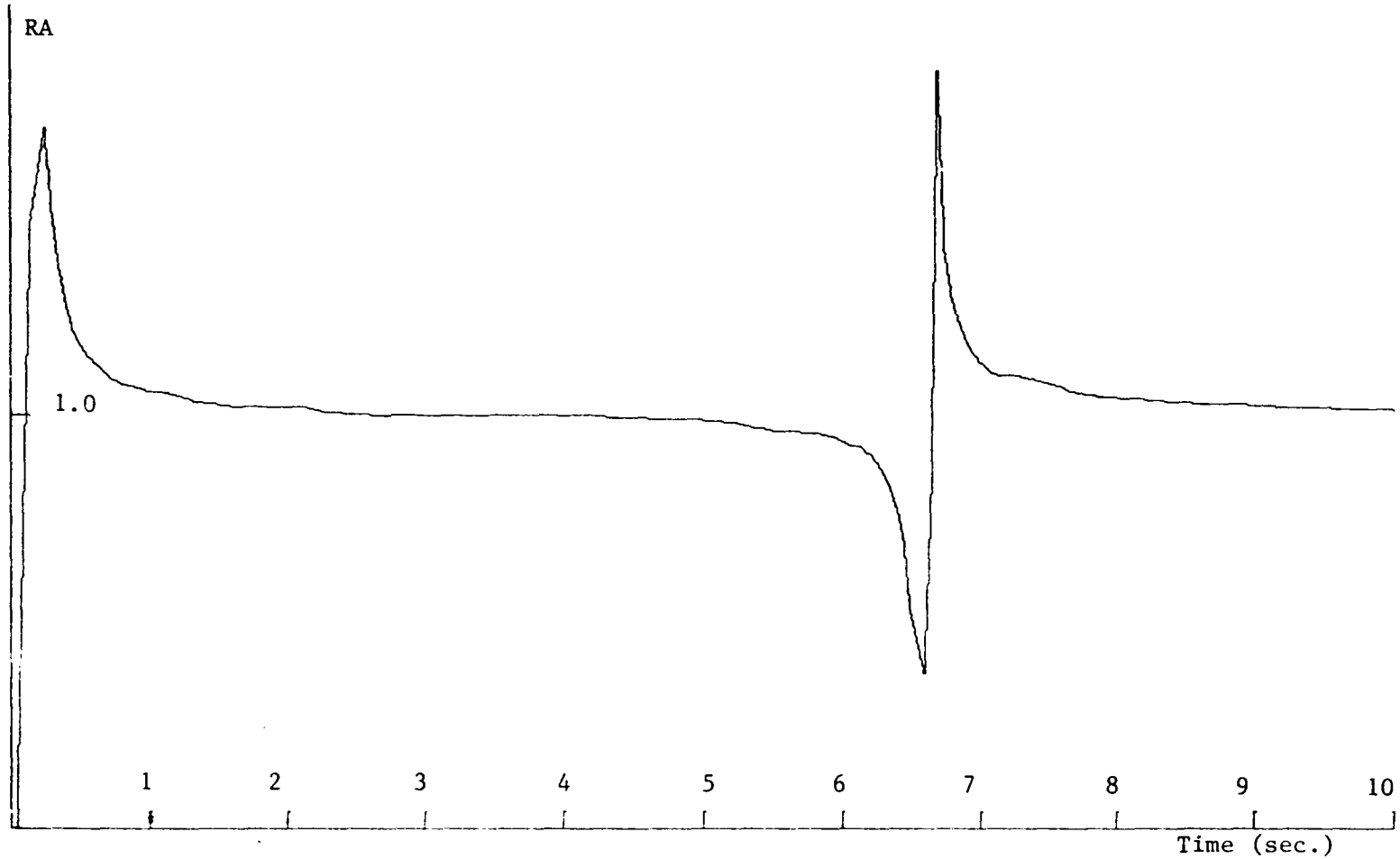

Figure 3.11 Average Ratio x_4/x_3 - Class I Vehicle, $\sigma_m^2=100$

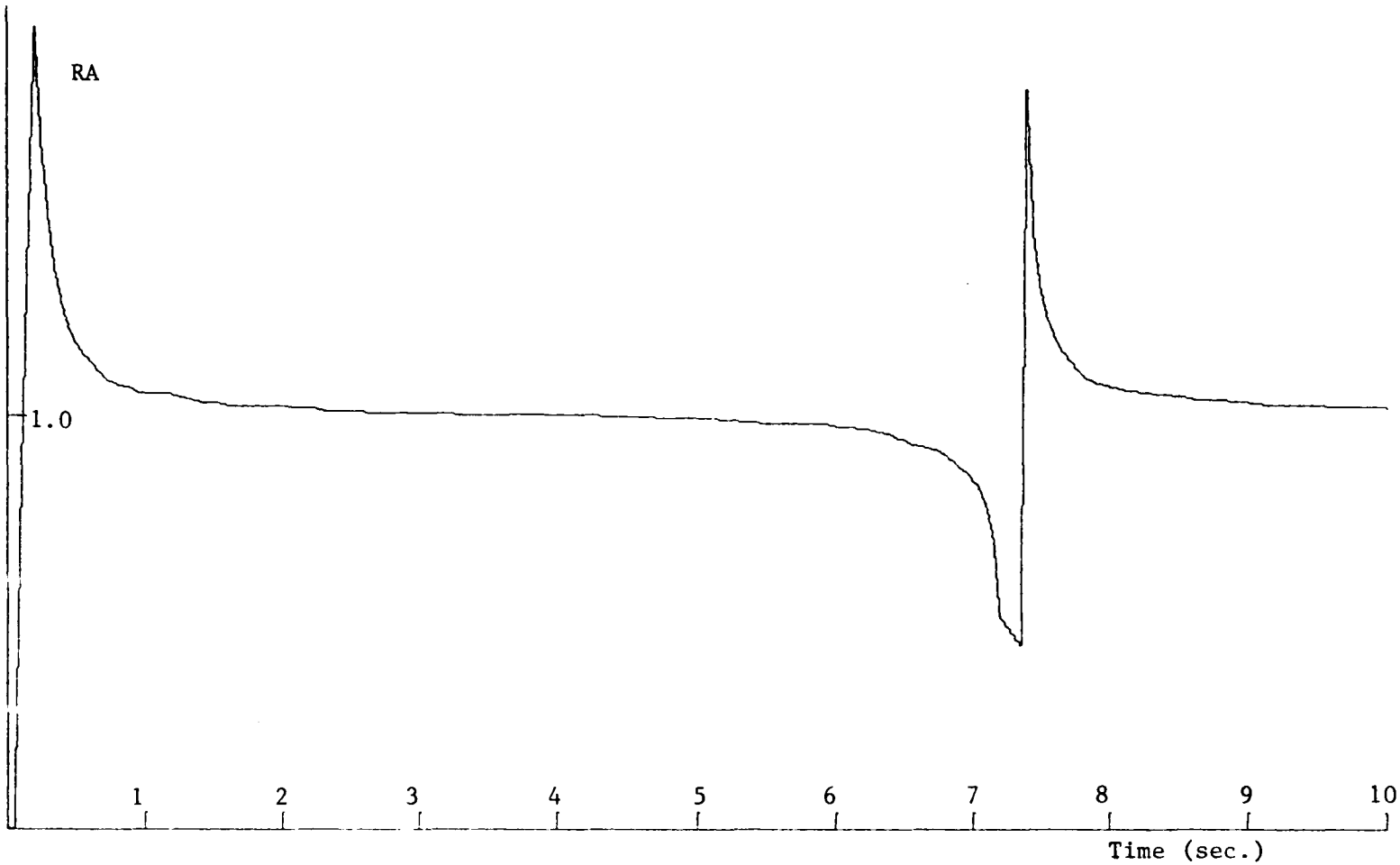

Figure 3.12 Average Ratio x_4/x_3 - Class II Vehicle, $\sigma_m^2=100$

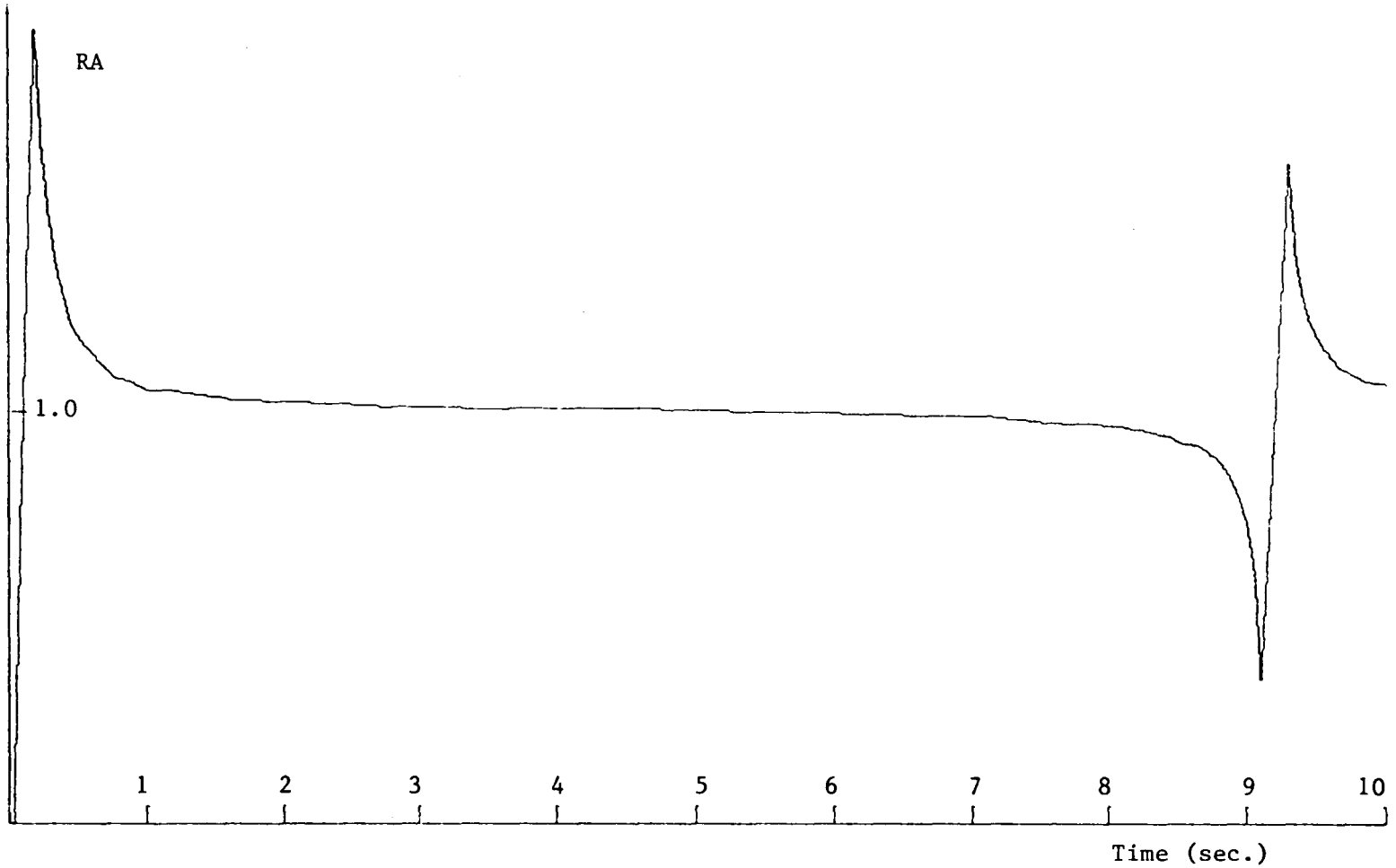

Figure 3.13 Average Ratio x_4/x_3 - ClassIII Vehicle, σ_m^2=100

$$x_1(k) = \frac{y_2(k) - .1u(k)}{.0947RA(k) - .09} \quad , \quad x_2(k) = RA(k)x_1(k) \tag{3.22}$$

This resetting must yield narrowband states with the same signs as their equvalent wideband states. Empirically it is seen that, in general, negative position estimates correspond to negative states and positive position estimates correspond to positive states. The exception to the above statement corresponds to a region around the origin which indicates a change in sign of the position estimate is eminent. In this transition region, the filter states are in the process of changing sign and negative values of R are possible. From 3.22 we see that, except for the transition region, the resetting will produce the proper sign on states x_1 and x_2 whenever

$$RA > .95 \tag{3.23}$$

It is also seen from Figures 3.11 through 3.13 that the region R<.95 corresponds to the transition region. Therefore, the resetting procedure of 3.22 will not work in the neighborhood of the origin when a sign change of position estimate is eminent.

The method of selecting the output of the double filter is based on observations of the estimates of the two α-β filters. For a given measurement noise variance, σ_m^2, 95% of the measurements will be within $2\sigma_m$ of the true position. The smoothed estimates of the wideband filter will have more than 95% of its estimates within $2\sigma_m$ of the true position. Assuming the narrowband filter is properly tracking the trajectory, a

large percentage of the estimates of filter #2 will be within $2\sigma_m$ of filter #1.

The filter output, $\hat{P}$, was selected in the following manner. If the filter output, $y_1(k)$ and $y_2(k)$, differ by less than a given threshold value, ξ, then the narrowband estimate is taken to be the filter output (i.e.,$\hat{P}(k)=y_1(k)$). If the difference is greater than ξ, the filter output is taken to be the wideband estimate and filter #1 is reset, if possible according to 3.22. A flow chart for the simulation of the double α-β filter is shown in Appendix 1. Figures 3.14 and 3.15 show the trajectory estimates of the double α-β filter for a class 1 vehicle, with $\sigma_m=50$, $\xi_1=2\sigma_m$, and $\xi_2=\sigma_m$. With $\xi=2\sigma_m$ it is seen that the filter outputs are choosen as y_1 for more regions than when $\xi=\sigma_m$ and therefore contain better noise smoothing qualities. However, in several regions of improved noise smoothing, the filter estimates contain a bias which grows with time. The result is that the mean squared error over the entire 10 seconds is better when $\xi=\sigma_m$. Therefore, for the remainder of the double α-β simulations, the threshold value was held at $\xi=\sigma_m$. Figures 3.16 through 3.21 show tracking trajectories of the double α-β filter for the various cases. Note that in each case, the estimates of the narrowband filter diverge in the neighborhood of the origin where the resetting procedure is not applicable (i.e.R<.95).

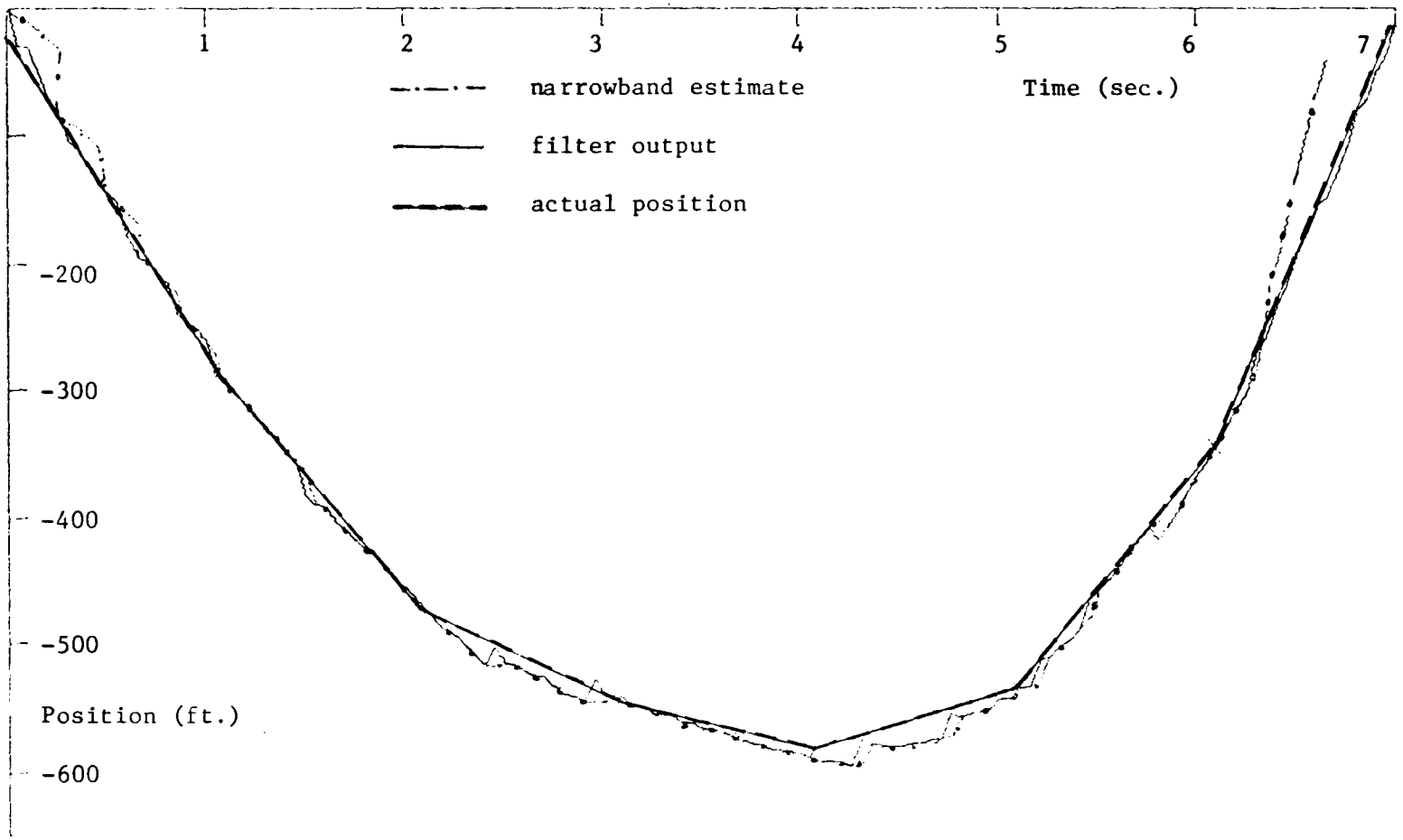

Figure 3.14 Double α-β Filter - Class II, $\sigma_m^2=50$, $\xi=2\sigma_m$

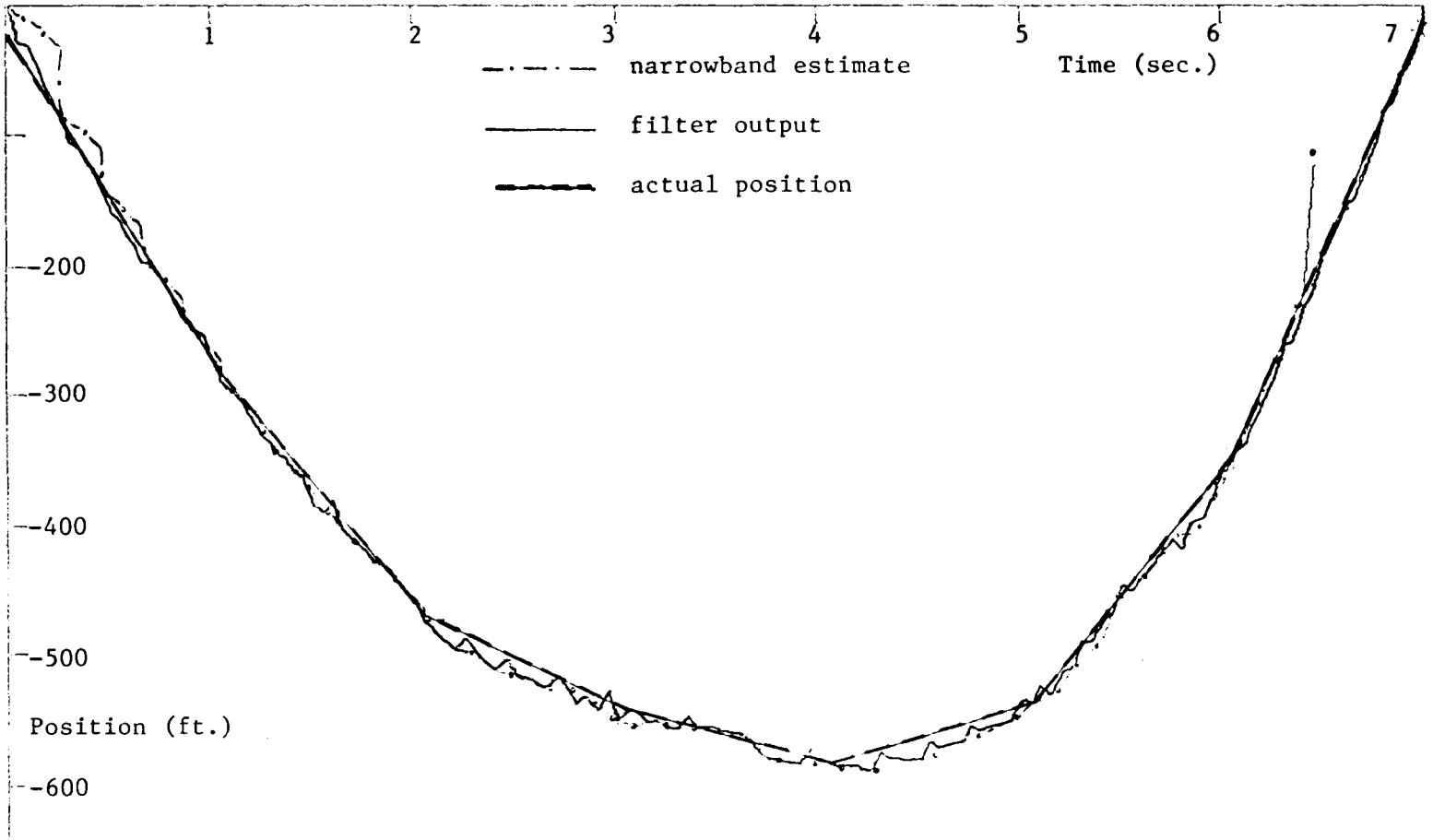

Figure 3.15 Double α-β Filter - Class II, $\sigma_m^2=50$, $\xi=\sigma_m$

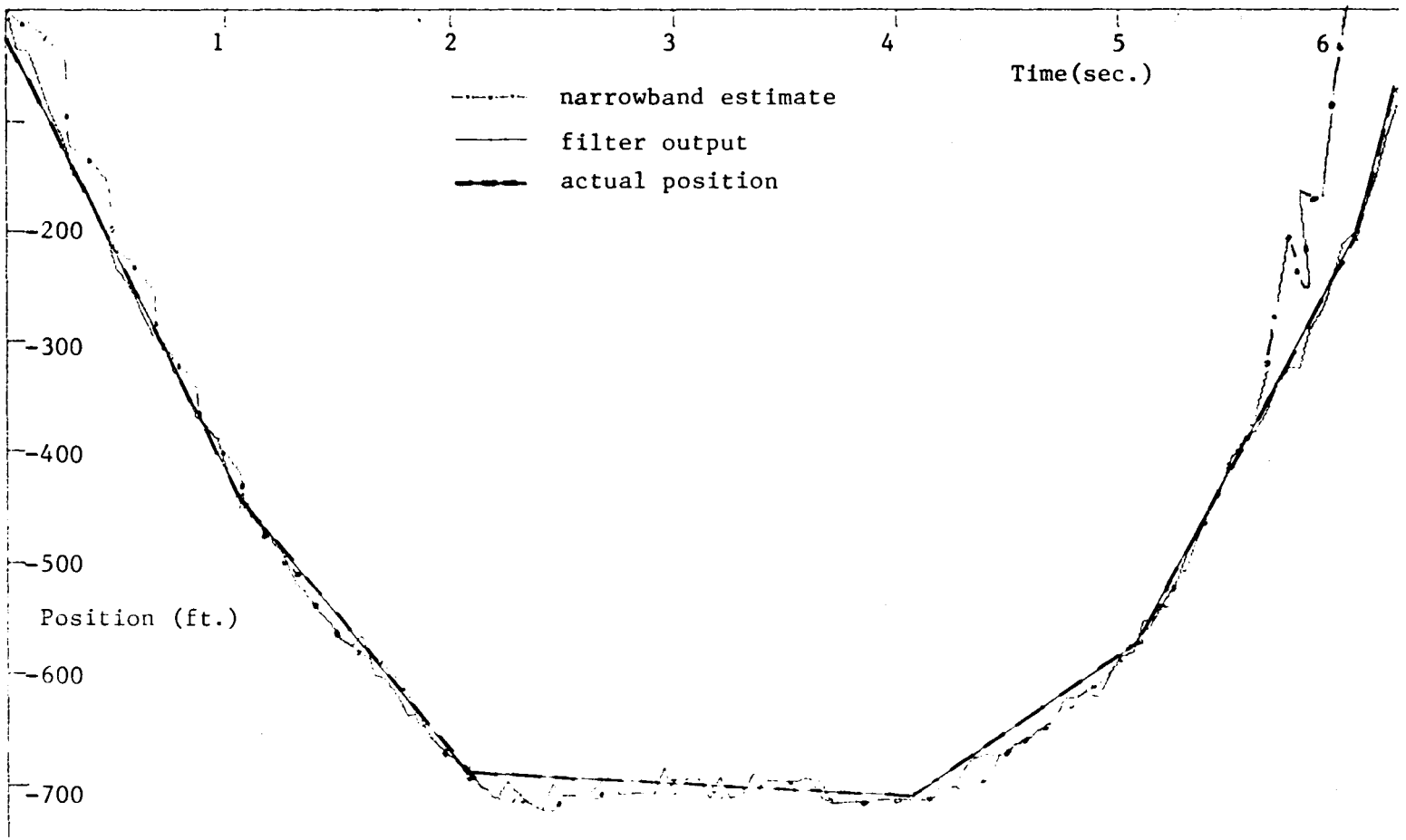

Figure 3.16 Double α-β Filter - Class I, σ_m^2=100

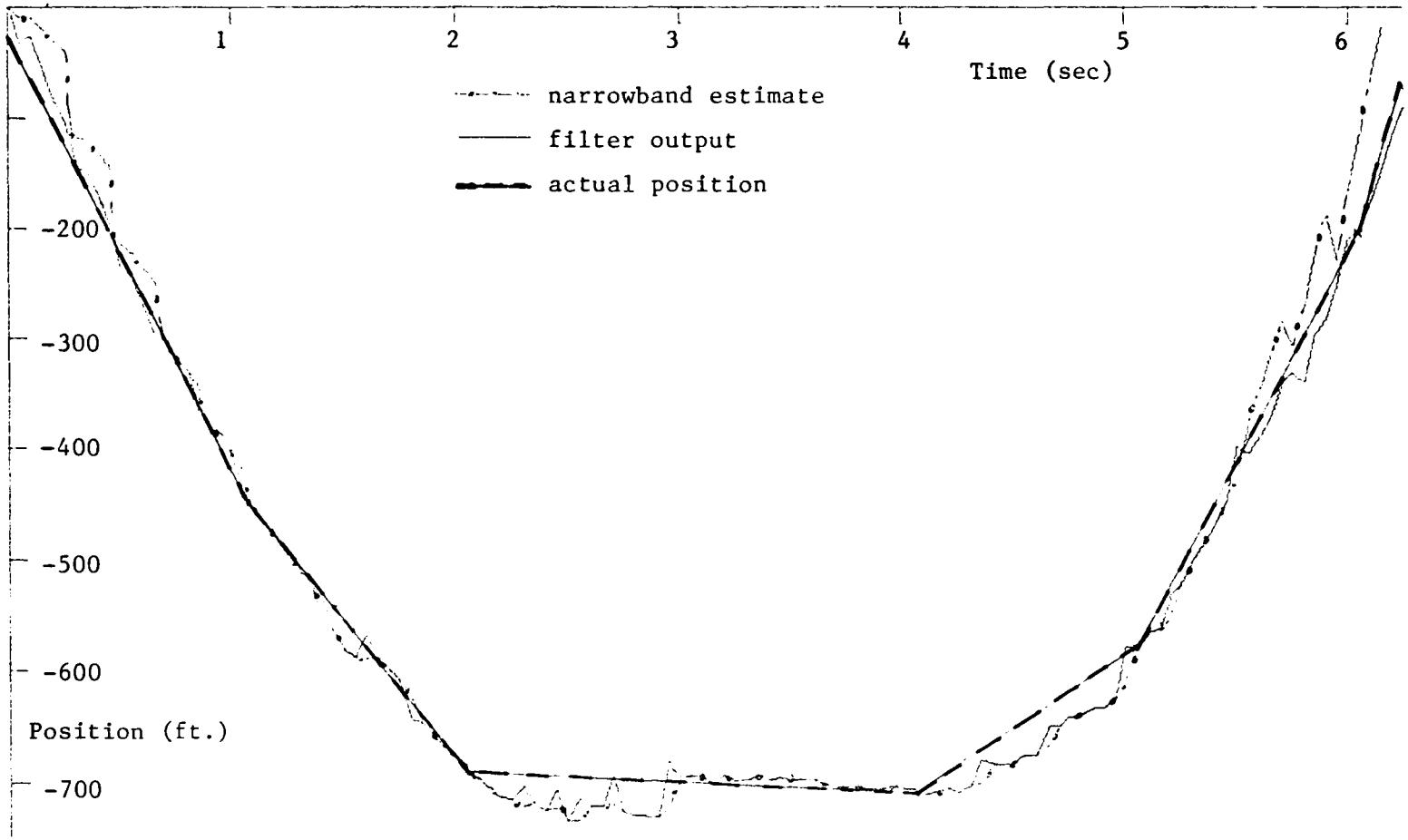

Figure 3.17 Double α-β Filter - Case I, σ_m^2=300

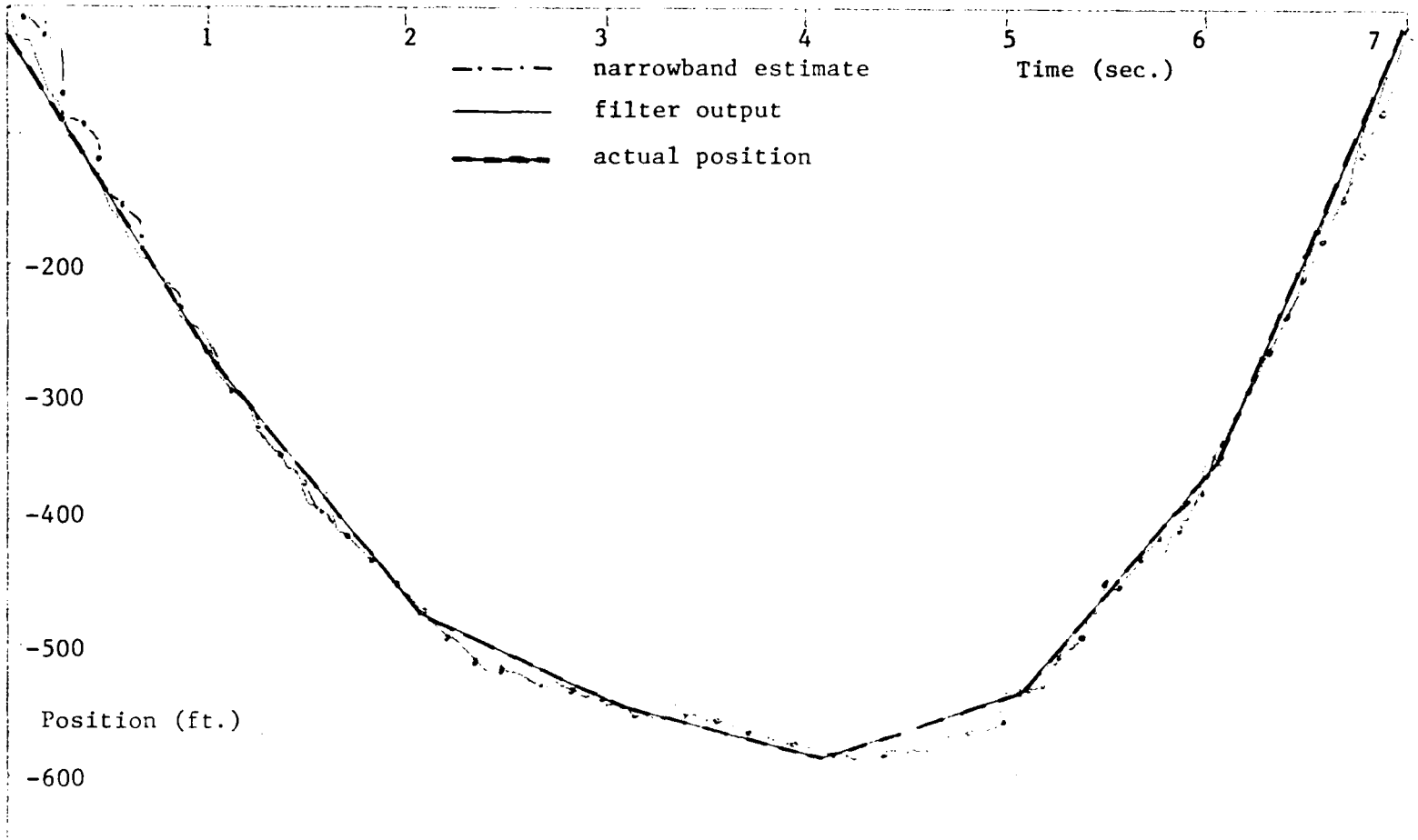

Figure 3.18 Double α-β Filter - Case II, σ_m^2=100

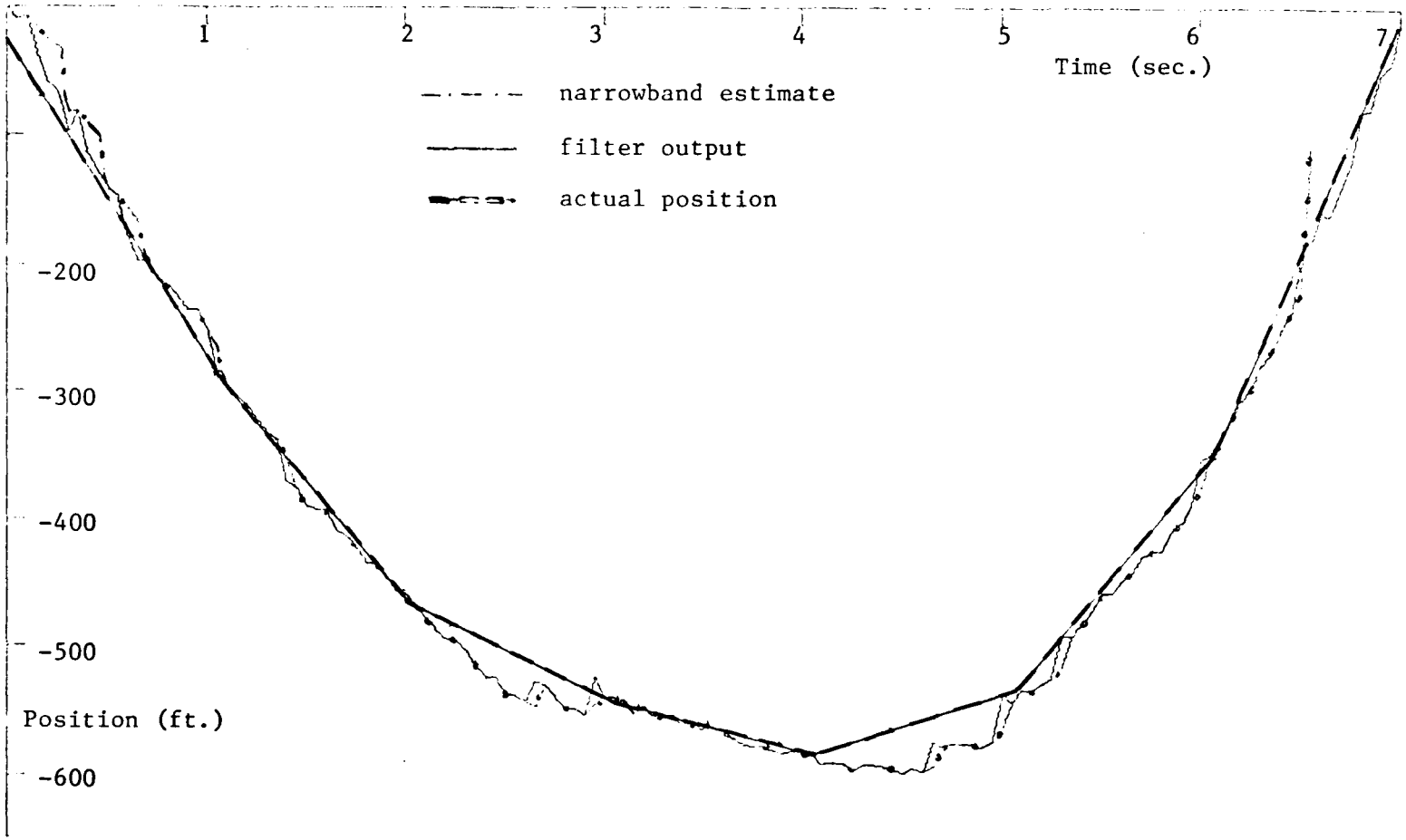

Figure 3.19 Double α-β Filter - Case II, σ_m^2=300

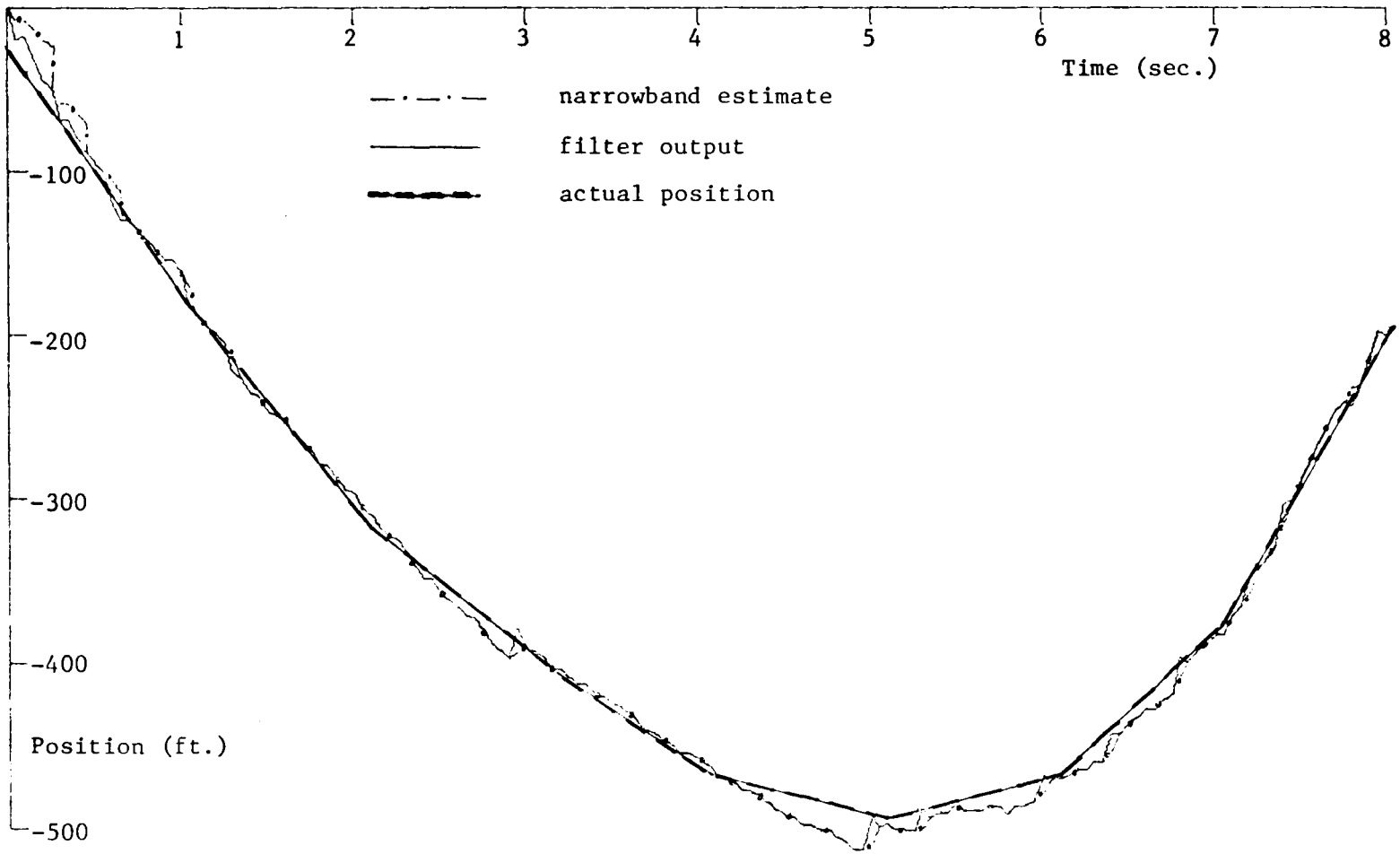

Figure 3.20 Double α-β Filter - Case III, σ_m^2=100

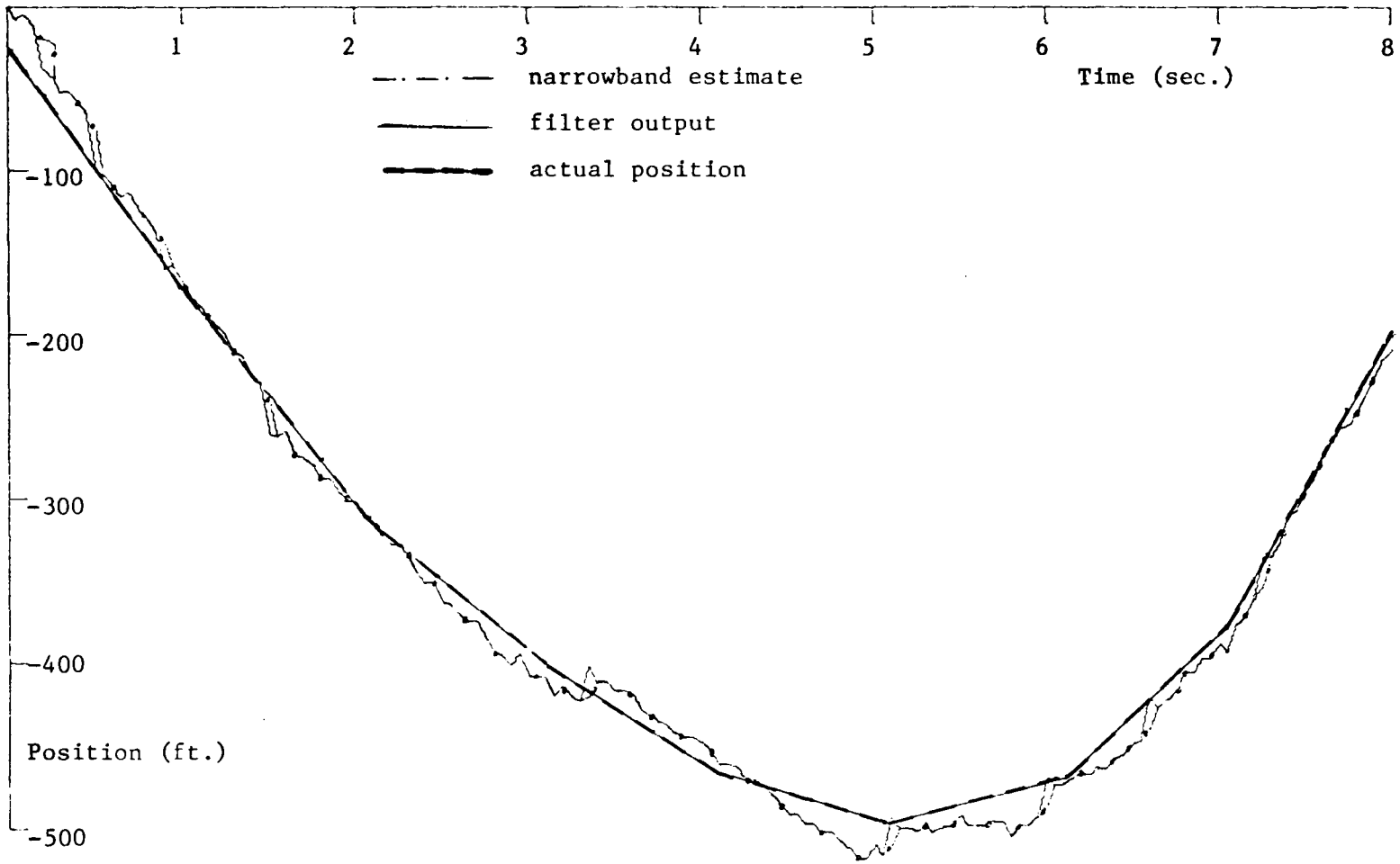

Figure 3.21 Double α-β Filter - Case III, σ_m^2=300

Chapter 4

Kalman Filters

4.1 Second Order Kalman Filter

From Chapter 2 we have the discrete-time plant model for the maneuvering vehicle as

$$\underline{x}(k+1)=\Phi x(k)+\Gamma a(k) \tag{4.1}$$

where

$$\Phi=\begin{bmatrix}1 & T\\ 0 & 1\end{bmatrix}, \qquad \Gamma=\begin{bmatrix}0\\ 1\end{bmatrix}, \qquad T=.05$$

and $a(k)$= input plant acceleration at time k

$$\underline{x}(k)=\begin{bmatrix}x_1(k)\\ x_2(k)\end{bmatrix}$$

$x_1(k)$ discrete position at time k

$x_2(k)$ discrete speed at time k

The output measurement process is

$$z(k)=H\underline{x}(k)+v(k) \tag{4.2}$$

where $H=[1 \quad 0]$

$v(k)$ is a zero mean white gaussian sequence with variance σ_m^2.

The above linear system formulation with process noise and measurement noise statistics known, lends itself to the implementation of the

Kalman filter. The Kalman filter is a linear recursive filter which is well documented in the literature. [12] In a linear system with process and plant noise which can be characterized as white gaussian sequences, the Kalman filter is the optimal filter. With the filter estimates at time k denoted as $\hat{\underline{x}}(k)$, the filter is chatacterized by two important properties. The first property is that the filter error is unbiased (i.e., $E[\hat{\underline{x}}(k)-\underline{x}(k)]=E[\tilde{x}(k)]=0$) and the second property is that it minimizes a weighted scalar sum of the diagonal elements of the error covariance matrix $P(k)=E[\tilde{\underline{x}}(k)^T\tilde{\underline{x}}(k)]$. Thus the estimate resulting from the Kalman filter is an unbiased estimate which minimizes the length of the error vector. [12]

The plant and measurement models are given by equations 4.1 and 4.2 with

$$\begin{aligned} &\underline{x}(0) \sim \text{Normal } (\underline{M},P(0/0)) \\ &a(k) \sim \text{Normal } (0,Q) \\ &v(k) \sim \text{Normal } (0,R) \end{aligned} \tag{4.3}$$

Filter Algorithms

State estimate:

$$\hat{\underline{x}}(k+1)=\Phi\hat{\underline{x}}(k)+K(k+1)[Z(k+1)-H\Phi\hat{x}(k)] \tag{4.4}$$

Prior covariance matrix:

$$P(k+1/k)=\Phi P(k/k)\Phi^T+\Gamma Q\Gamma^T \tag{4.5}$$

Kalman gain matrix:

$$K(k+1)=P(k+1/k)H^T[HP(k+1/k)H^T+R]^{-1} \qquad (4.6)$$

Posterior variance matrix:

$$P(k+1/k+1)=[I-K(k+1)H]P(k+1/k) \qquad (4.7)$$

where $P(k/j)=E[\tilde{x}(k)^T\tilde{x}(k)]$ given measurement data through time j.

The plant model and discrete Kalman filter are shown in Figure 4.1. Equations 4.3 indicate that the Kalman filter expects the initial distribution of the state vector to be normal with mean vector $\underline{M}$ and covariance matrix $E[\underline{x}(0)^T\underline{x}(0)]=P(0/0)$. The same notation applies to the system process and measurement noise (i.e., $E[a(k)]=E[v(k)]=0$ and $Q=E[a^T(k)a(k)]=\sigma_m^2$, $R=E[v^T(k)v(k)]=\sigma_m^2$. An additional requirement on the process and measurement noise sequences is that they be white, gaussian, and mutually uncorrelated (i.e., $E[v(k)v(j)]=E[a(k)a(j)]=E[a(k)v(k)]=0$). For the simulation and filtering of the noisy position data over the range of vechicle classes, the above assumptions hold true except for the assumption that a(k) be a white gaussian sequence. The actual distribution of accelerations is shown in Figure 2.1 and the acceleration sequence is correlated in time according to equation 2.1. Thus, for this simulation, the Kalman filter is suboptimal in the sense that all of the criterion for optimality are not met. The fact that the acceleration sequence is not gaussian is not a serious hinder to the filter performance. In many practical systems in which Kalman filters are performing well, the only things known about the noise are the second order statistics (mean, variance, and autocorrelation) with the

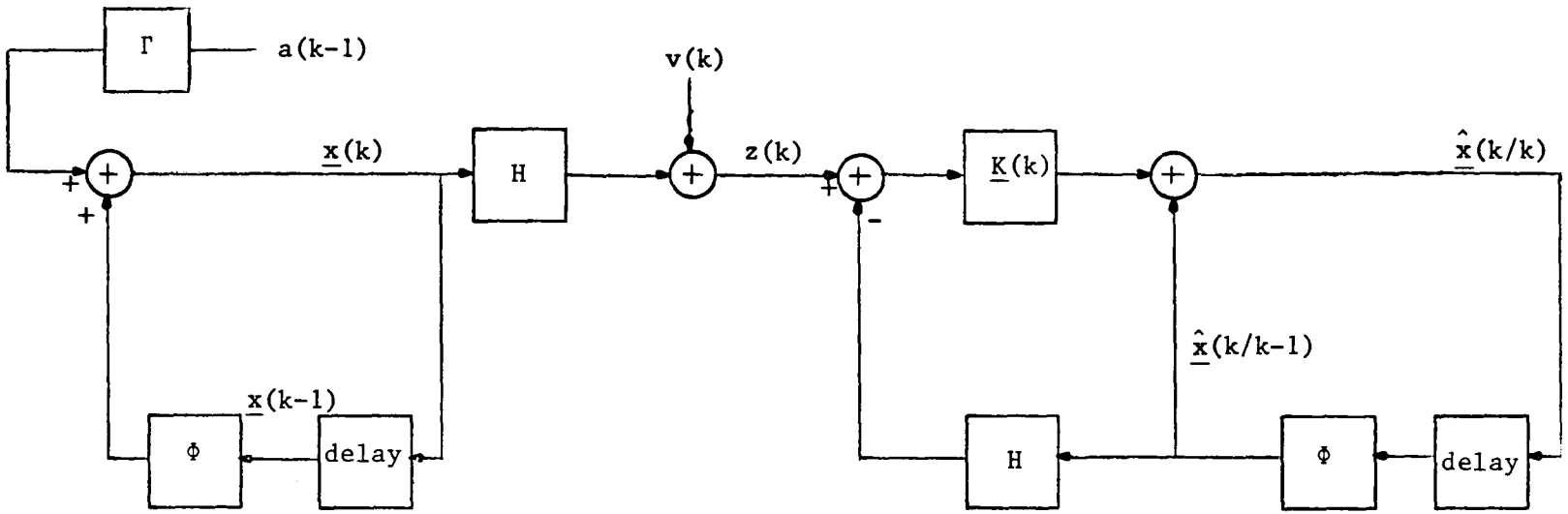

Figure 4.1 System Model and Discrete Kalman Filter

actual distribution being unknown. In such situations, the designer generally looses nothing by assuming a gaussian distribution for the noise. [10] However, assuming a white noise sequence when the noise is actually correlated can, in some cases, lead to suboptimal filter degradation. In the case at hand, it will be seen that the filter yields quite good results, even under the assumption of the acceleration sequence being white. The extension of the Kalman filter to include the correlation information will be discussed in section 4.2.

It is noted that the initial uncertainty of the state distribution must be known in order to initialize the Kalman filter (equation 4.5). In practice, two noisy measurements must be taken in order to aquire an initial estimate of position and velocity with mean $\underline{M}$ and covariance P(0/0). It is shown in appendix C that using this procedure with the system of equations 4.1 and 4.2 with the statistics of 4.3 yields

$$P(0/0) = \begin{bmatrix} \sigma_m^2 & \sigma_m^2/T \\ \sigma_m^2/T & \dfrac{2\sigma_m^2}{T^2} \end{bmatrix} \tag{4.8}$$

In the simulations, the Kalman filters were given a 2-step "head start". The filters were given an initial posterior covariance matrix as determined by equation 4.8 with an initial state estimate satisfying the first of equations 4.3.

4.2 Augmented Kalman Filter

Section 4.1 indicated that the second order Kalman filter is

suboptimal in the sense that the input sequence a(k) is not a white gaussian sequence. It was indicated that correlation of the input sequence, in some cases, could cause considerable filter degradation. This problem can be overcome by using the Wiener-Kolmogorov whitening procedure. [13] For a continuous time process with autocorrelation

$$r(\tau)=\sigma_a^2 e^{-\gamma|\tau|} \tag{4.9}$$

$$R(s)=\mathcal{L}\{r(\tau)\}=H(s)H(-s)W(s)$$

$$=\frac{-2\gamma\sigma_a^2}{(s-\gamma)(s+\gamma)} \tag{4.10}$$

where

$$H(s)=\frac{1}{s+\gamma} \quad \text{and} \quad W(s)=2\gamma\sigma_m^2 \tag{4.11}$$

The quantity H(s) is the Laplace transform of the whitening filter for a(t), and w(s) is the Laplace transform of the white noise w(t) that drives the filter H(s). [1] The input accelerations can then be considered as outputs of a linear filter H(s) which receives as its input white noise with variance $\sigma_w^2=2\gamma\sigma_a^2\delta(\tau)$. For the discrete time simulation, we let w(k) be a zero-mean white noise sequence with distribution as shown in Figure 2.1 with Am replaced by $\sqrt{2\gamma}$Am.

The sequence w(k) is processed through a digital filter with Z transform H(z) where

$$H(Z)=Z\{H(s)\}=\frac{1}{1-e^{-\gamma T}Z^{-1}} \tag{4.12}$$

The flow diagram for the augmented system is shown in Figure 4.2. With the augmented system, new system matrices for use in the Kalman filter (Φ_F,Γ_F, and H_F) can be defined where

$$\Phi_F=\begin{bmatrix} 1 & T & 0 \\ 0 & 1 & 1 \\ 0 & 0 & e^{-\gamma T} \end{bmatrix}, \qquad \Gamma_F=\begin{bmatrix} 0 \\ 0 \\ 1 \end{bmatrix} \tag{4.13}$$

and $H_F=$ [1 0 0]

As in the case of the second order Kalman filter, for simulation purposes, the filter was given a lead start with (Appendix C)

$$P(0/0)=\begin{bmatrix} \sigma_m^2 & \sigma_{m/T}^2 & 0 \\ \sigma_{m/T}^2 & 2\sigma_{m/T}^2 & 0 \\ 0 & 0 & \sigma_a^2[1+e^{-2\gamma}] \end{bmatrix} \tag{4.14}$$

Sample trajectories of both the second order Kalman filter and the augmented Kalman filter are shown in Figures 4.3 through 4.8. Note that the trajectories of the augmented Kalman filter show more variation than the trajectories of the second order Kalman filter. This degradation of the augmented filter is due to the piece-wise linear, constant velocities being tracked. The fact that the accelerations are considered to occur

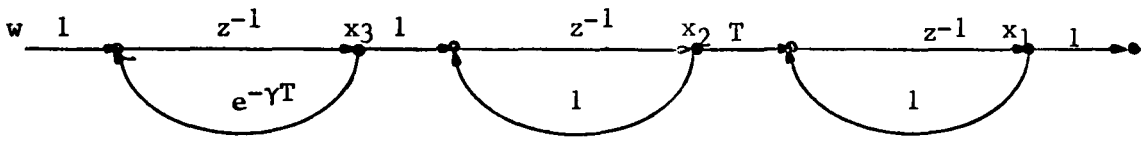

Figure 4.2 Augmented System

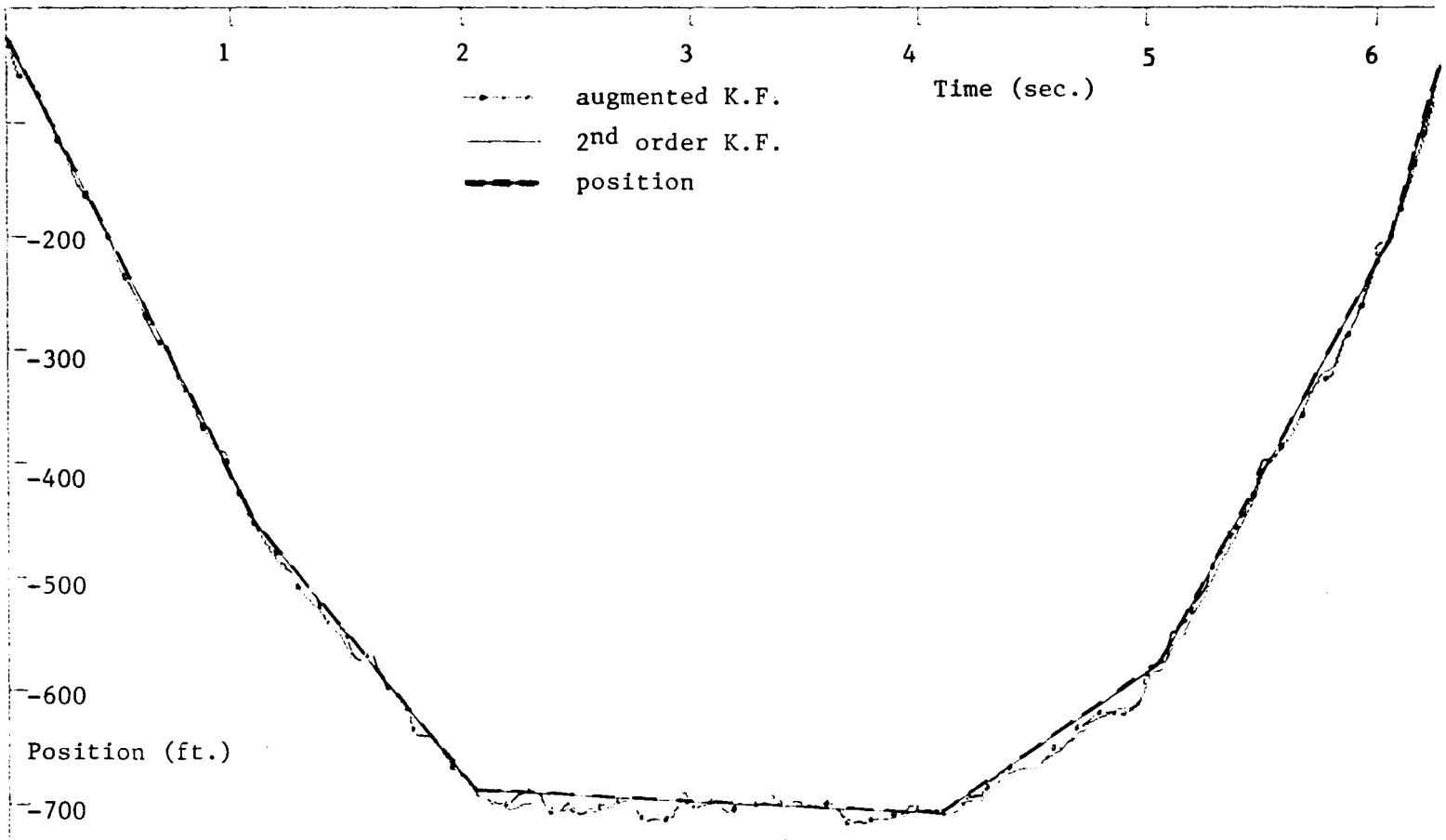

Figure 4.3 Second and Third Order Kalman Filters - Class I, $\sigma_m^2=100$

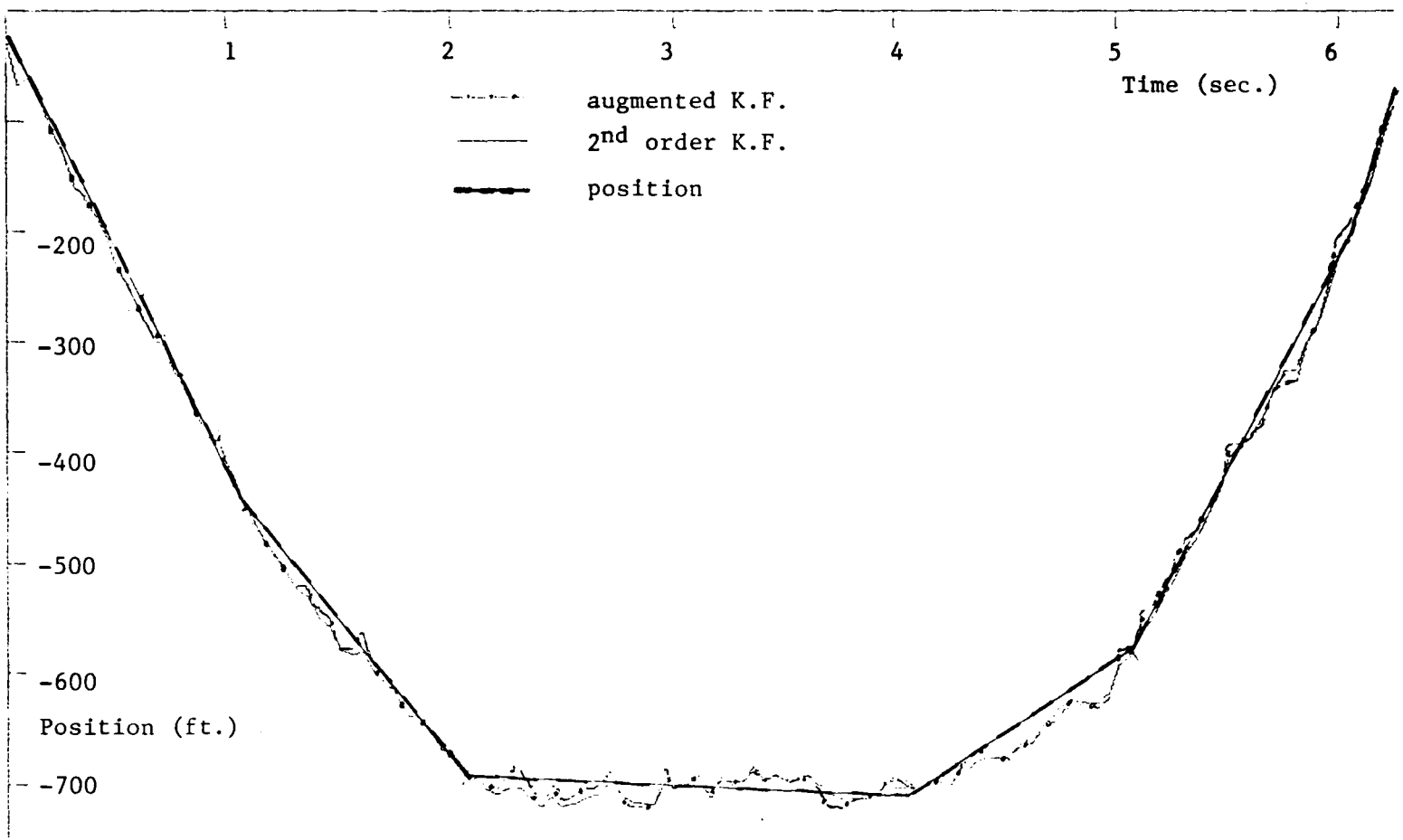

Figure 4.4 Second and Third Order Kalman Filters - Class I, σ_m^2=300

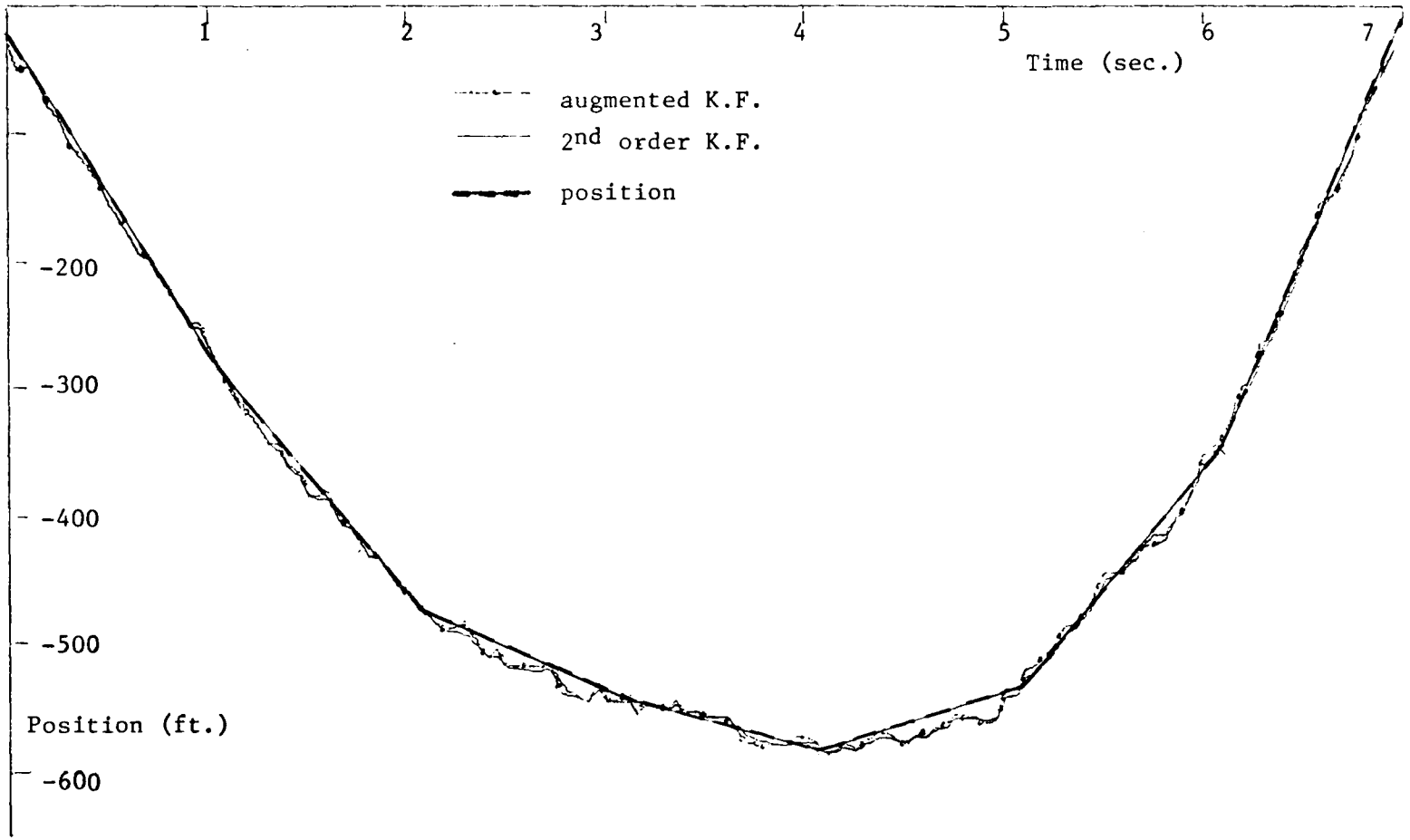

Figure 4.5 Second and Third Order Kalman Filters - Class II, $\sigma_m^2=100$

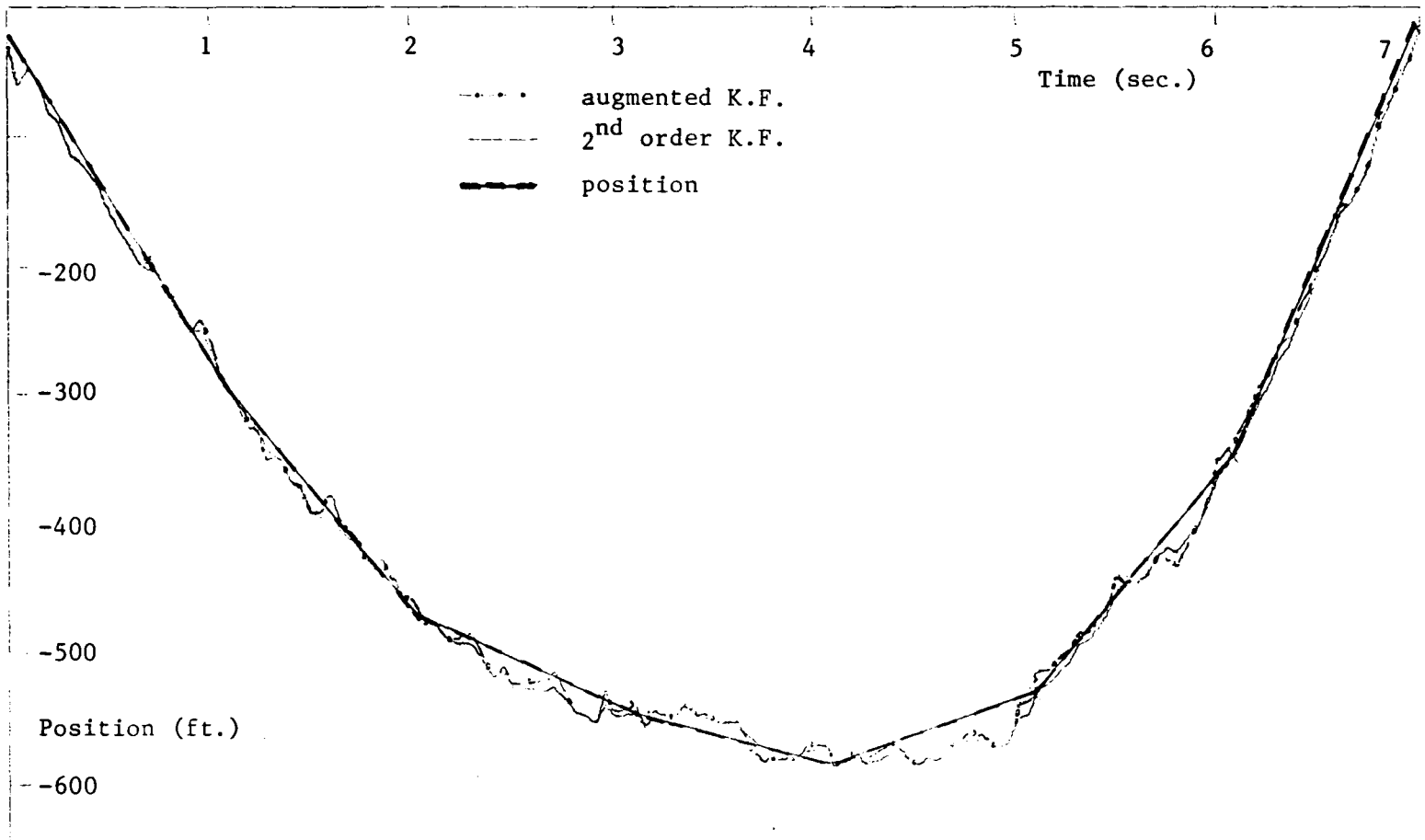

Figure 4.6 Second and Third Order Kalman Filters - Class II, σ_m^2=300

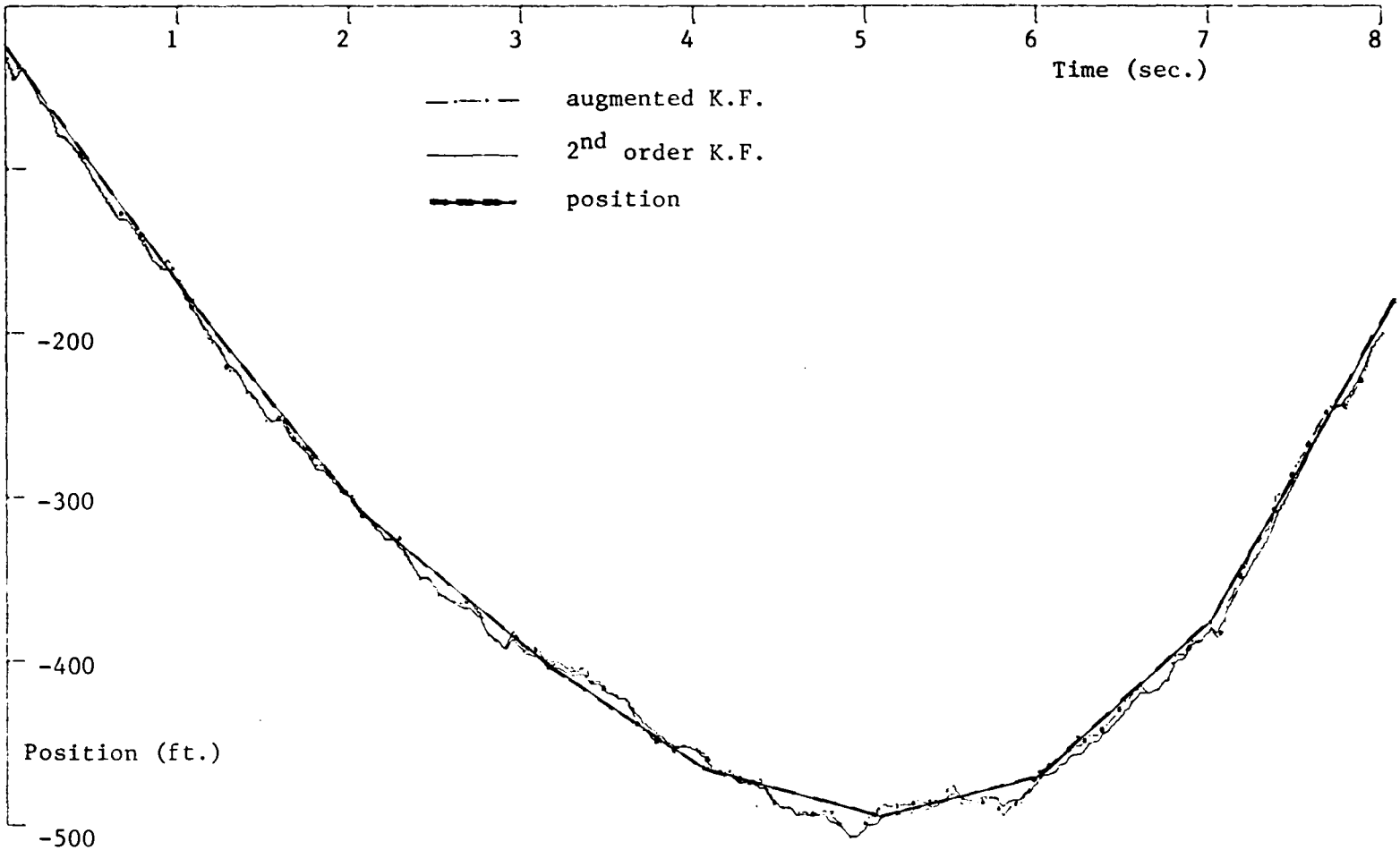

Figure 4.7 Second and Third Order Kalman Filters, - Class III, σ_m^2=100

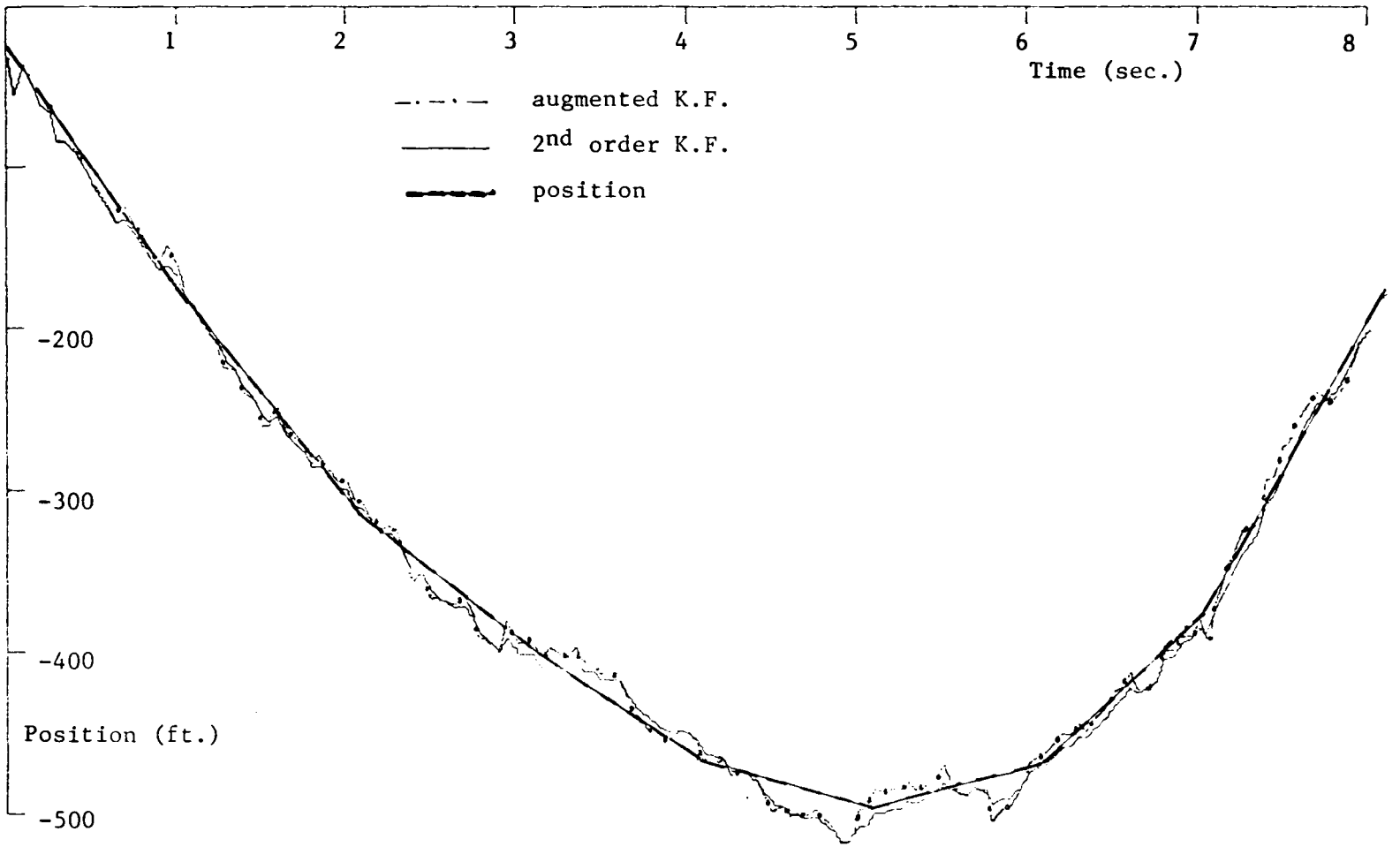

Figure 4.8 Second and Third Order Kalman Filters - Class III, $\sigma_m^2=300$

instaneously and at fixed time intervals is only reflected in the filter by the value Po=.95 which lowers the variance of the input forcing sequence (a(k) or w(k)). However, since the filter works only with the first order statistics, it cannot discriminate between a noise sequence as determined from Figure 2.1 and a gaussian white noise sequence with indentical statistics which is available at every sample instant. This fact is emphasized in the trajectories of the augmented filter which contains information about the correlation of the input accelerations. When the filter detects an acceleration input, it expects a correlated input on the very next sample instead of the twentith sample. Therefore, in track-white-scan systems in which the sample time is large compared to the vehicle maneuver time constant, the second order Kalman filter can perform better than the augmented Kalman filter.

In systems where the sample rate is small compared to the vehicle maneuver time constant, the trajectaries of Figures 2.2 through 2.4 are only approximations to a continuously varying maneuver. In such cases, it is expected that the augmented filter will outperform the second order filter.

4.3 The Double Kalman Filter

As in the case of the double α-β filter, descrimination between the outputs of two independent Kalman filters can add to the flexibility of the state estimate with respect to noise smoothing versus trend following. The basic idea is to have two Kalman filters, the first of which expects no input accelerations to the plant. In the linear, constant velocity regions of the plant's trajectory and with only white gaussian measurement noise, this filter produces the optimal estimate. However,

when an input acceleration occurs, the filter estimates will diverge from the true values and the filter must be reset in some manner. This reseting will be done via information obtained from a second Kalman filter which expects an input acceleration at every sample.

The implementation of Kalman filter 1 (K.F.#1) is straightforward. The variance of the input accelerations for filter #1, Q_1, as used in equation 4.5, is zero since no accelerations are expected. This has the effect of lowering the covariance matrix of filter #1 and therefore the Kalman gain matrix, K(n). Therefore, just prior to a non zero acceleration input, the uncertainty of the filter estimates, as reflected in the covariance matrices, will reach a low value and in turn lower the value of the Kalman gains. Following a non zero acceleration input, the filter will essentially ignore the new information as seen in equation 4.4

The implementation of Kalman filter #2 (K.F.#2) is also straightforward. To implement a filter which expects an acceleration input every sample instant, an acceleration variance, Q_2, as determined by equation 2.3 with Po=0 and Pm=.4, is used in equation 4.5. The effect of raising the input variance is to hold the steady state value of the Kalman gains at a higher level and thereby insure that adequate weighting is given new measurements during a maneuver as seen in equation 4.4 Because of the higher input variance associated with K.F.#2, it will yield estimates with larger variations than those of the filter of section 4.1. However, these larger variations enhance the decision making process of the double filter with respect to maneuver versus non

maneuver operation.

The ideal double Kalman filter scheme would use the estimates of K.F.#1 in the linear constant velocity regions. Then, in the process of detecting a maneuver and while there is still some doubt, the estimates of K.F.#2 would be the best estimates. Finally, when all criterion for maneuver detection have been met, the posterior variance and state estimate of K.F.#1 would be set to the corresponding values of K.F.#2.

In the double Kalman filter as implemented in this paper, all maneuver decisions were based on observations of the residuals of each Kalman filter over a five sample window. The filter residual is the quantity in equation 4.4 which is premultiplied by the Kalman gain matrix. The residual at time k+1 is the difference in the observed position measurement and the expected value of the position based on the last observation [i.e.,$Z(k+1)-H\Phi\hat{x}(k)$]. While in the tracking process, the average residual of each filter, denoted AR1 and AR2, over the last five samples is updated as each new measurement is taken. As extensions of the average residuals associated with each filter, there are also additional figures of merrit associated with each filter. Probability indicators, denoted PR1 and PR2, are associated with the respective filters, and are obtained by observing the relative sizes of AR1 and AR2, taking signs into account, and normalizing so that PR1 + PR2=1.

For the double Kalman filter as implemented in this paper, there are four threshold values (ξ,ε,ρ, and η) which are critical in the maneuver detection process. For maneuver detection, the probability indicator of filter #1 must be below a given threshold value (1.e.,

PR1<ε), the magnitude of the average residual of filter #1 must be above a given threshold (i.e.,|AR1|>ρ), and the magnitude of the average residual of filter #1 must have increased consecutively for a given number of sample intervals, η. When the above three criterion are met, the posterior variance and state estimate matrices of K.F.#1 are set to the values of the corresponding matrices of K.F.#2. When PR1 is greater than or equal to the upper threshold value ξ, the estimates of K.F.#1 is taken to be the best estimate. In all other cases (i.e.,ε<PR1<ξ,|AR1| <ρ), K.F.#1 is not reset but the estimates of K.F.#2 is taken to be the best estimate.

It takes little thought to realize that the effectiveness of the double Kalman filter is highly sensitive to the above threshold values. The optimal threshold values for a given situation may be functions of the input and measurement noise statistics and may therefore vary from one simulation to the next. However, in these simulations, the threshold values were held constant, except for ρ, and are given as follows:

$$\xi=.7, \qquad \varepsilon=.4, \qquad \eta=3, \qquad \text{and } \rho=1.5\sigma_m$$

Selected trajectories of the double Kalman filter are shown in Figures 4.9 through 4.14. The threshold values used seem to be better at the lower levels of measurement noise variance. At higher levels of measurement noise, the filter is driven much more by the noise, causing the unwanted reseting of K.F.#1 at infrequent sample times.

The above threshold valves can be adjusted according to the emphasis placed on noise smoothing versus trend following. For example, by

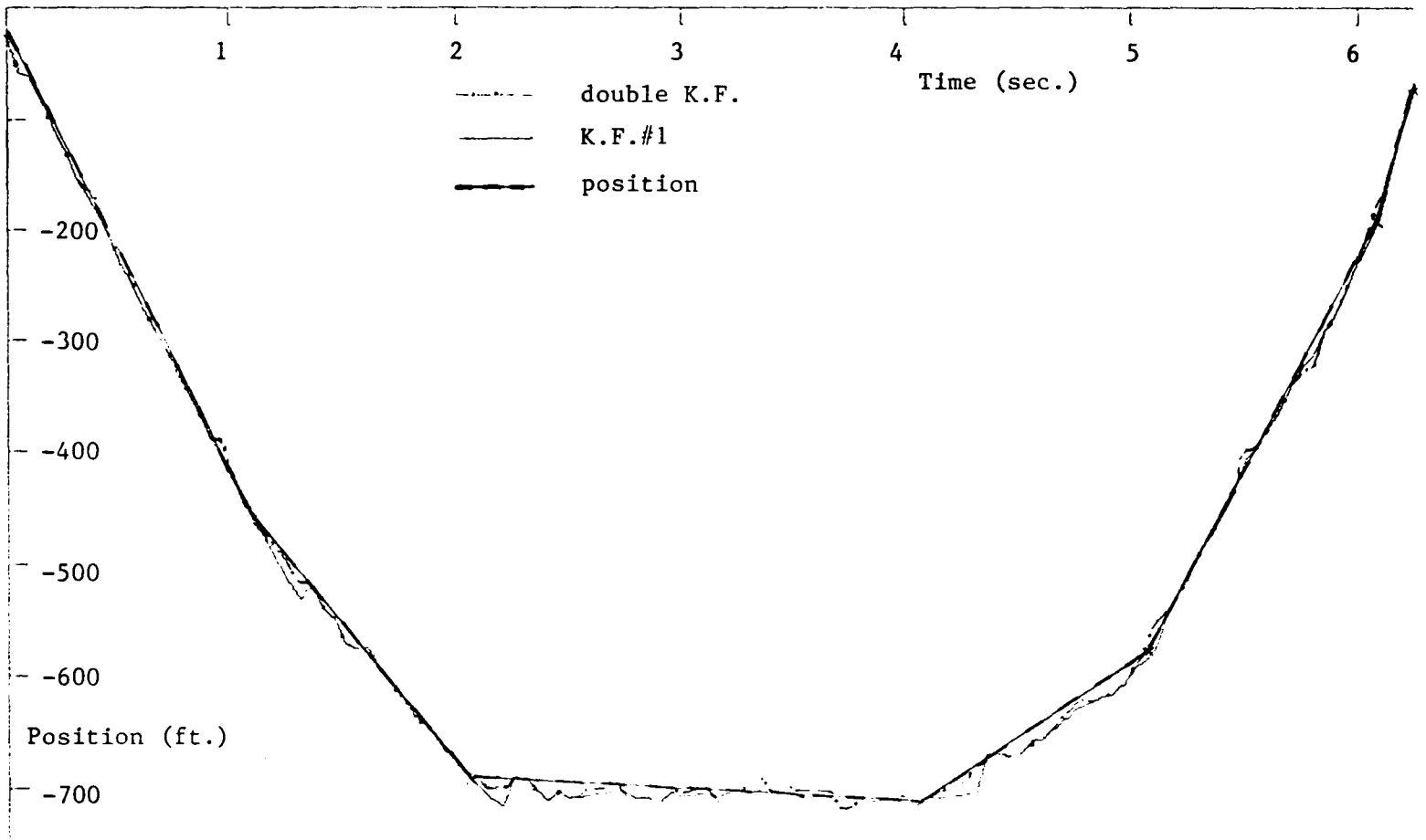

Figure 4.9 Double Kalman Filter - Class I, σ_m^2=100

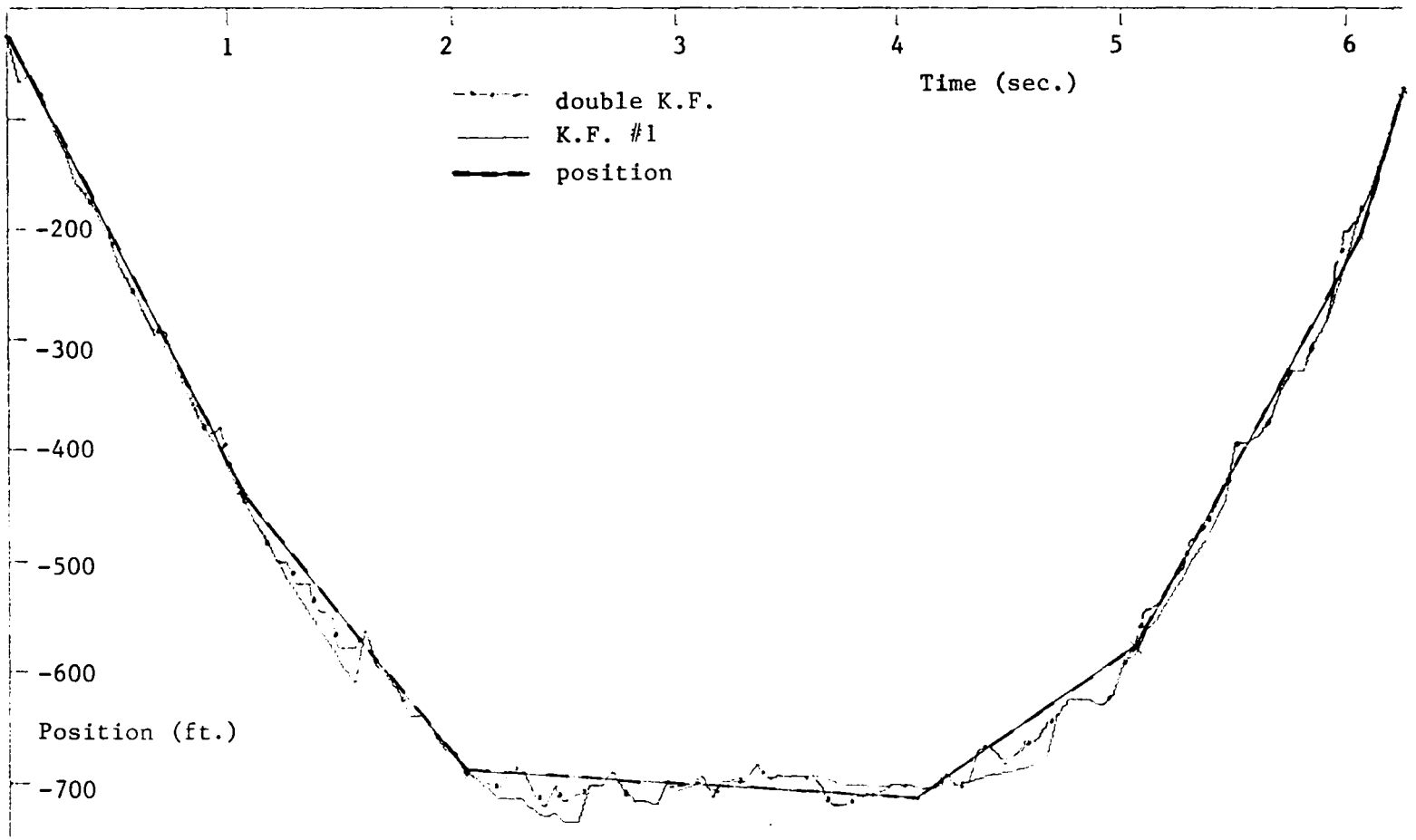

Figure 4.10 Double Kalman Filter - Class I, σ_m^2=300

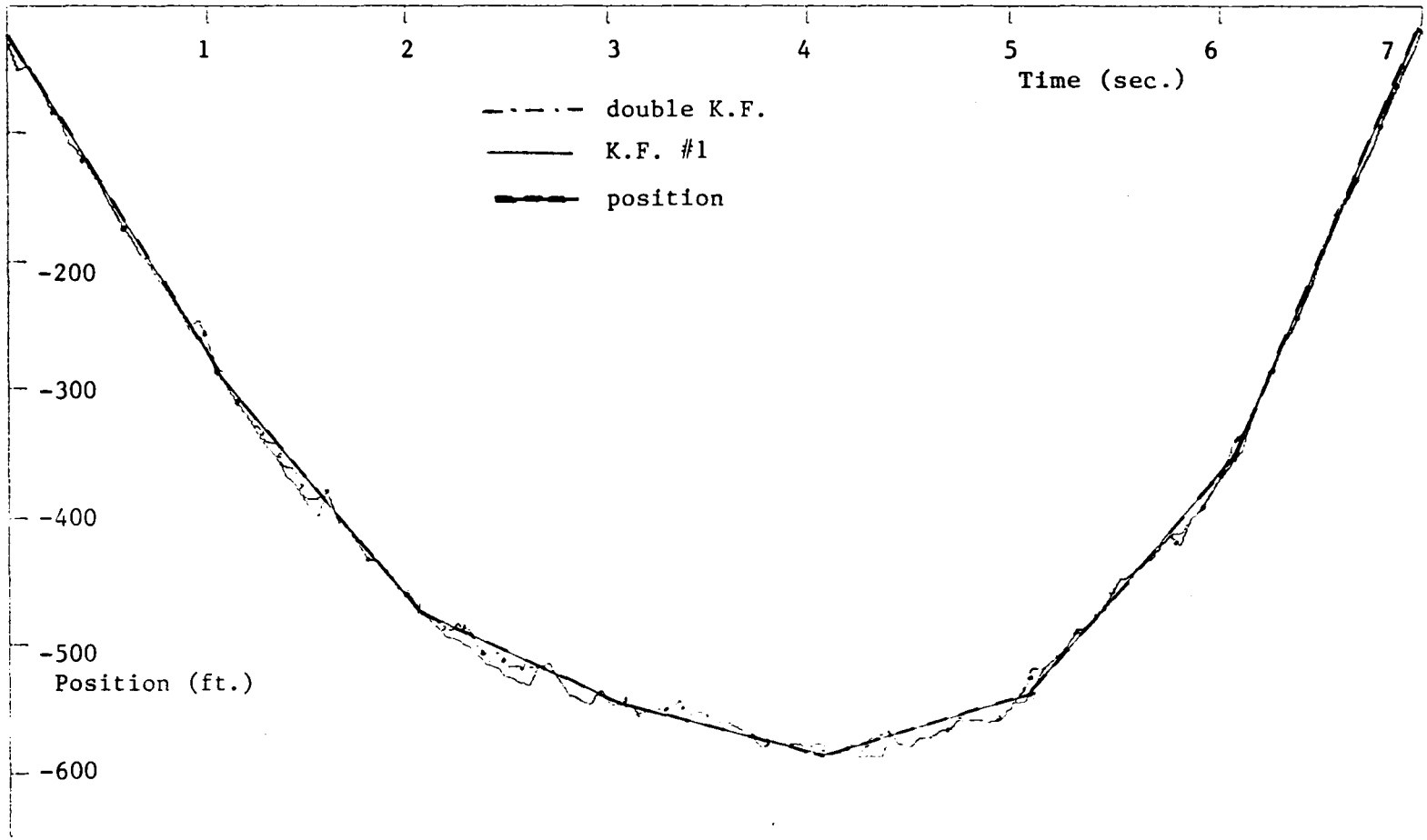

Figure 4.11 Double Kalman Filter - Class II, σ_m^2=100

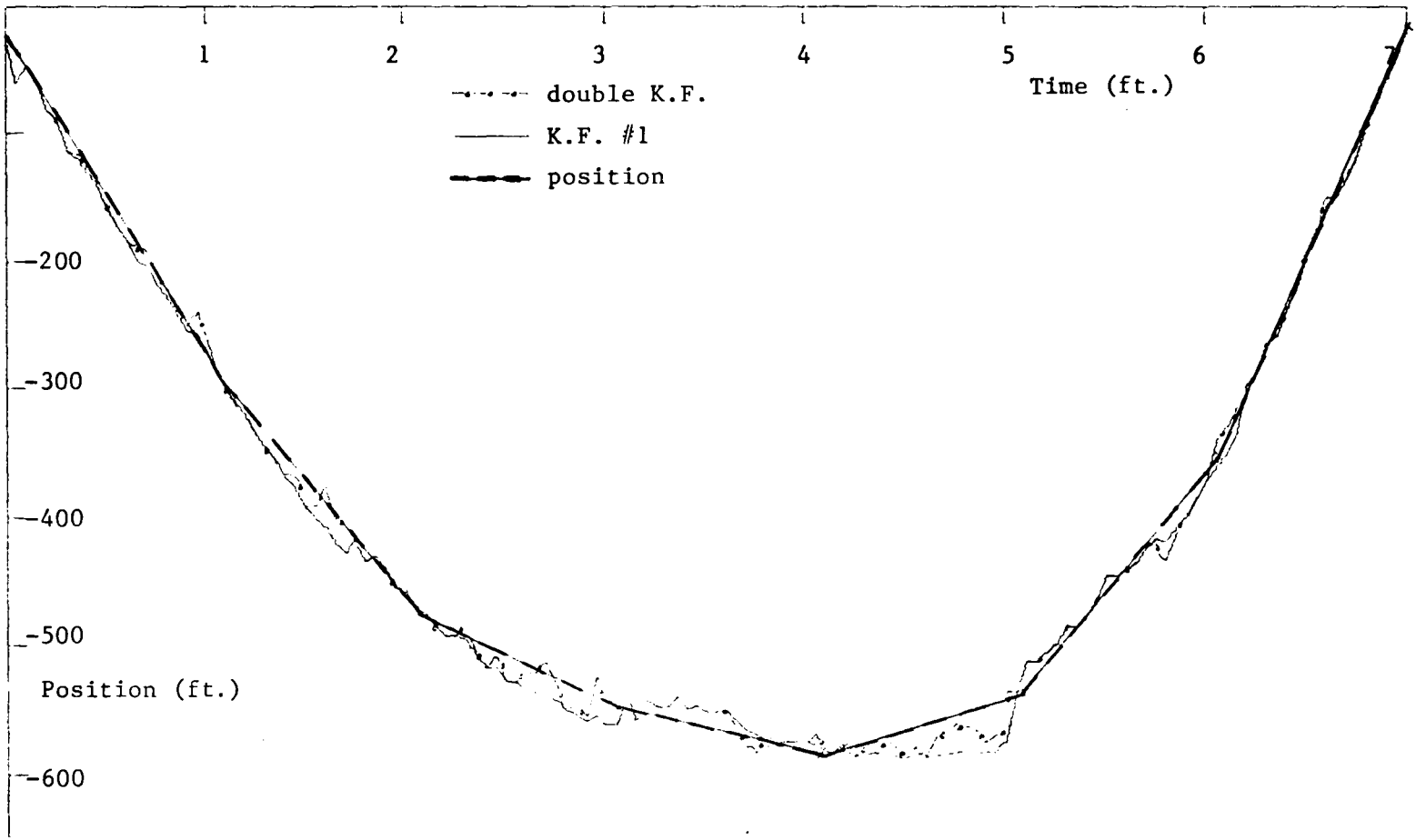

Figure 4.12 Double Kalman Filter - Class II, σ_m^2=300

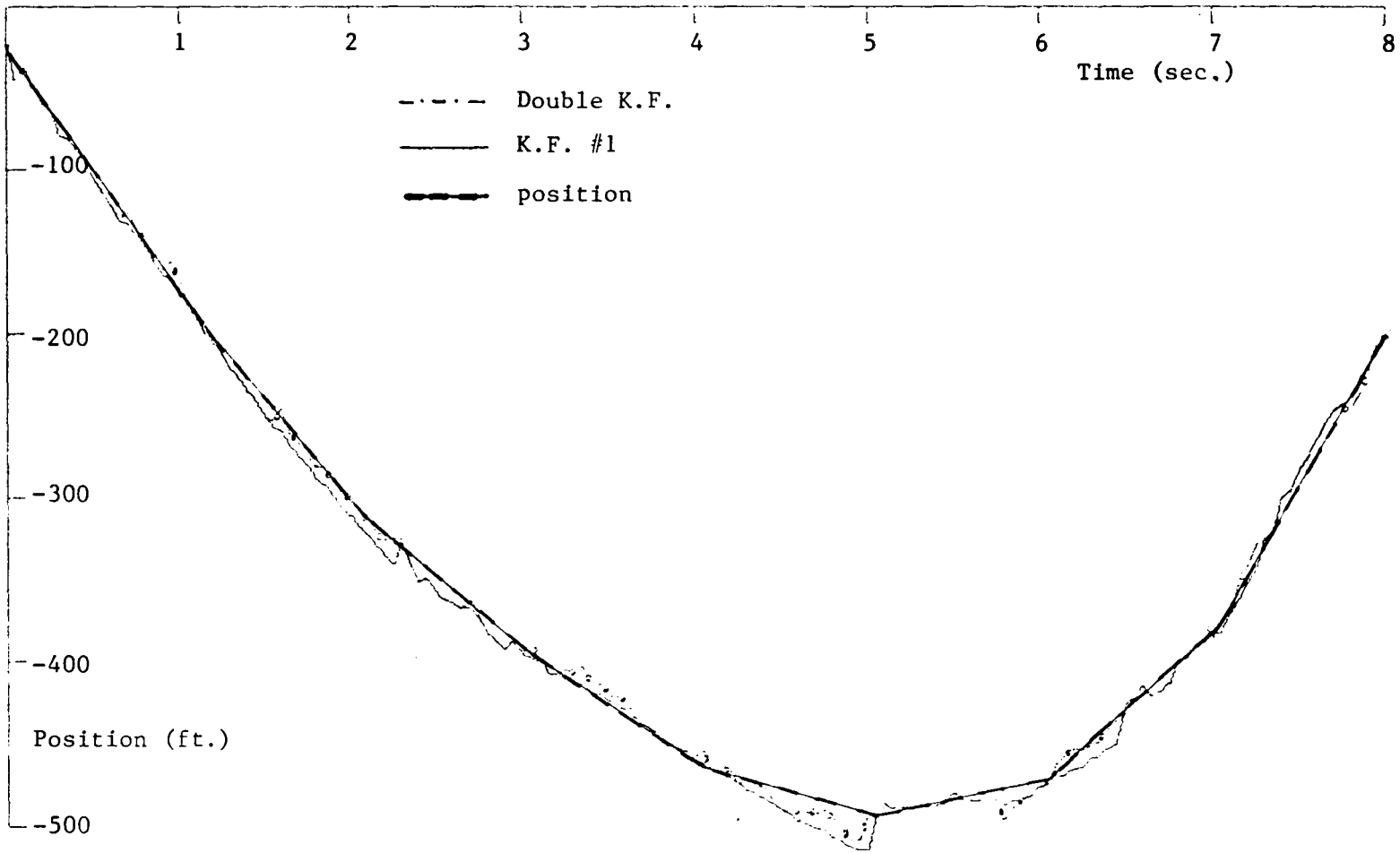

Figure 4.13 Double Kalman Filter - Class III, σ_m^2=100

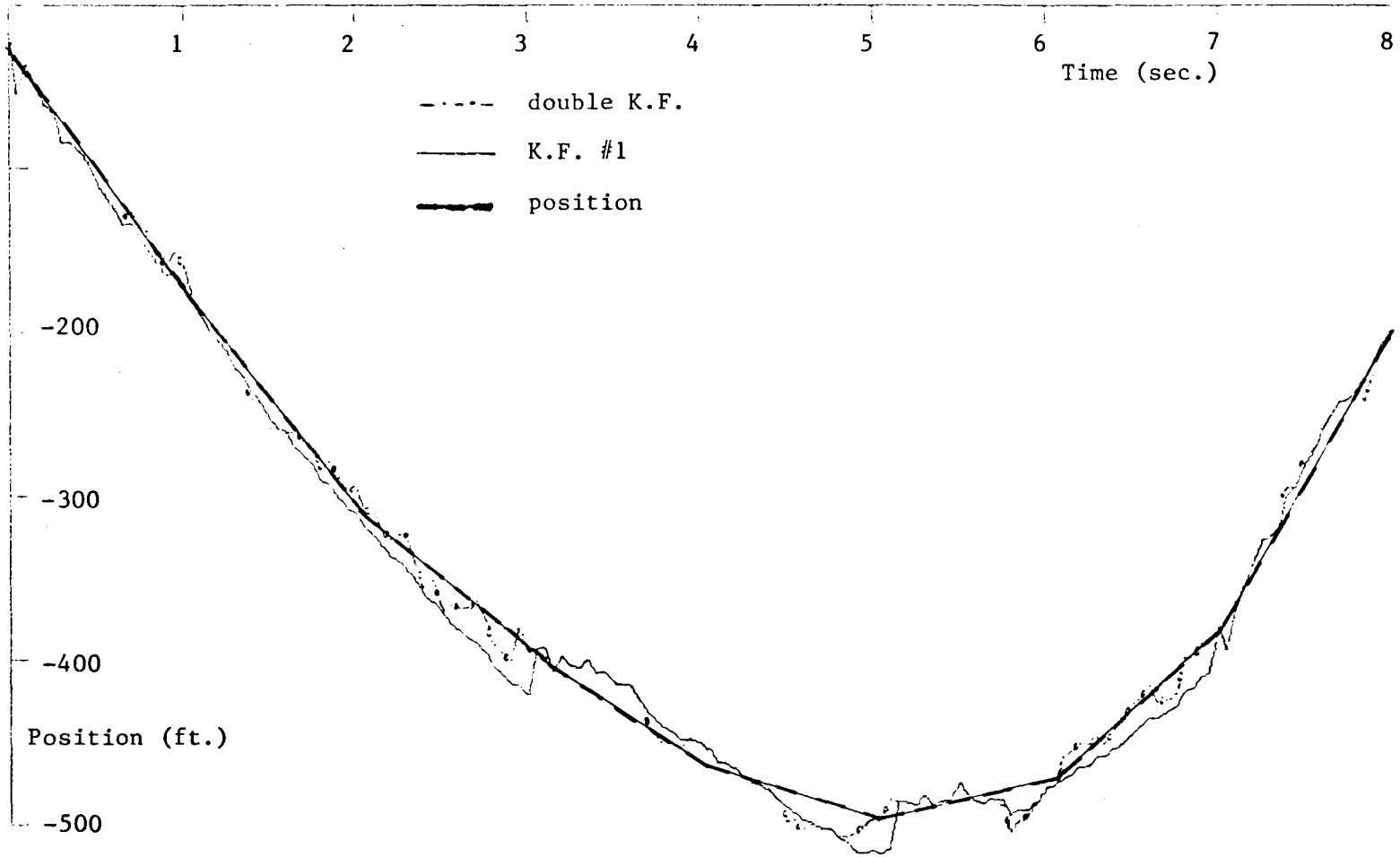

Figure 4.14 Double Kalman Filter - Class III, σ_m^2=300

fixing ξ=1, we essentially take the best estimates to be those of K.F.#2 which will quickly follow all maneuvers. By fixing ξ=0 and ϵ=1, we essentially take the best estimates to be those of K.F.#1 while risking an undetected maneuver. Although these simulations were in maneuver conditions with threshold values fixed, the double Kalman filter scheme lends itself to adaptive adjustments of ξ and ϵ in a general situation. As stated in Chapter 2, most vehicles travel in straight line constant velocity trajectories while not maneuvering. In such cases, where maneuver tracking time is a small percentage of the overall tracking time, a scheme for adaptive adjustments of ξ and ϵ seems reasonable. While in the linear, constant velocity mode, ξ could be set to a low value producing the optimal estimate of K.F.#1 as the output of the double filter. Once a maneuver had been detected, ξ and ϵ could be adjusted such that the estimate of K.F.#2 would be used as the best estimate until a specified amount of time had elapsed since the last maneuver detection. At that time ξ and ϵ could be readjusted to their original values. A flow chart for the double Kalman filter is shown in Appendix B with the added capability of adaptive adjustment of ξ and ϵ.

Chapter V

Conclusions

Figures 5.1, 5.2, and 5.3 show the percentage improvement, PI, for each of the filters under test as a function of process and measurement noise variances. The percentage improvement of each filter over the noisy measurements is taken to be

$$PI = \left| 1 - \frac{\bar{e}_f}{\bar{e}_m} \right| x100$$

where

$$\bar{e}_f = \frac{1}{200} \sum_{k=1}^{200} \left| \hat{p}(k) - p(k) \right|$$

$$\bar{e}_m = \frac{1}{200} \sum_{k=1}^{200} \left| z(k) - p(k) \right|$$

$\hat{p}(k)$ = filter position estimate at time k

$p(k)$ = actual position at time k

$z(k)$ = noisy position measurement at time k

It is seen that for each of the nonresetting filters (i.e., 2nd order K.F., 3rd order K.F., and fixed parameter α-β), the percent improvement increases as the measurement noise increases and the process noise decreases. The same trend is shown for the double K.F. In contrast,

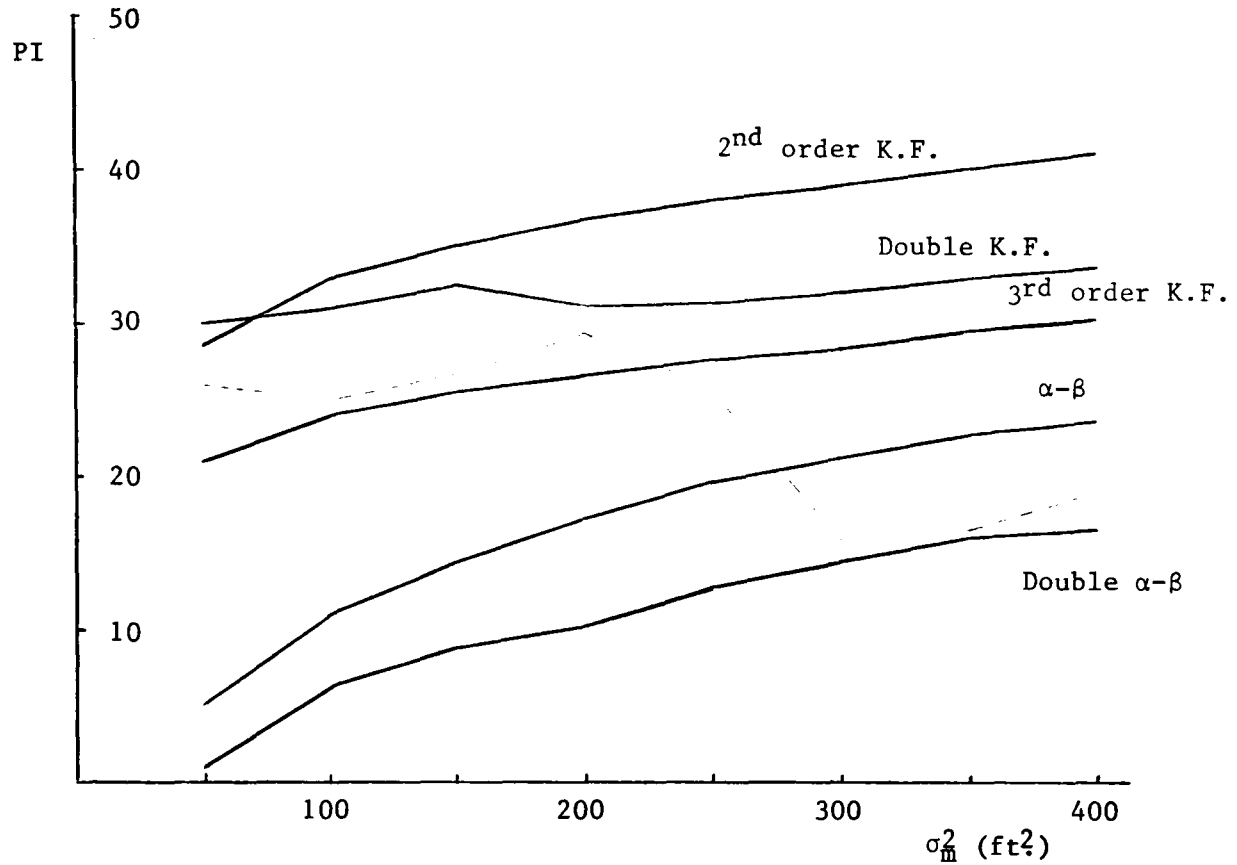

Figure 5.1 Percent Improvement - Class I

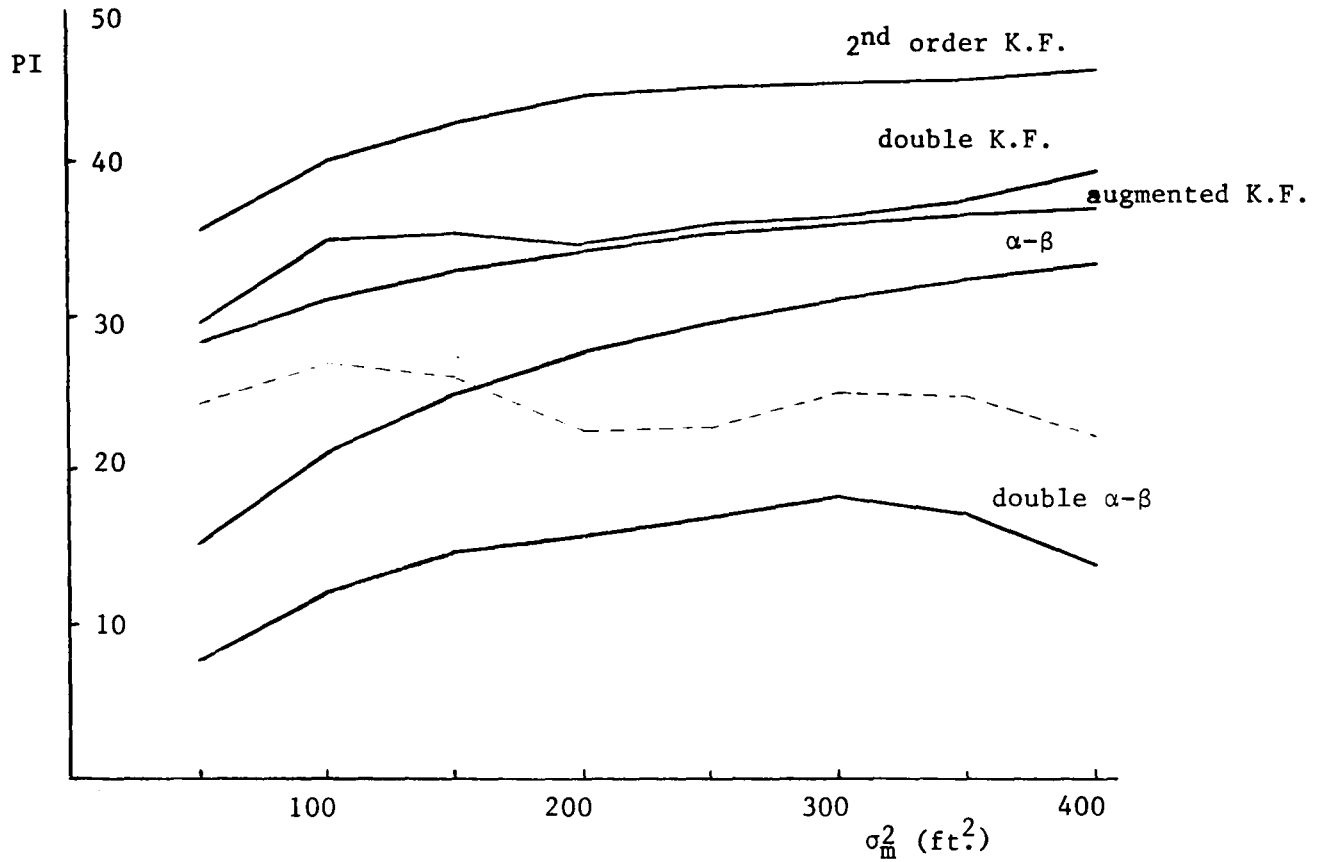

Figure 5.2 Percent improvement - Class II

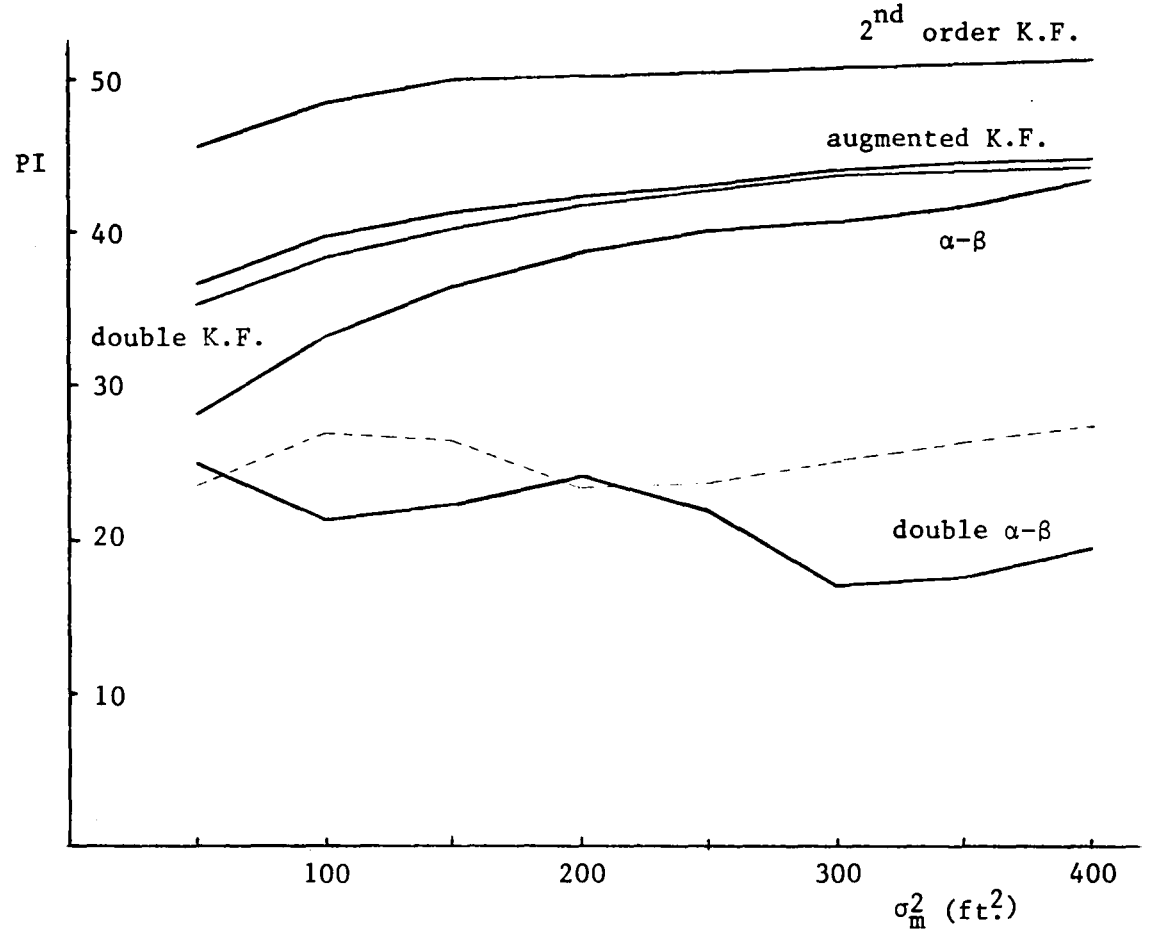

Figure 5.3 Percent Improvement - Class III

the performance of the double α-β filter decreases as both measurement and process noise is increased.

In each case, the 2nd order K.F. is the best. The degradation of the augmented K.F. is due to the linear, constant velocity trajectories used in these simulations. In real-time tracking situations where the trajectories used here are only approximations to a continuously maneuvering vehicle, it is expected that the 3rd order Kalmon filter will replace the 2nd order Kalman filter as the leader in percent improvement over the noisy measurements during a maneuver.

In each case, the curve for the double K.F. is slightly below that of the 2nd order K.F.. The dashed lines indicate the performance of K.F. #1 of the double K.F.. This is the filter which expects no accelerations and will yield the optimal estimate when the vehicle is not maneuvering. Adjustment of the threshold values associated with the double K.F. can yield percentage improvement plots which can be anywhere between the dashed curve and the plot for the 2nd order K.F.. Selection of these threshold values is determined by the relative importance placed on maneuver versus non-maneuver tracking. The double K.F. scheme lends itself to adaptive adjustments of the threshold values for maneuver versus non-maneuver operation.

The double α-β filter shows relatively low improvement for all process and measurement noise environments. The problem lies in obtaining the very accurate resetting needed for a narrowband filter from wideband information. It is suggested that further resetting procedures be investigated, using state models other than the controllable form

used here, before discarding the idea completely.

As a follow up investigation, it is recommended that the feasibility of using the simple 2nd order, fixed parameter α-β filter as a buffer to a Kalman filter using reduced measurement noise statistics, be studied. In such a case, the output of the α-β filter must be assumed to have a white noise component which it does not. However, the output spectral density of the fixed parameter α-β filter is still wideband compared to the frequencies associated with the maneuvering vehicle and the buffering may yield further improvement.

Bibliography

(1) Robert A. Singer, "Estimating Optimal Tracking Filter Performance for Manned Maneuvering Targets", IEEE-TAES, Vol. AES-6, No.4, July 1970, pp. 473-483.

(2) Kenneth W. Behnke and Robert A. Singer, "Real-Time Filter Evaluation and Selection for Tactical Applications", IEEE-TAES, Vol. AES-7, No.1, January 1971, pp. 100-110.

(3) T.R. Benedict and G.W. Border, "Synthesis of a Optimal Set of Radar Track-While-Scan Smoothing Equations", IRE-TAC, Vol. AC-7, No.4, July 1962, pp.27-32.

(4) C.C. Schooler, "Optimal Alpha Beta Filters for Systems with Modeling Inaccuracies", IEEE-TAES, Vol. AES-11, No.6, pp.1300-1306.

(5) Jack Sklansky, "Optimizing the Dynamic Parameters of a Track-While-Scan System", RCA Review, June 1957, pp. 163-180.

(6) H.F. Vanlandingham and C.M. Hubbard, "Adaptive and Optimal Linear Forcasting Algorithms", Virginia Polytechnic Institute and State University, Blacksburg Va., Naval Surface Weapons Center, Dalgren Va.

(7) Allen J. Kanyuck, "Transient Response of Tracking Filters with Randomly Interrupted Data", IEEE-TAES, Vol. AES-6, No.3, May 1970, pp. 313-323.

(8) James S. Thorp, "Optimal Tracking of Maneuvering Targets",

IEEE-TAES, Vol. AES-9, No.4, July 1973, pp. 512-518.

(9) H.F. Vanlindingham, "Class Notes for EE-5401(Discrete-Time Systems)", Department of Electrical Engineering, Virginia Polytechnic Institute and State University, Blacksburg Va., March 1976.

(10) H.F. Vanlandingham, "Class Notes for EE-5403(Stochastic Control Systems)", Department of Electrical Engineering, Virginia Polytechnic Institute and State University, Blacksburg Va., June 1976.

(11) H.F. Vanlandingham, "Class Notes for EE-6400(Stochastic System Theory)", Department of Electrical Engineering, Virginia Polytechnic Institute and State University, Blacksburg Va., Nov. 1976.

(12) Technical Staff, The Analytic Sciences Corporation, "Applied Optimal Estimation", The M.I.T. Press, 1974.

(13) Papoulis, "Probability, Random Variables, and Stochastic Processes", McGraw-Hill Inc., 1965.

Appendix A

Flow Chart for Double α-β Filter

Variables

RA - average ratio of x_3/x_4 over a three sample window

x_1, x_2 - states of narrowband filter

x_3, x_4 - states of wideband filter

y_1 - smoothed position estimate of narrowband filter

y_2 - smoothed position estimate of wideband filter

u - noisy input position measurement

$\hat{p}$ - double filter position output

ξ - threshold value for output selection

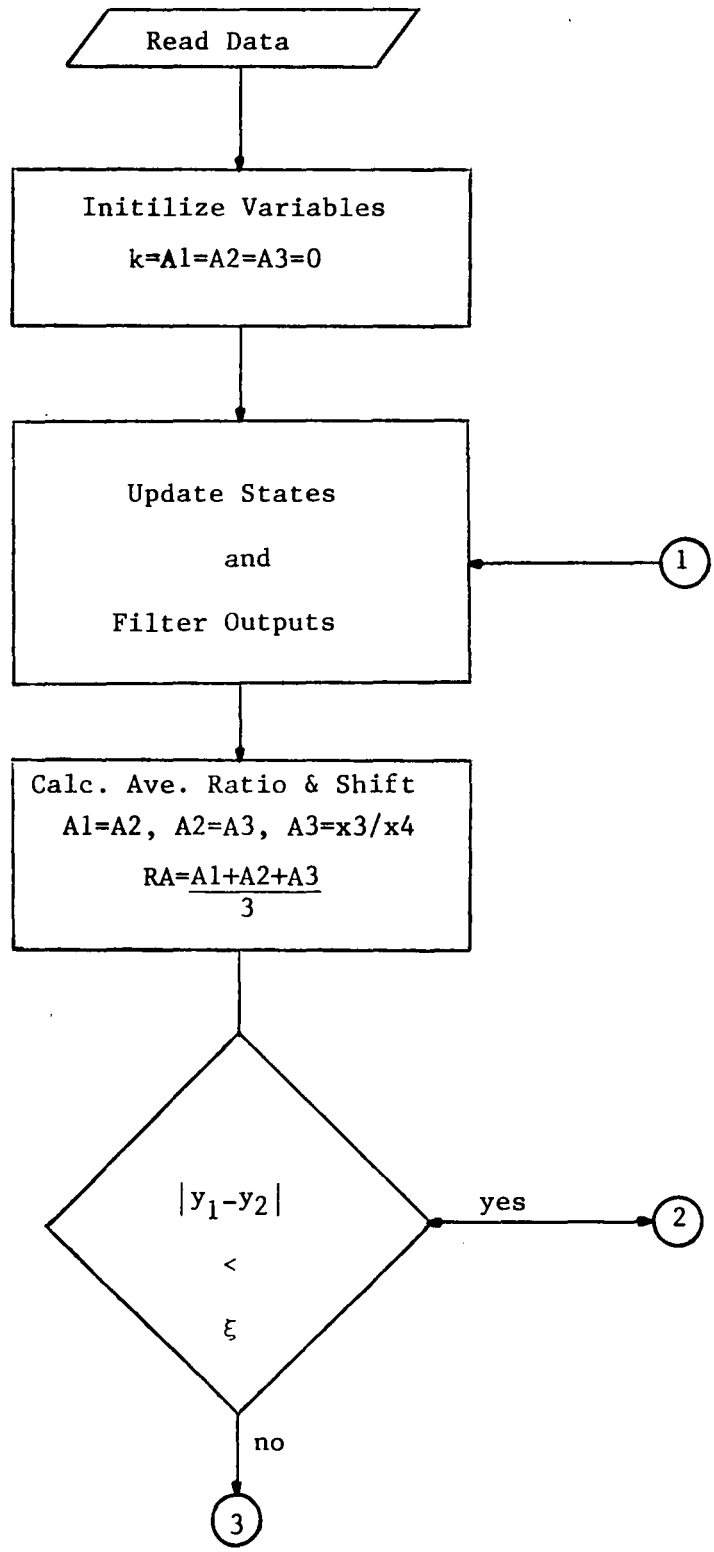
Read Data
Initilize Variables
k=A1=A2=A3=0
Update States
and
Filter Outputs
1
Calc. Ave. Ratio & Shift
A1=A2, A2=A3, A3=x3/x4
RA=A1+A2+A3
3
|y1-y2|
<
ξ
yes
2
no
3

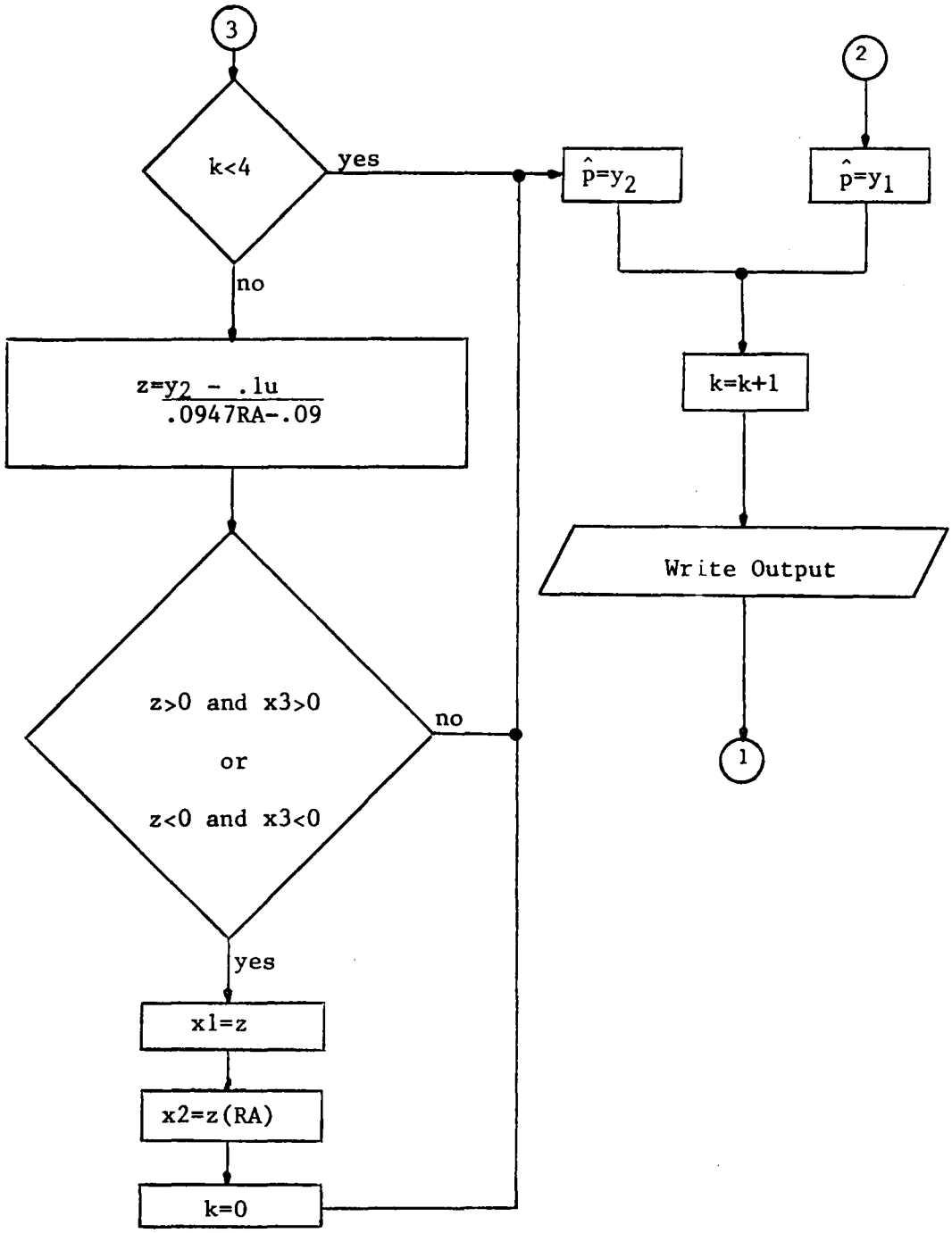
3
k<4
yes
no
$\hat{p}=y_2$
2
$\hat{p}=y_1$
$z=\frac{y_2 - .1u}{.0947RA-.09}$
k=k+1
Write Output
z>0 and x3>0
or
z<0 and x3<0
no
1
yes
x1=z
x2=z(RA)
k=0

Appendix B

Flow Chart for Double Kalman Filter

Variables

$\hat{p}$ - estimated position

p_1 - posterior covariance matrix of K.F. #1

p_2 - posterior covariance matrix of K.F. #2

$\underline{\hat{x}}_1$ - state vector of K.F. #1

$\underline{\hat{x}}_2$ - state vector of K.F. #2

$\hat{x}_{11}$ - position estimate of K.F. #1

$\hat{x}_{21}$ - position estimate of K.F. #2

AR1 - average residual of K.F. #1 over 5 sample window

AR2 - average residual of K.F. #2 over 5 sample window

PR1 - probability indicator = $|AR1|/(|AR1|+|AR2|)$

J - counts # of sample intervals since last maneuver detection

k - counts # of continuous increases in $|AR1|$

m - indicates maneuver versus non-maneuver operation

ξ - threshold value of PR1 above which $\hat{x}_{11}=\hat{p}$

ϵ, p, η - threshold values which sense a maneuver

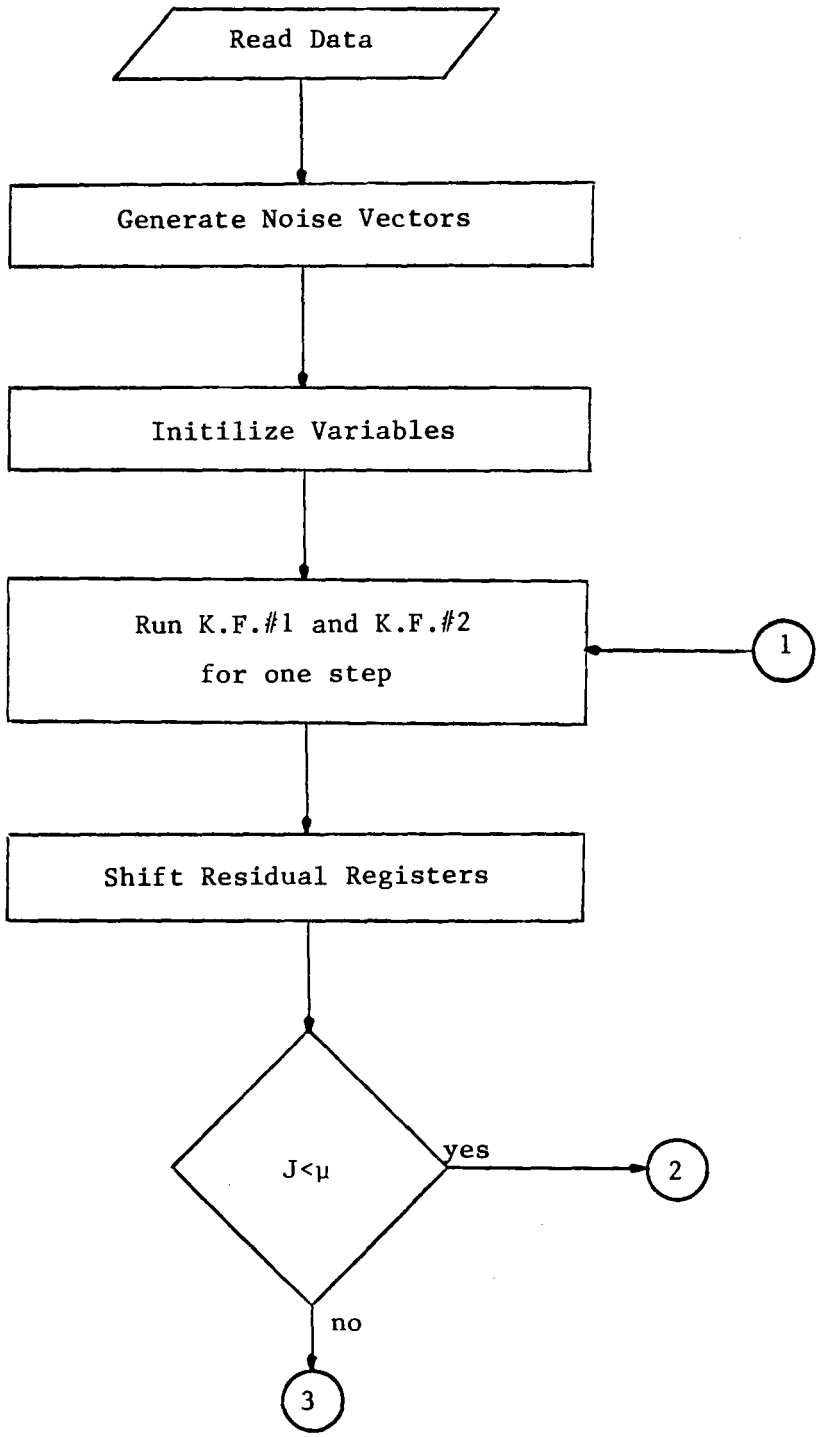
Read Data
Generate Noise Vectors
Initilize Variables
Run K.F.#1 and K.F.#2
for one step
1
Shift Residual Registers
J<μ
yes
2
no
3

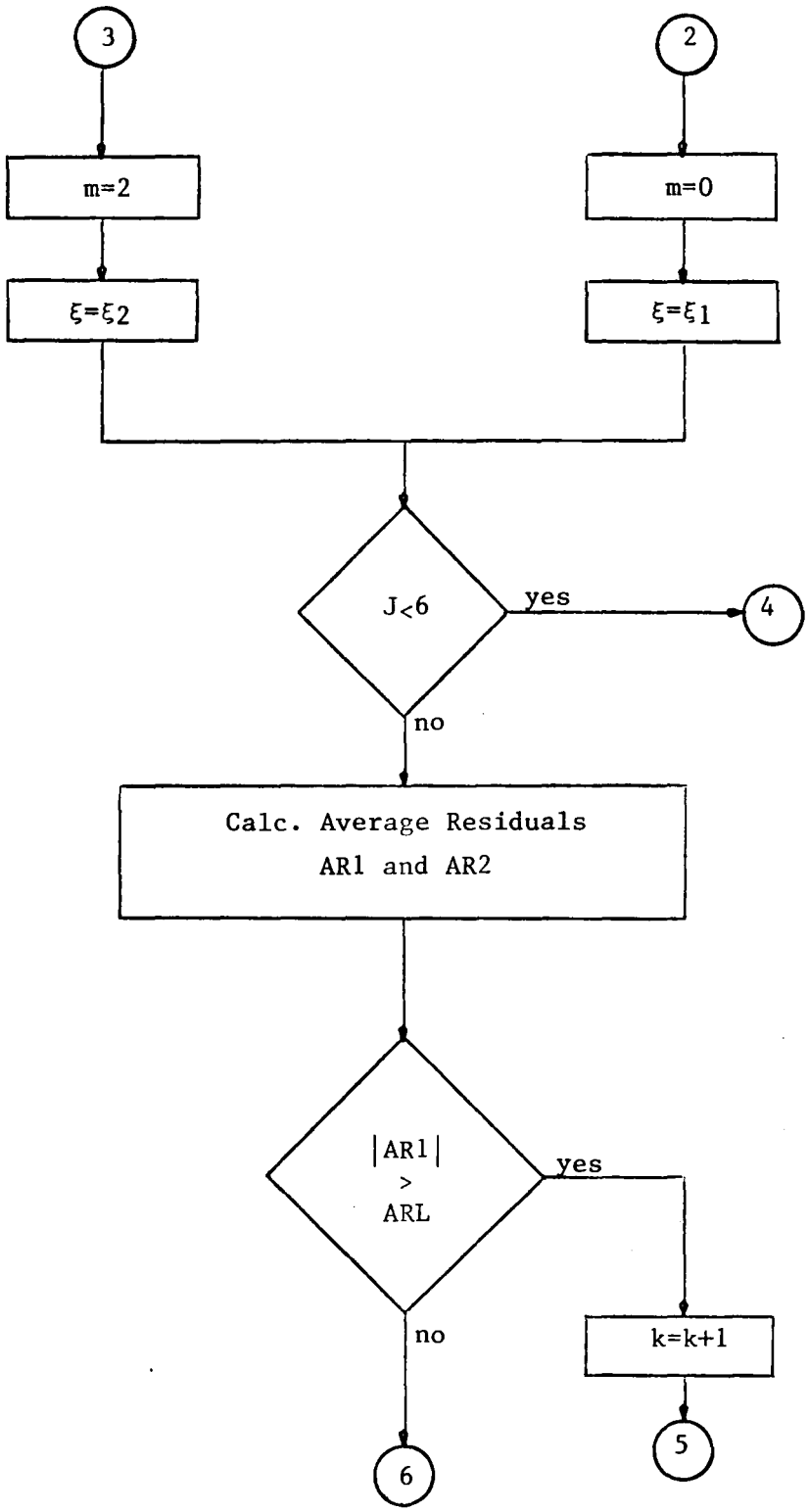
3
2
m=2
m=0
ξ=ξ2
ξ=ξ1
J<6
yes
4
no
Calc. Average Residuals
AR1 and AR2
|AR1|
>
ARL
yes
no
k=k+1
5
6

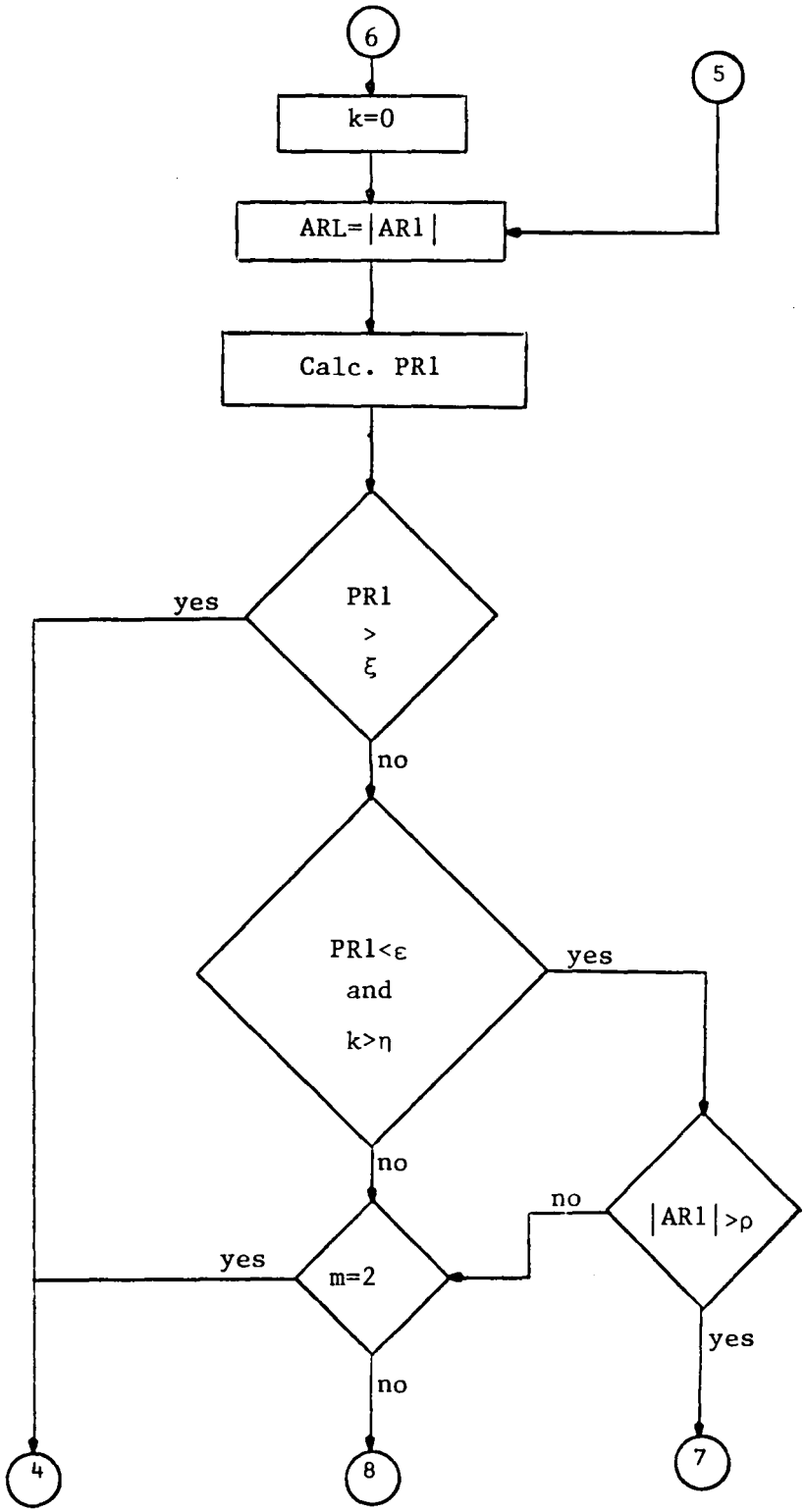
6
5
k=0
ARL=|AR1|
Calc. PR1
PR1
>
ξ
yes
no
PR1<ε
and
k>η
yes
no
|AR1|>ρ
no
m=2
yes
yes
no
4
8
7

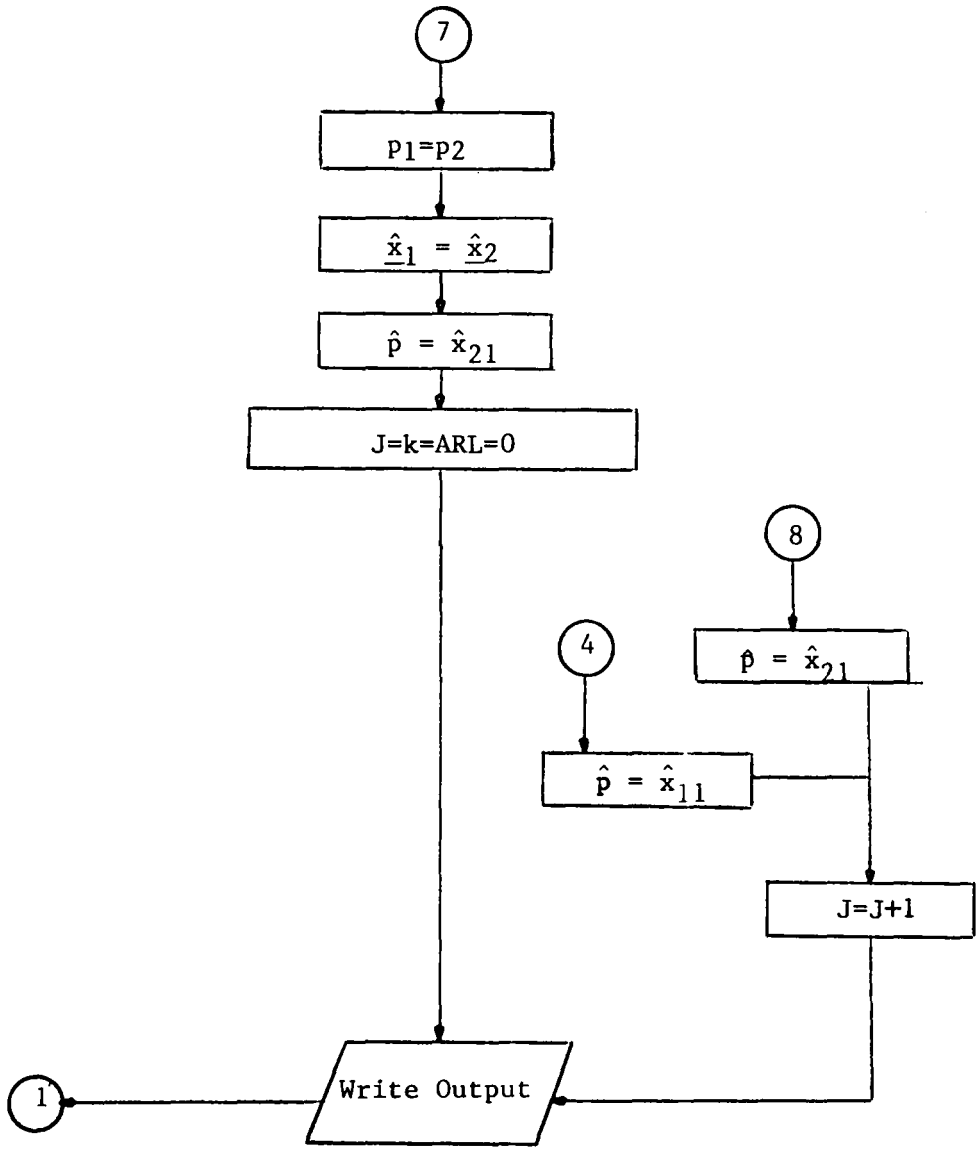
7
P1=P2
$\underline{\hat{x}}_1 = \underline{\hat{x}}_2$
$\hat{p} = \hat{x}_{21}$
J=k=ARL=0
8
$\hat{p} = \hat{x}_{21}$
4
$\hat{p} = \hat{x}_{11}$
J=J+1
Write Output
1

Appendix C

Derivation of Initialization Equations For The Kalman Filters

$$\underline{x}(k+1)=\begin{bmatrix} 1 & T & 0 \\ 0 & 1 & 1 \\ 0 & 0 & e^{-\gamma T} \end{bmatrix}\underline{x}(k)+\begin{bmatrix} 0 \\ 0 \\ 1 \end{bmatrix}w(k)$$

$$z(k)=[1 \quad 0 \quad 0]\underline{x}(k)+v(k)$$

v(k) and w(k) are white, zero-mean, gaussian sequences, therefore

$$E[v(k)]=E[w(k)]=E[v(k)v(j)]=E[w(k)w(j)]=E[v(k)w(k)]=0$$

$$P=E\begin{bmatrix} \tilde{x}_1^2 & \tilde{x}_1\tilde{x}_2 & \tilde{x}_1\tilde{x}_3 \\ \tilde{x}_2\tilde{x}_1 & \tilde{x}_2^2 & \tilde{x}_2\tilde{x}_3 \\ \tilde{x}_3\tilde{x}_1 & \tilde{x}_3\tilde{x}_2 & \tilde{x}_3^2 \end{bmatrix}$$

With $\underline{\tilde{x}}=\underline{\hat{x}}-\underline{x}$

Let $\hat{x}_1(1/1)=z(1)=x_1(1)+v(1)$

$\hat{x}_2(1/1)=(z(1)-z(0))/T$

$\hat{x}_3(1/1)=0$

$$E[\tilde{x}_1^2]=E[(\hat{x}_1(1)-x_1(1))^2]$$

$$=E[(x_{1(1)}+v(1)-x_1(1))^2]=E[x(1)^2]=\sigma_m^2$$

$$E[\tilde{x}_1\tilde{x}_2]=E[(x_1(1)+v(1)-x_1(1))(x_1(1)+v(1)-x_1(0)-v(0)-x_1(1)+x_1(0))/T]$$

$$=E[v(1)^2/T]-E[\frac{v(1)v(0)}{T}]=\frac{\sigma_m^2}{T}$$

$$E[\tilde{x}_1\tilde{x}_3]=E[(x_1(1)+v(1)-x_1(1))(x_3(1)-x_3(1))]$$

$$=E[v(1)(0-e^{-\sigma T}x_3(0)-(0))]=0$$

$$E[\tilde{x}_2\tilde{x}_3]=E[(\frac{v(1)}{T}-\frac{v(0)}{T})(-e^{-\sigma T}x_3(0)-w(0))]=0$$

$$E[\tilde{x}_2^2]=E[(\frac{v(1)}{T}-\frac{v(0)}{T})^2]$$

$$=\frac{1}{T^2}E[v(1)^2-2v(1)v(0)+v(0)^2]=\frac{2\sigma_m^2}{T^2}$$

$$E[\tilde{x}_3^2]=E[(-e^{-\sigma_T}x_3(0)-w(0))^2]$$

$$=e^{-2\sigma T}E[x_3^2(0)]-2e^{-\sigma T}E[x_3(0)]E[w(0)]+E[w(0)^2]$$

$$=\sigma_a^2\ [1+e^{-2\sigma T}]$$

The vita has been removed from the scanned document

A COMPARISON OF FIXED PARAMETER VERSUS ADAPTIVE DIGITAL TRACKING FILTERS

by

Charles Keith Colonna

(ABSTRACT)

The simulation and testing of several state tracking techniques over a range of process and measurment noise environments is considered. The problem is placed in the context of tracking a maneuvering vehicle from noisy position data with the vehicle accelerations considered as a random process about which the first and second order statistics are known. The tracking filters under test are the fixed α-β filter, the double α-β filter, the second order Kalman filter, the augmented Kalman filter, and the double Kalman filter.

All filters show improved performance as the measurment noise increases and the process noise decreases. The superiority of the Kalman filter over the simpler deterministic digital trackers decreases as the measurment noise increases and the process noise decreases. The double Kalman filter, with the capability of adaptive adjustments of threshold values, indicates the best overall tracking for combined maneuver and non-maneuver tracking.